THE HONG KONG

POLYTECHNIC UNIVERSITY

Institute of Textiles and Clothing

Chitosan Nanoparticles for Functional Textile Finishes

by Hu Zhigang

(A thesis submitted in partial fulfilment of the requirements

for the Degree of Doctor of Philosophy)

February 2007

CERTIFICATE OF ORIGINALITY

I hereby declare that this thesis is my own work and that, to the best of my knowledge and belief, it reproduces no material previously published or written, nor material that has been accepted for the award of any other degree or diploma, except where due acknowledgement has been made in the text.

_____(Signed)

Hu Zhigang_____(Name of student)

Abstract

In this thesis, the research work mainly focused on the preparation of nano-scale chitosan, and its applications in textile.

Firstly, a new method to prepare the emulsions containing chitosan nanoparticles was developed through a dissolving-precipitating-dispersing process with the assistance of ultrasound, and emulsions of the pure chitosan nanoparticles or the composite chitosan/silver oxide nanoparticles were accordingly prepared. Then the emulsions were studied in the applications of textile antibacterial and deodorizing finishing.

On the other hand, research works was done on the investigation and applications of the pure chitosan nanoparticles in the dyeing process of textile. This section included the study of the interaction between the pure chitosan nanoparticles and the acid dye molecules, and the application of the emulsion of the pure chitosan nanoparticles on the dyeability improvement of silk fabrics and nylon fabrics.

Published Work

1. **Hu Z.G.**, Chan W.L., Szeto Y.S.; *Nanocomposite of chitosan and silver oxide and its antibacterial property* **Journal of Applied Polymer Science,** 108(1):52-56, 2008.

2. **Hu Z.G.**, Zhang J., Chan W.L., Szeto Y.S.; *The sorption of acid dye onto chitosan nanoparticles* **Polymer** 47 (16): 5838-5842 2006.

3. Szeto Y.S., **Hu Z.G.**, *The preparation of chitosan nanoparticles* **Chinese Patent**, Appl. Code 200610139605.4, 2006; **WO Patent**, WO/2008/038134, 2007.

4. **Hu Z.G.**, Zhang J., Chan W.L., Szeto Y.S.; S*uspension of Silver Oxide Nanoparticles in Chitosan Solution and its Antibacterial Activity in Cotton Fabrics* **Mater. Res. Soc. Symp. Proc.** 920, Warrendale, PA, U.S.A., 2006.

5. **Hu Z.G.**, Chan W.L., Szeto Y.S.; *Dyeability improvement of silk with chitosan nanoparticles* **Abstracts of papers of the American Chemistry Society** 230: U4033-U4033 70-POLY, Washington D.C., U.S.A., 2005.

6. **Hu Z.G.**, Chan W.L., Chan K.W., Szeto Y.S.; *New chitosan/silver oxide nanocomposite and its antibacterial activity in cotton fabrics* **Abstracts of papers of the American Chemistry Society** 230: U4058-U4058 126-POLY, Washington D.C., U.S.A., 2005.

Acknowledgements

I would like to express my deep and sincere gratitude to my supervisor, Dr. Szeto Yau Shan, assistant professor of the Institute of Textiles and Clothing, the Hong Kong Polytechnic University. His wide knowledge and his logical way of thinking have been of great value for me. His understanding, encouraging and personal guidance have provided a good basis for the present thesis. I am deeply grateful to my co-supervisor, Dr. Chan Wing Lai, assistant professor of the Department of Applied Biology and Chemical Technology, the Hong Kong Polytechnic University, for his detailed and constructive comments, and for his important support throughout this work.

During this work I have collaborated with many colleagues for whom I have great regard, and I wish to extend my warmest thanks to all those who have helped me with my work in the Institute of Textiles and Clothing and Department of Applied Biology and Chemical Technology.

I owe my loving thanks to my father, mother and brother. They have lost a lot due to my research abroad. Without their encouragement and understanding it would have been impossible for me to finish this work.

The financial support of the Hong Kong Polytechnic University is gratefully acknowledged.

Contents

List of Figures

List of tables

List of Abbreviations

CSNPs	the Chitosan Nanoparticles
E. coli	Escherichia coli
S. aureus	Staphylococcus aureus
D.I. water	Deionic Water
MW	Molecule Weight
DD	Degree of Deacetylation
TPP	Tripolyphosphate
DSC	Differential Scanning Calorimeter
Mv	Viscosity Molecule Weight
SEM	Scanning Electronic Microscopy
TEM	Transmission Electron Microscopy
IR	Infrared Ray Spectroscopy
UV-vis	Ultraviolet-visible Spectroscopy
XRD	X-ray Diffraction
^{1}HNMR	Hydrogen Nuclear Magnetic Resonance
AFM	Atomic Force Microscopy
AATCC	American Association of Textile Chemists and Colorists
ASTM	American Society for Testing and Materials

Chapter 1

Introduction

1.1 Research background

Chitosan is the deacetylated derivative of chitin that is the second most abundant polysaccharide next to cellulose on the earth. Chitin is the main component in the shells of crustaceans such as shrimp, crab, and lobster, and also be found in exoskeletons of mollusks and insects and the cell walls of some fungi [1-3]. Every year plenty of crabs and shrimp shells are abandoned as wastes by seafood companies worldwide, and considerable scientific and technological interest arouses in the attempt to utilize chitin and chitosan in these renewable wastes . In the past 30 years, it was demonstrated by a number of researchers that chitosan had a great potential for a wide range of uses due to its biodegradability, biocompatibility, antibacterial activity, non-toxicity, and versatile chemical and physical properties [1]. The applications of chitosan covers a variety of fields, such as pharmaceutical and medical applications, paper production, textiles, waste water treatment, biotechnology, cosmetics, food processing, and agriculture [4-8]. **Figure 1.1** summarizes such advantages and applications.

In its chemical structure, chitosan is the N-deacetylated derivative of chitin, and most of its glucopyranose residues are 2-2-deoxy-b-D-glucopyranose. **Figure 1.2** lays out the chemical structures of chitin and chitosan. Generally, chitosan is produced through the deacetylation reaction of chitin using a concentrated sodium hydroxide solution of concentration of over 40% (w/v) [3].

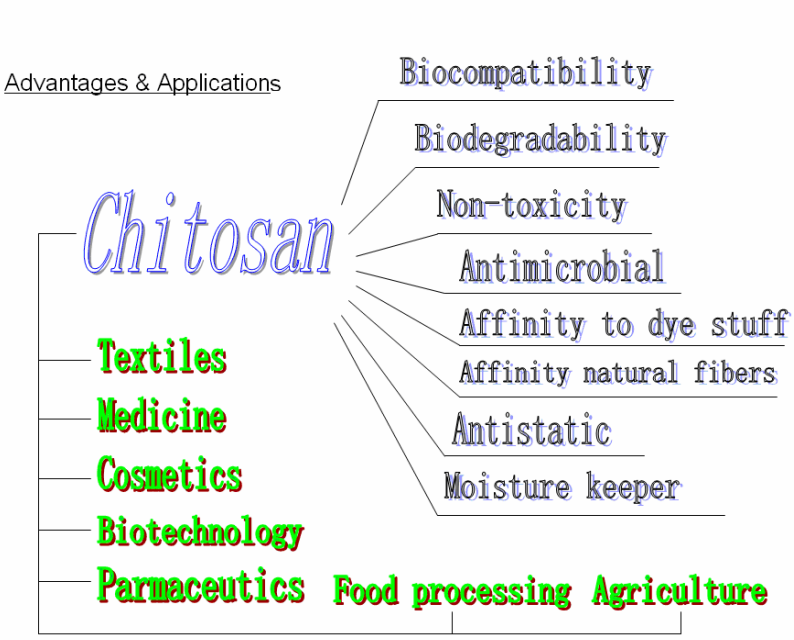

Figure 1.1 Advantages and applications of chitosan

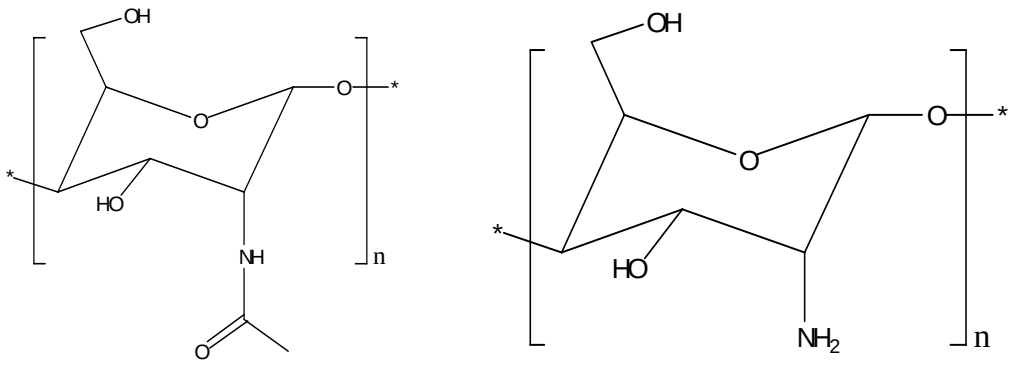

Figure 1.2 Chemical structures of chitin and chitosan

1.1.1 Physical and chemical characters of chitosan

Generally speaking, commercial chitosan with lower degree of deacylation (DD) is a white fragment of a loose macrostructure. Fine chitosan for food or medical is

white powder with DD of over 80 %. The production process is illustrated in **Figure 1.3**. Among these physical and chemical properties of chitosan, its solubility and chemical activities are of most concerns because they are the main factors affecting its various applications.

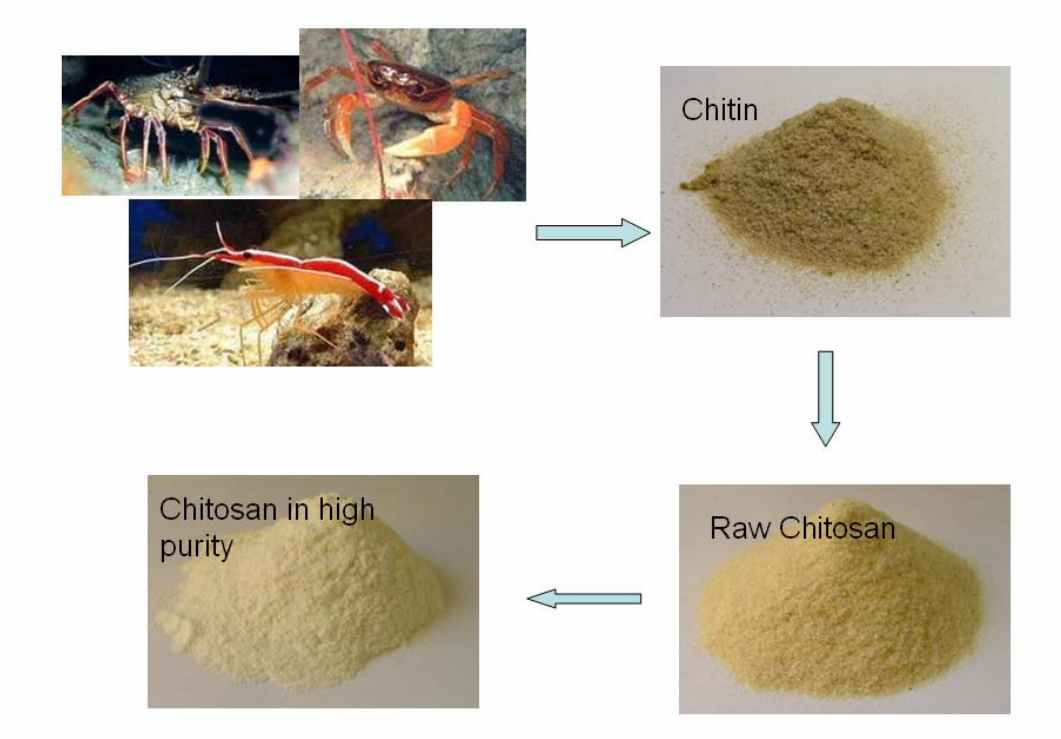

Figure 1.3 Illustration of chitosan production

Both chitin and chitosan are insoluble in water at pH 7. Although many solvents have been developed, most of them are not applicable due to their toxic, corrosive, or mutagenic properties. Chitosan are more tractable than chitin because it readily dissolves in dilute mineral or organic acids due to the protonation of free amino groups at low pH.

Meanwhile, chitosan is also more chemically active than chitin. Chitosan has three reactive groups. They are the primary and secondary hydroxyl groups on each repeat unit, and the amino group on each deacetylated unit, as shown in **Figure 1.4**. These reactive groups are readily subject to chemical modification to alter mechanical and physical properties of chitosan.

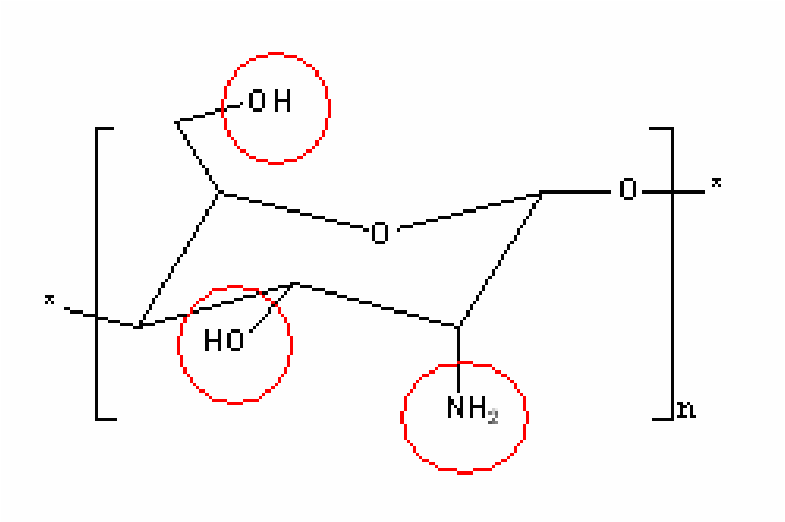

Figure 1.4 Reactive groups of chitosan

1.1.2 Antibacterial application of chitosan

The antibacterial property of chitosan is well known. This unique property, due to the polycationic nature of chitosan, enables its applications in various fields, including food science, agriculture, medicine, pharmaceutics, and textiles.

1.1.2.1 Mechanisms of the microbial inhibition by chitosan

Several different mechanisms for microbial inhibition by chitosan have been proposed, though its exact mechanism remains unknown. The most accepted one is the interaction of the positively charged chitosan with the negatively charged

residues on the cell surface of many fungi and bacteria, causing extensive cell surface alterations and altering cell permeability [48,50-52,57,60,71]. Consequently, it causes the leakage of intracellular substances, such as electrolytes, UV-absorbing materials, proteins, amino acids, glucose, and lactate dehydrogenase. As a result, chitosan inhibits the normal metabolism of microorganisms and finally leads to the death of these cells.

Another popular mechanism is that the positively charged chitosan interacts with cellular DNA of some fungi and bacteria, and thus inhibits the RNA and protein synthesis [54, 62]. In this mechanism, chitosan must be hydrolyzed to a lower molecule weight (MW) to penetrate the cell of microorganisms. However, this mechanism remains controversial.

1.1.2.2 Factors affecting the antibacterial activity of chitosan

The extent of the antibacterial property of chitosan is affected by factors both intrinsic and extrinsic, such as MW [62, 63], DD, pH value, temperature, etc. It is found that larger MW of chitosan promised more inhibited fungi, and the antibacterial activity increased as the polymer size increased. Monomer and dimer units do not show any antibacterial activity at the concentration of 1 mg/mL. Tests suggested that the MW of chitosan is critical for the inhibition of microorganisms, and MW higher than 10,000 is a preferred level for better antibacterial effects.

The antibacterial activity of chitosan is also under strongly influence by pH [48, 52, 54]. Previous work disclosed that the greatest activity was observed at pH 5.0 against E. coli; the activity decreased with the increasing of the pH value and chitosan has little antibacterial activity at pH 9.0. Other researchers reported that chitosan had no antibacterial activity at pH 7.0 due to the deprotonation of amino groups and poor solubility in neutral water.

On the other hand, the increase of DD means more amino groups on chitosan, thus more protonated amino groups in an acidic condition and more interaction chances between chitosan and negatively charged cell walls of microorganisms. Thereby chitosan with higher DD was more antibacterial [54, 55, 60, 63]. Meanwhile, the antibacterial activity was found to be directly proportional to temperature [52].

1.1.2.3 Antibacterial performance of chitosan nanoparticles (CSNPs)

There are several methods for the preparation of CSNPs. The first is the ionotropic gelation method, basing on the reaction between the cationic amino groups of chitosan and additional anionic chemicals or cross-link agents, such as tripolyphosphate (TPP) and calcium salts, etc. The other is water-oil reversed-phase micro-emulsion method using organic solvents, emulsifiers, supernatants and cross-linking agents. In the reversed-phase micro-emulsion, chitosan solution is mixed with an organic solvent to form a water-in-oil

micro-emulsion, and then an aqueous solution of polyanion is added into the micro-emulsion under a high speed stirring. Nanoparticles are formed in the micro-droplet in the emulsion through the ionotropic gelation. In some cases, a cross-linking agent is used instead of polyanions. Chitosan is also coated onto the surface of polymer nanoparticles, such as PMMA, to form core-shell particles.

So far, the antibacterial activity of CSNPs was seldom reported. The unique character of nanoparticles for their small size and quantum size effect could make CSNPs exhibit superior activities. Some studies showed that CSNPs and copper-loaded CSNPs could inhibit the growth of microorganisms markedly and exhibited higher antibacterial activity than macro-chitosan itself or doxycycline.

1.1.2.4 Antibacterial application of chitosan in textile

Textiles especially those made from natural fibers provide an excellent environment for the growth of bacteria because of their large surfaces and moisture retainability. A number of chemicals were used to impart antibacterial activity to textiles [65]. Many of these chemicals, however, are toxic and not biodegradable. These facts facilitate chitosan as a new antibacterial agent for textiles.

A lot of research was done on the application of chitosan in textile for antibacterial purpose, and the studies were focused on the effects of DD, MW and

other characters of chitosan to the antibacterial activity in textile. It is found that the activity increased with the increase of DD and MW of chitosan, and the MW effect was more distinctive at low concentrations. The antibacterial activity also increased as the amount of chitosan applied increased, and reached its maximum value at a certain concentration of chitosan. Studies suggested that incorporation of chitosan with citric acid (CA) provided cotton fabric antibacterial activity as well as wrinkle resistance. The fabrics treated with CA/chitosan showed better mechanical and antibacterial properties than the fabric treated with CA alone.

However, it is suggested that the efficiencies of antibacterial activity of fabrics between different work could not be directly compared with each other because the result varied depending on different test parameters, such as the size of test fabrics, number of bacteria used for the test, test temperature, contact time between test organisms and fabrics, etc.

1.1.2 Chitosan application in dyeing of textile

Chitosan can easily adsorb anionic dyes, such as direct, acid and reactive dyes, by electrostatic attraction due to its cationic nature in an acidic condition. It is postulated that the affinity of chitosan to cotton would be by Van der Waals forces between them because of the similar structures of chitosan and cotton. Another possibility for the bonding of the chitosan to cellulose was a cross-link by the formation of Schiff base between reducing end (–CO–H) of cellulose and the

amino group of chitosan. Hydrogen bonds also play an important role. It is reported that chitosan pretreatment increased the exhaustion of direct dyes and enabled immature fibers to be dyed to the same depth of shade as mature fibers. The application of chitosan to cotton could reduce the uses of dyes and residual dyes in wastewaters due to the increased dye exhaustion. On the other hand, studies claimed that the use of chitosan could decrease the amount of salt required in the dyeing by direct and reactive dyes by about 50% to produce a comparable shade to that of the untreated fabric.

1.2 Project significance and values

The source of chitosan is chitin which is mainly from the shell of crustaceans. Although chitosan is highly valuable in many industries, its raw material to produce from is a waste in the food industry. Thus, the utilization of chitosan lands results in alleviating the solid waste problem by converting the otherwise dumped crustacean shell into an invaluable asset.

In recent years, chitosan has already been utilized in many fields. Much work was conducted to study its applications in textile. However, a lot of the work was limited in the chitosan solution. The low pH and relative high concentration of the chitosan resulted in the loss of the original properties of treated fabrics. It is also infeasible for the chitosan solution to achieve stable chitosan-based composites in light of controllable functions by proper chemo-physical modification. The

insolubility of some of the chitosan derivatives in water limits their applications to enable the treated textile of more capabilities besides those of pure chitosan.

Meanwhile, the value-added property of nano-treated textiles is increased. Nanotechnology provides a versatile tool to modify the properties of textile substrates. It also offers opportunities to use nano-scale chitosan for property enhancement because of the unusual nano-effects. The much higher surface area to volume ratio is the most important reason behind it.

The nano-scale chitosan cannot only overcome the scarcity of chitosan solutions, it also acts as a kind of excellent host. After incorporating other new functional groups to this host by chemical or physical methods, these new functional groups could be fixed onto the textiles due to the good affinity of chitosan to cellulose and protein. At the same time, the good dispersing property of nano-scale chitosan would give the textile a uniform property enhancement. Plenty of cross-link agents could be chosen for the chitosan to promote the durability.

On the other hand, the textile industry brings serious pollution to the environment in the process of the production. Pollution prevention is a key strategy in product design and manufacture. This trend can be evidenced from the latest development of large corporations in the line such as DuPont (biosynthesis of propanediol); Shell (fuel-cell); Cargill-Dow (polyl(actic acid) fibre), and Marks and Spencer

(machine-washable suits). Though chitosan is a biodegradable and no-toxic polymer, current methods for the preparation of chitosan nanoparticles, as mentioned above, are weak in respect with environment compatibility. The use of organic solvents and other chemical additives are not environment-friendly, when the remains of these chemicals are also toxic. The critical experimental conditions result in energy waste too. So it is significant to develop new green methods for the preparation of nano scale chitosan products that is suitable for the application in the textile and low cost.

Last but not least, nano-scale chitosan does also command desirable wonderful potential in the dyestuff remove from the waste effluent of the textile industrial since both macro- or micro-chitosan proved to have excellent sorption ability to various dyes.

The project significance and values are embodied in following aspects:

a. To develop new green methods and processes for the preparation of nano-scale chitosan, which are environment-friendly and suitable for low-cost industrial applications.

b. To study the new methods, in a including stabilizing, size controls, to expand these methods to the synthesis of chitosan nano-composites and complexes with

various controllable functions, especially the antibacterial application on textile.

c. To study the adsorption of chitosan nanoparticles towards the dye molecules, and disclose the potential applications of the nano scale chitosan in environment protection, especially in the textile industry.

d. To study the interaction between the nano-scale chitosan and textiles, especially cotton, silk and nylon, to modify these methods continuously to achieve a series of products of nano scale chitosan with various controllable functions, which meets the critical environment and health requirements.

1.3 Research methodology

Most research methodology and research progress is described in the following sections of this thesis separately. The required knowledge structure and contents are summarized in the literature review section. Research methodology and plan here focuses on the methods and techniques which were employed in the subsequent progress and research work.

1.4 Objectives of project

There was little work done on the application of chitosan nanoparticles in the textile. On the other hand, nano-scale materials exhibit perfect advances in many fields because of their unique properties, which lead us to believe that the chitosan

nanoparticles will also bring us considerable properties at its applications in textile.

The lack of research work on the applications of chitosan nanoparticles in the textile and our previous development in this area leave us much room to expand the significant project objectives when the achieved results show a brilliant future:

a. To develop new methods and process for the preparation of chitosan and chitosan-contained nanoparticles applicable in textile industry;

b. To study the experimental conditions and other aspects in imparting functional properties such as antibacterial properties, freshness, and better dyeability on different fabrics; and to optimize the treatment processes for a better durability.

1.5 Scope of research

1.5.1 Adsorption of dye molecules using chitosan nanoparticles

In this research, the CSNPs, prepared via the ionotropic gelation method basing on the reaction between the cationic amino groups of chitosan and tripolyphosphate (TPP), was used as an adsorbent to remove Acid Green 27 (AG27), an acid dye, from its aqueous solution. The dye concentration at equilibrium (Qe mg/g) was calculated using the weight of the nanoparticles in the mixed solution (Qes) and the weight of chitosan in the nanoparticles (Qep).

The experimental isotherm data were analyzed using the Langmuir equation for each chitosan sample; the Langmuir monolayer adsorption capacity (Q0) was calculated with Qes and Qep.

1.5.2 Preparation of pure CSNPs

In this research, a novel method was developed for the preparation of pure CSNPs through an ultrasound dispersing process without the assistance of other chemicals. Stable emulsion of pure CSNPs was achieved with average particle sizes from 200 nm to 500 nm determined by laser scan. The thermal character and zeta potential of the emulsion were studied through laser scan and differential scanning calorimeter (DSC), disclosing that the emulsion is positively charged and stabilized by hydrogen bonds between water and chitosan.

The changes of the characters of the emulsion with different treatment duration and ultrasound intensities, including changes of particle size, viscosity molecular weight (Mv), degree of deacetylation (DD) and crystallinities, were also investigated. The results indicated that these changes of the studied characters mainly happened in the early nonlinearly sonolysis, but the DD kept invariant. The nanoparticles were characterized through scanning electron microscopy (SEM) and transmission electron microscopy (TEM), uncovering the spherical profiles of the dried nanoparticles with sizes from 100 nm to 300 nm.

1.5.3 Antibacterial finishing of cotton fabrics

First, the emulsion of the pure CSNPs was applied to finish cotton fabrics for the antibacterial purpose. The relationship between the antibacterial activity and the usage of chitosan was investigated compared with the traditional chitosan solution of dilute acetic acid. The antibacterial activity of the finished cotton fabrics was found to be activated efficiently by using either the emulsion or the solution although the emulsion behaved better. The washing durability of the emulsion-finished cotton fabrics was also investigated.

Subsequently, the nanoparticles of chitosan/silver oxide composite were prepared using a mixture of $AgNO_3$ solution and chitosan solution of dilute acetic acid. The complex interactions between silver ions and chitosan during the preparation were also investigated through various instrumentation methods. The emulsion of the nanoparticles was charactized through laser scan, infrared ray spectroscopy (IR), ultraviolet-visible spectroscopy (UV-vis) and X-ray diffraction (XRD). The measurements of the nanoparticles using SEM and TEM disclosed the spherical profiles of these nanoparticles, which were about 100nm encapsulating silver oxide nanoparticles of 10-20nm. Cotton fabrics finished using this emulsion were marked with remarkable antibacterial activity against S. aureus and E. coli at pH 5 and 7 with litter color effect and good washing fastness.

1.5.4 Dyeability improvement of textiles

In this research, first silk fabric was finished with the emulsion of pure CSNPs to improve its dye affinity to acid dyes and reactive dyes. The dyeability of the finished silk was investigated with five different acid dyestuffs and five reactive dyestuffs. The K/S values of these dyed silk fabrics were studied to show the dyeability improvement through the finishing using the emulsion.

Also, the advantage of the emulsion comparing traditional chitosan solution was tested. The color fastness to washing and the dry rubbing fastness were studied too. Then further work, mainly focusing on investigation of the micro surface structures, including those of the emulsion-finished, the solution-finished and unfinished silk fabrics, were carried out using SEM technology. The dyeability of the emulsion-finished silk was remarkably increased when compared with that of the untreated silk and of the solution-treated silk due to a rough nano-structure formed by the CSNPs on their surface.

The emulsion was then applied to finish nylon fabrics. The dyeability of the finished nylon fabrics was studied through a traditional exhausting dyeing process with four of acid dyestuffs. The results proved improvements in the emulsion’s dyeability in the exhaustion dyeing process.

Chapter 2

Literature review

2.1 Introduction of chitosan

Chitosan is the deacetylated derivative of chitin. Chitin, the second most abundant polysaccharide found next to cellulose, the main component in the shells of crustaceans, such as shrimp, crab, and lobster [1], and also in exoskeletons of mollusks and insects and in the cell walls of some fungi [2-3]. Though chitosan is also found in some fungi at small quantity, it is mainly produced commercially through alkaline deacetylation of chitin [3]. Huge amounts of crab and shrimp shells are abondoned as wastes by seafood companies worldwide, leading to considerable scientific and technological interest in chitin and chitosan as an attempt to use these renewable wastes. Chitosan has become the preferred commercial form of these materials because it is more tractable to solution processes than chitin.

In the past, it was demonstrated by many researchers that chitosan had a great potential for a wide range of uses due to its biodegradability, biocompatibility, antibacterial activity, non-toxicity, and versatile chemical and physical properties [1-3]. The applications of chitosan include a variety of areas, such as pharmaceutical and medical applications, paper production, textiles, waste water treatment, biotechnology, cosmetics, food processing, and agriculture [4-8].

2.1.1 Chemical structure and preparation of chitosan

Chitin has the same backbone with cellulose except for its acetamide group

instead of a hydroxy group. As shown in **Figure 2.1,** chitosan is naturally presenting ß-1,4-linked linear polysaccharides, and most of its glucopyranose residues are 2,2-deoxy-b-D-glucopyranose. The DD is the proportion of glucosamine monomer residues in chitin, and has a striking effect on the solubility and solution properties of chitin. There are several methods for the measurement of DD, including infrared resonance spectroscopy[9-13], UV-vis spectroscopy [14], circular dichroism [15], proton nuclear magnetic resonance (^{1}HNMR) spectroscopy [16-17], ^{13}C solid-state NMR spectroscopy[18], gel permeation chromatography [14], and titration methods [12, 18-21].

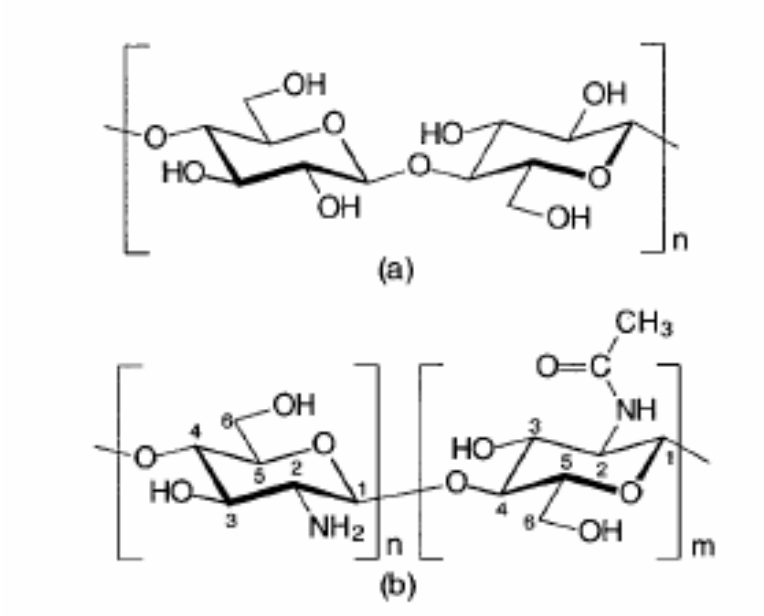

Figure 2.1 Chemical structures of cellulose (a) and chitosan (b)[1]

Generally speaking, chitosan is prepared through the deacetylation of chitin in a sodium hydroxide solution with a concentration of over 48 % (w/v). **Figure 2.2** illustrates the deacetylation reaction in which the amino acetyl group is changed

into the amino group. The deacetylation reaction happens quickly at the beginning and reaches equilibrium after certain duration with no more chitosan produced. So this requires altering the reaction solution with fresh sodium hydroxide solution after a certain time interval, such as one hour, to keep the reaction going for chitosan with higher DD. Great amounts of sodium hydroxide are costly in the deacetylation reaction; it leads to environmental pollution. Efforts to reduce to usage of sodium hydroxide were committed by many researchers. For instance, Wang et al. [22] treated swollen chitosan using a water/alcohol mixture with usage of sodium hydroxide three times to that of treated chitin. The author reported that chitosan with high DD was obtained using an amount of sodium hydroxide less than 10% (w/v).

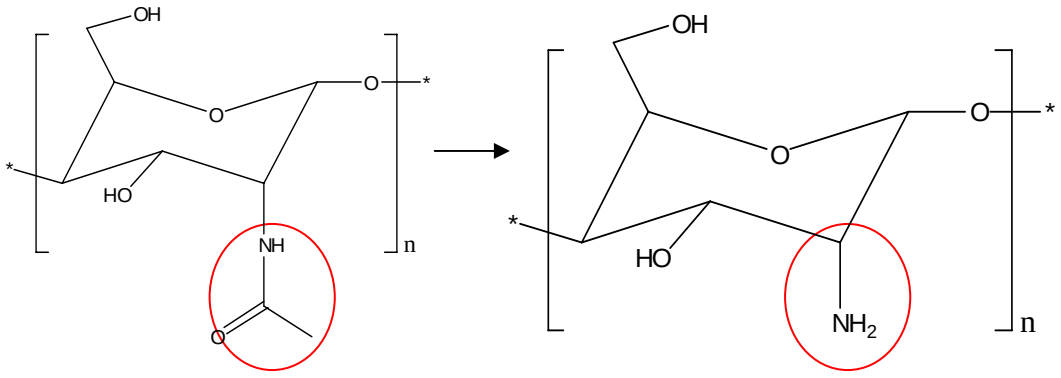

Figure 2.2 Deacetylation reaction of chitin

2.1.2 Physiochemical characters of chitosan

Commercial chitosan is a white fragment with a loose macrostructure. Fine chitosan in food or medicine grade is white powder with high DD of over 80% generally. Among these physical and chemical characters of chitosan, its solubility

and chemical activity are of most concern because they are the main factors impacting its various applications.

2.1.2.1 Solubility of chitosan

Neither chitin nor chitosan dissolves in neutral water. Chitin is a semi-crystalline polymer with extensive inter- and intra-molecular hydrogen bonds, making it difficult to dissolve in dilute acids or organic solvents under mild conditions. Although many solvents were found, most of them are useless due to their toxic, corrosive, or mutagenic properties. Chitosan is more tractable than chitin, and readily dissolves in dilute mineral or organic acids because of protonation of its free amino groups at low pH values. This cationic nature from the protonation is the basis of a number of applications of chitosan. Acetic and formic acids are most widely used for research and applications of chitosan while many solvents for chitin and chitosan can be found in the literature [23].

Generally speaking, the solubility of chitin and chitosan decreases with an increase of molecule weight (MW). Oligomers of chitin and chitosan with a degree of polymerization (DP) of 8 or less are water soluble regardless of the pH value [24]. Water-soluble chitin, however, can be prepared by either homogeneous deacetylation of chitin [25] or homogeneous N-acetylation of chitosan [26, 27]. I would emphasize that the water-soluble chitin is obtained by a homogeneous reaction instead of heterogeneous reaction. The former treatment gives a random

copolymer of N-acetyl-D-glucosamine and D-glucosamine units, whereas the latter produces a block copolymer of these two units. X-ray diffractometry revealed that the random copolymer was almost amorphous, but the block copolymer was highly crystalline, although the DD of the two polymers were the same. Kurita et al. [25, 27] concluded that the water solubility was attributed to the greatly enhanced hydrophilicity resulting from the random distribution of acetyl groups and the destruction of the tight crystalline structure of chitin.

2.1.2.2 Chemical properties

Chitosan has three reactive groups, including primary and secondary hydroxyl groups on each repeat unit, and the amino group on each deacetylated unit. These reactive groups are readily subject to chemical modification to alter mechanical and physical properties and solubility of chitosan.

The typical reactions involving the hydroxyl groups are etherification and esterification. Selective O-substitution can be achieved by protecting the amino group during the reaction. As N-protected chitosan derivatives, several Schiff bases [28-30] of chitosan and N-phthaloyl chitosan [31] were reported. The presence of a nucleophilic amino group allows selective N-substitution, such as N-alkylation and N-acylation by reacting chitosan with alkyl halides and acid chlorides, respectively. The alternative method for the N-alkylation is reductive alkylation, where the amino group is converted into amine with a variety of

aldehydes or ketones and subsequently reduced to N-alkylated derivative. Chitosan can also be modified by either cross-linking or graft copolymerization.

2.1.3 Preparation of CSNPs

2.1.3.1 Preparation of pure CSNPs

Many reports were published on the preparation of CSNPs. In summary, several methods are generally adopted. The first is ionotropic gelation method, based on the reaction between the cationic amino groups of chitosan and additional anionic chemicals or cross-linking agents such as TPP or calcium salts [32-36]. The other is the water-oil-reversed-phase micro-emulsion method, in which organic solvents, emulsifiers, supernatants and cross-linking agents are applied [35]. Using the reversed-phase micro-emulsion, a chitosan solution is mixed into an organic solvent to form a water-in-oil micro-emulsion. Then aqueous solution of polyanions is added into the micro-emulsion under a high speed stirring. Nanoparticles are formed in the micro-droplet in the emulsion through the ionotropic gelation. In some cases, cross-linking agents are used instead of polyanions.

For instance, Calvo et al. [32] prepared CSNPs by inducing the gelation of a chitosan solution with TPP, as **Figure 2.3** shows.

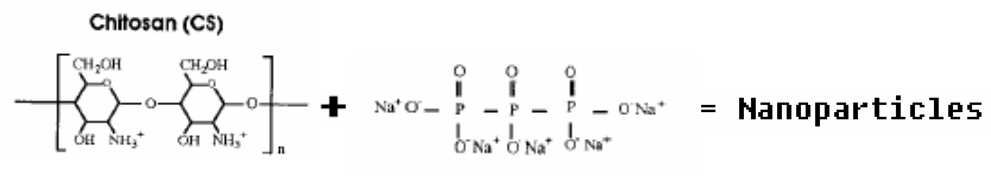

Figure 2.3 Preparation of CSNPs with TPP [32]

The researchers studied the relationship of nanoparticles with the concentrations of chitosan and TPP. At different concentrations, three different systems were identified: a clear solution, an opalescent suspension and an aggregate. The zone of the opalescent suspension, responding to a suspension of very small particles, is illustrated in **Figure 2.4**, the TEM photo of the CSNPs is also shown in **Figure 2.4**.

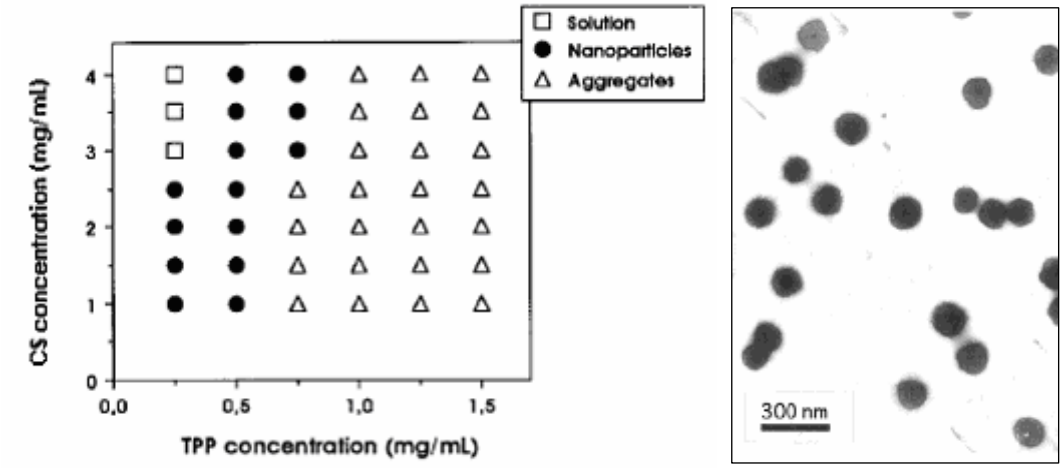

Figure 2.4 Zone of the nanoparticles (left) and their TEM microscopy (right) [32]

Tang et al. [36] also prepared CSNPs by inducing the gelation of a chitosan solution with TPP. Furthermore, they studied the effect of ultrasound to the particle size and DD of the prepared nanoparticles, and reported that changes of

particle size and polydispersity could have resulted from ultrasound-mediated depolymerization of chitosan chain while the DD and chemical characters of chitosan seemed unchanged.

Chang et al. [37] synthesized nano-scale chitosan/poly(acrylic acid)(PAA) particles by a dropping method based on the reaction between chitosan and PAA. The PAA solution was used as a base material into which the chitosan solution was dropped into. After incubation in the solution, the chitosan-PAA mixed solution was freeze-dried to obtain the nanoparticles. In this study, extremely fine chitosan-PAA particles with a size of 30 nm were synthesized successfully.

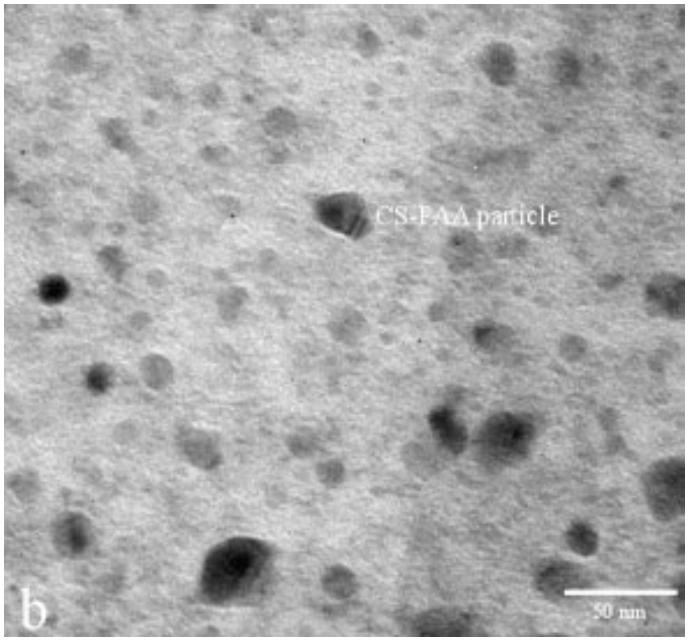

Figure 2.5 TEM micrograph of chitosan-PAA nanoparticles [37]

On the other hand, Banerjee et al. [38] described the preparation of cross-linked chitosan nanoparticles with a diameter size of less than 100nm using reverse micelles as the media. The process is shown in **Figure 2.6**. AOT (sodium

bis(2-ethylhexyl) sulfosuccinate) was used as a surfactant and glutaraldehyde was used as a cross-linking agent.

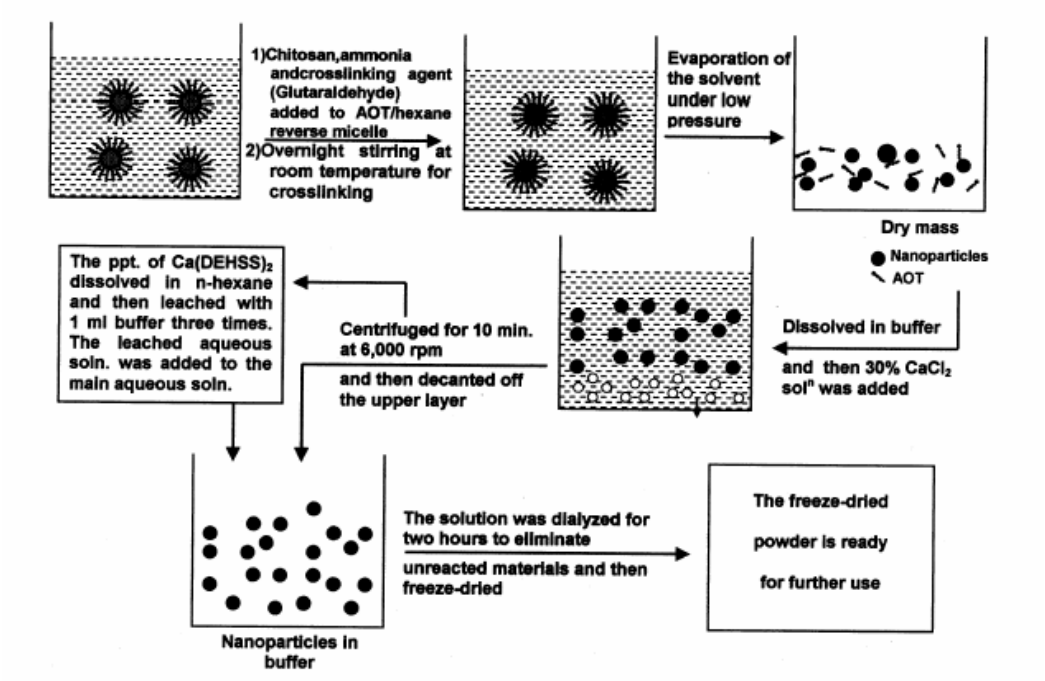

Figure 2.6 Flow chart of preparation of cross-linked CSNPs [38]

2.1.3.2 Core-shell nanoparticles using chitosan

Another widely used approach for nano-chitosan preparation is the core-shell nanoparticles in which chitosan generally plays the role of shell materials [39-44]. **Figure 2.7** illustrates an example of the nanoparticles [44].

For example, in the research of Ye et al. [39,41], chitosan-shelled nano-spheres with different core flexibilities were synthesized via a surfactant-free emulsion copolymerization in aqueous chitosan using cores of poly(n-butyl acrylate) (PBA)

and crosslinked poly(N-isopropylamide). Chen et al. also reported the preparation of chitosan/b-lactoglobulin core–shell nanoparticles for developing a biocompatible carrier for the oral administration of nutraceuticals [42]. Amiji et al. prepared alginate/chitosan core-shell micro-capsules with core formed by crosslinking sodium alginate with calcium or barium ions and shell of sodium tripolyphosphate (Na-TPP)-cross-linked chitosan membrane [43]. The aforesaid two kinds of core-shell nanoparticles were developed as a biocompatible carrier for medicines or enzymes. On the other hand, Cheng et al. also studied an one-step sequential method for preparing AgCl@polypyrrole/chitosan core-shell nanoparticles and subsequently prepared the formation of polypyrrole/chitosan hollow nano-spheres with a typical diameter of 50±5 nm [44]. The size of the core and thickness of shell could be controlled by adjusting the reaction parameters.

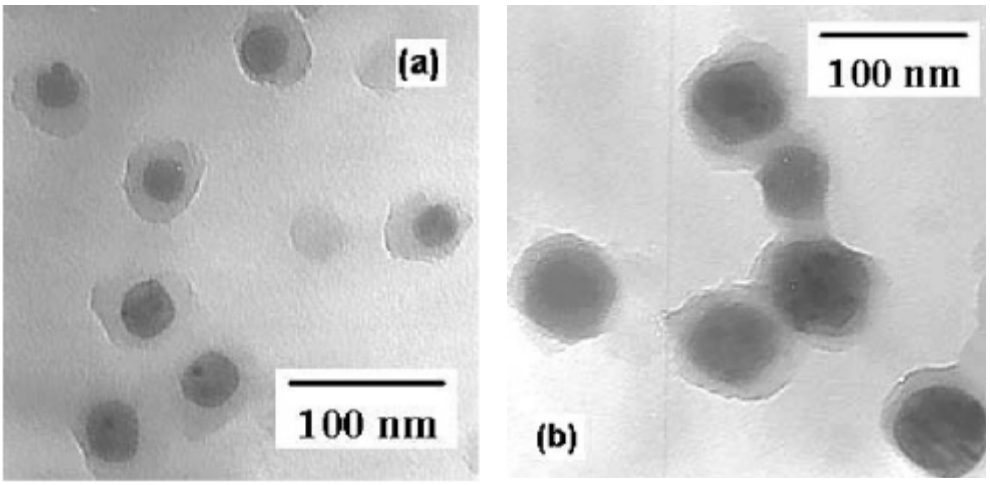

Figure 2.7 Core-shell chitosan nanoparticles [44]

2.1.3.3 Overview of the preparation of chitosan-based nanoparticles

In conclusion, all of these widely used methods were based on certain chemical reactions, such as gelation and polymerization, assisted by other chemical additives. With TPP, it is difficult to determine the particle content in the achieved emulsion and avoid the effect of dissolved chitosan as only part of chitosan in the original solution forms nanoparticles. In the water-in-oil method, emulsion-droplet method and core-shell system, these additional chemicals are difficult to remove from the system, and can cause negative effects to the applications. On the other hand, the damage of organic solvents to protein causes limited applications in the biochemical field. A number of spray drying processes were developed [45]. However, these preparation procedures are usually complex, which limit their applications.

2.2 Application of chitosan in antibacterial finishing

There is a growing demand for antibacterial finishes on textile goods because consumers are becoming more aware of the potential advantages of these materials. Clothing or fabrics with efficient antibacterial activity could be very helpful to avoid bacterial infection in some emergent environments, for instance, self-protection during the SARS outbreak, or wound protection in wars and battles. A number of chemicals are applied in textile processes for this purpose. Many of these chemicals, however, are also toxic and do not easily degrade. The industry continues its effort in seeking for eco-friendly processes that can either substitute

for toxic textile chemicals or reduce dyes in dyehouse wastewater.

The antibacterial activity of chitosan against various bacteria and fungi is well known, as reported by many researchers [46-54]. Its unique property, due to the polycationic nature, facilitated its applications in a variety of fields, including food science, agriculture, medicine, and pharmaceutics. These facts have facilitated the use of chitosan as a new textile chemical.

2.2.1 Mechanism of antibacterial activity of chitosan

Several mechanisms for microbial inhibition by chitosan have been proposed, but the exact mechanism remains uncertain. The most accepted one is the interaction of the positively charged chitosan with the negatively charged residues at the cell surface of many fungi and bacteria. The interaction causes extensive cell surface alterations and alters cell permeability [48,50-52,56,60,72], leading to the leakage of intracellular substances, such as electrolytes, UV-absorbing material, proteins, amino acids, glucose, and lactate dehydrogenase. Consequently, chitosan inhibits the normal metabolism of microorganisms, finally kills the cell.

For example, Fang et al. [50] reported that the growth of Aspergillus niger was inhibited by chitosan. Chitosan at the concentration of 5.0 mg/ml induced considerable leakage of UV-absorbing and proteinaceous materials from A. niger at pH 4.8. In contrast, chitosan at pH 7.6 and chitin at pH 4.8 did not induce the

leakage, which suggested that the antifungal activity of chitosan is related to the polycationic nature of chitosan, and is directly affected by the pH value. The leakage of nucleic acid and protein from Escherichia coli was observed by Hwang et al. [51] in their study on the bactericidal activity of chitosan on E. coli. TEM microscopy revealed that the outer cell wall of E. coli was greatly distorted and frayed, and the cytoplasmic membrane was detached from the inner part of the cell wall after chitosan treatment. Tsai and Su [52] observed the chitosan-induced leakage of glucose and lactate dehydrogenase from E. coli cells, and suggested that the death of cells resulted from the interaction between chitosan and the E. coli cell, changing in membrane permeability and causing the leakage of intracellular components, such as glucose and lactate dehydrogenase. Young et al. [60, 61] suggested that chitosan induces the leakage of electrolytes, protein, and UV-absorbing material from Glycine max and Phaseolus vulgaris cells. Severe damage to the G. max cell membrane by chitosan was indicated by reduced staining with fluorescein diacetate and the leakage of fluorescein from preloaded cells [60].

Another mechanism is that the positively charged chitosan interacts with cellular DNA of some fungi and bacteria, which consequently inhibits the RNA and protein synthesis [54, 62]. In this mechanism, chitosan must be hydrolyzed to a lower MW to penetrate into the cell of microorganisms. However, this mechanism remains controversial.

2.2.2 Factors impacting the antibacterial activity

The extent of the antibacterial action of chitosan is influenced by intrinsic and extrinsic factors, such as MW, DD, pH, temperature, etc.

2.2.2.1 Effect of MW

Tanigawa et al. [60] reported that D-glucosamine hydrochloride (salt of chitosan monomer) did not show any growth inhibition against several bacteria. This result suggested that the antibacterial activity of chitosan relates to not only its cationic nature but also its chain length. Hirano et al. [46] examined the relationship between the degree of polymerization (DP) of chitosan and the growth inhibition of several phytopathogens. It was observed that the increase in MW of chitosan increased the number of inhibited fungi.

Kendra et al. [62] examined the antifungal effect of chitosan oligomers on Fusarium solani f. sp. pisi and Fusarium solani f. sp. phaseoli. In the assessment of the minimum concentration (mg/ml) at which no fungal growth was detected, the antifungal activity was found to increase as the polymer size increased. Monomer and dimer units did not show any antifungal activity at the concentration of 1000 mg/mL.

Yalpani et al. [63] also suggested that the antibacterial activity was heavily dependent on the MW of chitosan. Several oral bacteria were treated with the same concentration of chitosan with four different MW (DD 0.99) from squid

chitin in 1% lactate buffer (pH 5.8) for 1 min, and incubated at 37 ^{o}C for 24 hours. It was found that the chitosan with MW 220,000 was most effective and MW 10,000 was the least effective in their bactericidal activities. The antibacterial activities of chitosan with MW of 70,000 were better than MW 426,000 for some bacteria, but for the others, the effectiveness was reversed. These findings suggested that the antibacterial activity of chitosan varies depending on the microorganisms targeted.

Many researchers reported the antibacterial activity of chitosan against E. coli. Jeon et al. [55] suggested that the MW of chitosan was critical for the inhibition of microorganisms, and the required MW higher than 10,000 for a better antibacterial activity. Although it is difficult to find a clear correlation between MW and antibacterial activity, generally the antibacterial activity increases as the MW of chitosan increases. However, the activity decreases over a certain high MW. The discrepancies between the reported data may result from the different DD and MD distributions of chitosan. The evaluation of only the MW dependence of the antibacterial activity requires a wide MW range of chitosan samples with the same DD and MW distributions. It is almost impossible to achieve this effect because chitosan is a natural polymer. There is always variation from batch to batch, and the properties of chitosan are very sensitive to DD and MWD. Therefore, from the existing data, it is difficult to determine what the most optimal MW for the maximal antibacterial activity is. The selection of MW of chitosan

could be regarded to be more dependent on its applications.

2.2.2.2 Effect of pH value

The antibacterial activity of chitosan is strongly affected by the pH value. Tsai et al. [52] examined the antibacterial activity of chitosan (DD 0.98) against E. coli. at different pH values of 5.0, 6.0, 7.0, 8.0,and 9.0. The greatest activity was observed at pH 5.0. The activity decreased as the pH increased, and chitosan had little antibacterial activity at pH 9.0. Other researchers [48, 54] reported that chitosan had no antibacterial activity at pH 7.0 due to the deprotonation of amino groups and poor solubility in water at pH 7.0. These findings suggest that the antibacterial activity of chitosan comes from the cationic nature of chitosan.

2.2.2.3 Effect of DD

The antibacterial activity of chitosan was directly proportional to the DD of chitosan [54-55, 60, 63]. The higher DD meant an increased number of amino groups on chitosan, consequently increased the number of protonated amino groups of chitosan in an acidic condition, and led to higher antibacterial activity.

2.2.2.4 Effect of temperature

Tsai et al. [52] examined the effect of temperature on the antibacterial activity of chitosan against E. coli. The cell suspensions in phosphate buffer (pH 6.0) containing 150 ppm chitosan were incubated at 4, 15, 25, and 37 ^{o}C for various

time intervals, and the surviving cells were counted. The antibacterial activity was found to be directly proportional to the temperature. At temperatures of 25 ^{o}C and 37 ^{o}C, the E. coli cells were completely killed within 5 hours and 1 hour respectively. But at lower temperatures of 4 ^{o}C and 15 ^{o}C, the number of E. coli declined within the first 5 hours and then stabilized. The authors concluded that the reduced antibacterial activity resulted from the decreased rate of interaction between chitosan and cells at a lower temperature.

2.2.3 Antibacterial activity of CSNPs

The antibacterial activity of CSNPs was seldom reported. The unique characters of nanoparticles for their small size and quantum size effect supposedly promised CSNPs to exhibit superior antibacterial activity. Qi et al. [64] prepared CSNPs and copper-loaded CSNPs based on the ionic gelation of chitosan with TPP, and studied their antibacterial activity against E. coli and S. aureus. Their result showed that CSNPs and copper-loaded CSNPs could inhibit the growth of microorganisms remarkably and exhibited higher antibacterial activity than macro chitosan itself or doxycycline.

2.2.4 Applications of chitosan in textile for antibacterial function

Textiles especially those made from natural fibers provide an excellent environment for bacteria to grow because of their large surface area and ability to retain moisture. In recent years, demand has increased greatly for textile products

with antibacterial properties. A number of chemicals were applied to impart antibacterial activity to textiles, including inorganic salts, organometallics, iodophors, phenols and thiophenols, onium salts, antibiotics, etc [65]. Many of these chemicals, however, are toxic and slow to degrade. These facts prompted the use of chitosan as a new antibacterial agent for textiles.

2.2.4.1 Evaluating the antibacterial activity of finished textile

The most commonly used quantitative methods for testing the antibacterial activity of textiles are the Shake Flask method developed by Dow Corning Corporation and the AATCC TM 100. In the Shake Flask method, fabric swatches are shaken in a suspension of test organisms for a desired contact time. The suspension, both before and after contact, is serially diluted and cultured to determine the number of surviving bacteria. For the AATCC TM 100, a suspension of test organisms is inoculated to the test fabrics and incubated over the desired contact period. The fabrics are serially diluted and the number of surviving bacteria is counted. The antibacterial activities, in both methods, are reported in terms of percent reduction of bacteria calculated by comparing the numbers of surviving bacteria before and after contact. The most frequently used test organisms are S. aureus (gram-positive) and E. coli (gram-negative) which are both commonly found in the human body [65].

2.2.4.2 Research developments

Yoo et al. [67] reported the effect of the DD of chitosan on the antibacterial activity of chitosan-treated cotton fabrics. Cotton fabrics were treated using chitosan solution of 2 % (w/v) acetic acid through a pad-dry (100 ^{o}C for 5 min)-cure (150 ^{o}C for 3 min) method. As evaluated by the Shake Flask method, the antibacterial activity of the treated fabrics against S. aureus. was found to increase with the increase in DD of chitosan. The antibacterial activity also increased as the amount of chitosan applied increased and reached its maximum value (%reduction: approximately 40% with DD 0.65, approximately 90% reduction with DD 0.78,and 100% reduction with DD 0.84 and 0.95) at the chitosan concentration of 0.5% (w/v), and no obvious change was observed at higher concentrations.

Shin et al. [67] examined the MW effect on the antibacterial activity of chitosan-treated cotton fabrics. The antibacterial activity of treated fabrics was found to rise along with the increase in the MW of chitosan, and the MW effect was more distinctive at low concentrations of chitosan. At a higher treatment concentration of chitosan (1.0% w/v), all chitosan showed above 90% reduction against E. coli, Proteus Vulgaris, and S. aureus, but they were less effective against Klebsiella pneumoniae and Pseudomonas aeruginosa.

The evaluation of the chitosan-treated fabrics indicated that the increase of MW

and treatment concentrations of chitosan led to increase in add-on (%), stiffness, moisture regain, and a slight decrease in tensile strength. Shin's research group [68] also examined the application of chitosan oligomers to PP nonwoven fabrics by a pad–dry method for diaper. The chitosan-treated PP nonwoven showed over 90% reduction of bacteria against S. aureus, E. coli, and P. vulgaris at 0.01–0.05% w/v of the chitosan oligomer. The chitosan oligomer was most effective against P. vulgaris, which caused diaper rashes. The addition of a nonionic wetting agent (Triton X-100) in the finishing bath caused a decrease in the antibacterial activity of the fabric. For example, the percent reduction of S. aureus was reduced from 100% to approximately 45% at chitosan concentration of 0.1% w/v by the addition of the non-ionic wetting agent (0.1% w/v). They concluded that the interactions between the protonated amino groups of chitosan and the weak anionic ethylene oxide groups in the wetting agent reduced the function of the amino groups of chitosan, which related to its antibacterial activity. It was reported that the chitosan-treated PP non-woven showed higher add-on, stiffer handle, higher absorbency, and lower air permeability as the MW and concentration of chitosan increased [69].

Chung et al. [70] suggested that incorporation of chitosan with citric acid (CA) provided cotton fabric antibacterial activity as well as wrinkle resistance. The chitosan (MW 2700, DD 0.90) dissolved in an aqueous solution of CA (3,5,7,and 10% w/v) containing a catalyst (sodium hypophosphite) was applied to cotton

fabrics by a pad-dry-cure method. The authors expected cross-linking of chitosan with cellulose by esterification reactions not only between cellulose and CA but also between CA and the hydroxyl groups of chitosan. Another possible interaction was the ionic interaction between the free carboxylate groups of CA and the protonated amino groups of chitosan. The fabric treated with CA/chitosan showed better mechanical properties (tensile and tear strength retention) than the fabric treated with CA alone. The cotton treated with 7% w/v CA and 0.8% w/v chitosan showed almost 100% reduction of S. aureus (by the Shake Flask method), and the antibacterial activity remained over 80% reduction of bacteria after 20 laundering cycles. Also a satisfactory wrinkle resistance was retained. The authors concluded that chitosan and CA were firmly linked to the cotton. However, it is questionable if the antibacterial activity of the fabric after 20 launderings came from chitosan or CA, because the authors observed 100% reduction of bacteria from the fabric treated with CA alone before the launderings.

However, it is suggested that the efficiencies of antibacterial activity of fabrics in different published works could not be directly contrasted to each other because the result varies due to different test parameters, such as the size of test fabrics, number of bacteria used for the test, test temperature, contact time between test organisms and fabrics, etc.

2.4.2.3 Application of nano-chitosan in textile antibacterial finishing

Little work was conducted about the application of CSNPs in the antibacterial finishing of textile. Li et al. [39] applied their chitosan-based core-shell particles to finish cotton fabric by a pad-dry-cure method. It is reported that the antibacterial tests revealed an excellent and durable fabric antibacterial activity with a 99% bacterial reduction after the treatment and over a 90% reduction after 50 times of laundering cycles. At the same time, better properties, such as better handle and better air permeability, were also obtained with a slight reduction in the fabric tensile strength.

But to our knowledge, the antibacterial activity of fabrics finished using pure nano-chitosan is not reported. One possible reason is the limited preparation of chitosan nanoparticles. Using of pure nano-chitosan can overlap the synthesis of these polymer cores, avoiding possible pollution and saving cost. This situation leaves room for challenges among fellow researchers.

2.3 Applications of chitosan in dyeing of textile

The unique properties of chitosan, such as biodegradability, non-toxicity, antibacterial activity, and polycationic nature, make it suitable for many textile applications. The applications of chitosan in textiles can be categorized into two main topics: the production of man-made fibers and textile wet processing, which include dyeing and finishing. Chitosan may be considered as a multifunctional

finish, and those chemical attributes that contribute to the antibacterial properties also contribute to other functional utilizations of chitosan.

Chitosan absorbs anionic dyes easily, such as direct, acid and reactive dyes, by electrostatic attraction due to its cationic nature in an acidic condition. In the manufacture and dyeing of cotton fabrics, immature cotton causes dyeing problems. Thus the cotton does not absorb dye evenly and creates small lightly colored or white spots are resulted. This is the result of the small groups of immature cotton fibers known as neps. Rippon [71] evaluated the applications of chitosan to improve the dyeability of immature cotton fibers. The chitosan, which was dissolved in dilute acetic acid, was applied to cotton fabric by three different methods: pad-batch-rinse, pad-dry-rinse and exhaustion-rinse. The author postulated that the affinity of chitosan to cotton would be by van der Waals forces because of the similar structures of chitosan and cotton. Another possibility mentioned for binding the chitosan to cellulose was cross-linking by formation of Schiff base between cellulose's reducing end (–CO–H) and the amino group of chitosan. In addition to the two possible binding forces suggested by the authors, hydrogen bonds also played an important role. It was reported that a chitosan pretreatment increased the exhaustion of direct dyes and enabled immature fibers to be dyed to the same depth of shade as mature fibers. When the chitosan-treated fabrics were after-treated with a quaternary ammonium compound after dyeing, its fastnesses were comparable to those of untreated cotton.

Canal et al. [72] evaluated the dye exhaustion of chitosan-treated cotton fabrics compared the result with the untreated. The most uniform distribution of chitosan on the fabric was obtained by the pad method. The treated fabric was dyed with a direct dye, and it was subject to consecutive washes for the evaluation of durability of chitosan on the fabric. It was found that the first washing led to the largest color loss of the dyed fabric, and the color loss was stabilized after 15 washes. At this stage, the fabric kept 35% higher K/S (color strength) values than those of the untreated fabrics. The authors suggested that the applications of chitosan to cotton could reduce the use of dyes and dyes in wastewaters due to the increased dye exhaustion. The washing and wet rubbing fastnesses of chitosan-treated fabric were reduced by about one point, and the dry rubbing fastness was not affected.

Direct and reactive dyes are widely used for the dyeing of cotton fabrics because of their complete color ranges and easy applications, when these anionic dyes have a low affinity to the cotton fiber because cotton fibers develop anionic surface charges (zeta potential) in water. The charge repulsion between dyes and cotton can be overcome by adding an electrolyte, such as sodium chloride or sodium sulfate, which screens the surface charge of cotton. However, the large amount of salts required in dyeing can cause serious pollution. As an attempt to reduce salt usage, a number of researchers cationized cotton fibers through chemical modifications with chemicals containing cationic groups. Most of the

chemicals used for the cationization of cotton are not environmentally safe. Therefore, the use of chitosan, a polycationic biopolymer, is more eco-friendly. Bondyopadhyay et al. [67] applied chitosan as a substitute for synthetic chemicals to cationize cotton fabrics. A chitosan solution (with 2% w/v aqueous acetic acid) was applied to cotton fabrics by the pad-dry method. The treated fabrics were then dyed with several reactive dyes. When the fabrics were treated with chitosan solutions of 1% and 2% (w/v), it was possible to decrease the amount of salt required by about 50% to produce a comparable shade to that of the untreated fabric.

The chitosan-treated fabric also showed an improvement in the fixation of reactive dyes. This result was explained by the increased exhaustion of negatively charged reactive dyes onto the cotton, whose negative potential on the fiber surface was suppressed by the cationic chitosan treatment. Consequently, when an alkali was added to the dyebath, a substantial quantity of dye was available for the reaction with cotton. It was also suggested that the amino groups of chitosan reacted with the reactive group (vinylsulfone group) in the dye and the fixation was further improved. The chitosan-treated fabric showed comparable color fastness to that of the untreated fabric.

Chapter 3

Dye adsorption by the CSNPs in aqueous phase

3.1 Research background

In the textile industry, large quantities of aqueous wastes and dye effluents are discharged from the dyeing process with strong persistent color and high BOD loading which are aesthetically and environmentally unacceptable [73]. Most of these dye wastes are toxic and may be carcinogenic, and this poses a serious hazard to aquatic living organisms [74]. As a result, the removal of dyestuffs from effluents becomes important, and many governments have stipulated environmental restrictions with regard to the quality of colored effluents and have forced dye-using industries to decolorize their effluents before discharging. A number of conventional treatment technologies for dye removal were investigated extensively [75-81], such as the trickling filter, activated sludge, chemical coagulation, carbon adsorption, and photo-degradation processes. Among these chemical and physical methods, the adsorption process is fairly effective to produce a high-quality effluent without the formation of harmful substances, such as ozone and free radicals in the photo-degradation process using UV. Methods were developed using many adsorbents, such as peat [82-83], activated carbon [77], pith [84-88], fuller's earth [89-90], and wood [91-92].

Meanwhile, chitosan has extremely high affinity for many classes of dyes such as disperse, direct, reactive and acid dyes [93-100]. In an acidic aqueous medium, the cationized amino groups can adsorb anionic dye molecules by the electrostatic attraction. Yoshida et al. [98-100] studied the sorption of various dyes onto chitosan

fibers and reported its high potential for dye adsorption. Chiou et al. [101] also reported the adsorption of chemical cross-linked chitosan beads to Reactive Red 189 (C.I. 18210) at pH 3.0 and at 30 ^{o}C. However, the adsorption of nano-chitosan is scarcely reported. It is believed that the nano-chitosan should have a larger capacity because of the large surface area. Chang et al. [102] studied the sorption behavior of the carboxymethylated-chitosan-binded Fe_3O_4 nanoparticles to Acid Orange 12 (AO12) and Acid Green 25 (AG 25), and found that the adsorption capacities of AO12 (1883 mg/g) and AG25 (1471 mg/g) were very high due to the large surface area.

On the other hand, the ionotropic gelation is widely used to prepare chitosan nanoparticles. The reaction happens when the positively charged amino groups in chitosan interact with the negatively charged sodium tripolyphosphate (TPP) [32]. Different concentrations of chitosan and TPP will result in three different systems: a clear solution, opalescent suspension and aggregate. The emulsion system corresponds to a suspension of very small particles. Also, the particles size changes with the variety of the concentrations both chitosan and TPP in the emulsion. The more dilute the solutions, the smaller the particle size. Calvo et al. [32] obtained chitosan nanoparticles with the size of 260 nm (measured by a ZetasizerIII) at room temperature under magnetic stirring.

The aim of this research is to explore the potential of nano-chitosan in the dye

removal application. Chitosan nanoparticles were prepared using the gelation reaction between chitosan and TPP [32]. The adsorption ability of the nanoparticles was studied using anthraquinone type Acid Green 27 (AG 27) (**Figure 3.1**). The equilibrium sorption capacities of the dyes on chitosan were studied using the adsorption isotherm technique. The experimental data were then fitted in the Langmuir equation.

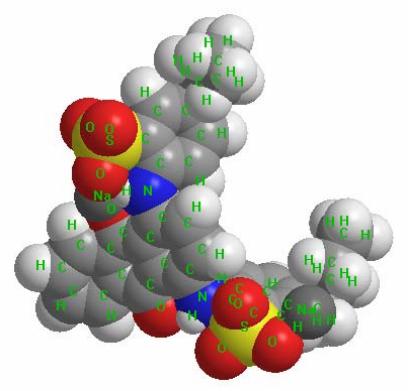

Figure 3.1 Molecule structure of Acid Green 27

3.2 Materials and experimental

3.2.1 Materials

Chitosan of 85% degree of deacylation (DD) and Acid Green 27(AG 27, purity ~65%) were purchased from Aldrich Chem. Co. Ltd.. Chitosan of 74% DD was prepared through the treatment of chitin (Sigma Chem. Co. Ltd.) with aqueous sodium hydroxide solution. Other chemicals were chemical grade and from Aldrich Chem. Co. Ltd. and used as received.

3.2.2 Preparation of CSNPs emulsion

The emulsion was prepared using the method reported before [32]. Typically, a TPP solution (95.4 mL, 1.45 mg/mL) was slowly dropped (10 mL/min) into a chitosan solution (150 mL, 2 mg/mL in 0.5% dilute acetic acid) in a 500 mL round-bottom flask under mechanical stirring (1200 rpm/min). After a further stirring of 20 min, a milky emulsion was obtained at pH of 5.0.

The solid nanoparticles were obtained through a freezing-thawing-centrifuging process. The emulsion was frozen at -4 ^{o}C, and then thawed in the atmosphere. The deposited nanoparticles were collected through centrifugation for one hour. They were subsequently washed with D.I. water and vacuum dried at 60 ^{o}C for 24 hours. Finally, the weight of the dried nanoparticles was measured and regarded as the solid content of the nanoparticles in the emulsion.

3.2.3 Dye adsorption

The emulsion (75 mL) was extracted into a sealable glass vessel with 50mL of AG27 solution of specified concentrations (from 0.4 mg/mL to 2.0 mg/mL), followed by a shaking process of 24 hours at 25 ^{o}C and at pH of 5.5. The mixed emulsion was then centrifuged (27200G, 4 ^{o}C for 60 min). The PPT and the filtrate were analyzed with a visible spectrometer. The dye concentration was calculated in the standard calibration curve obtained from standard AG27 solutions of known concentrations.

3.2.4 Characterization

A Zetasizer 3000HSA laser scanning instrument was used for the size analysis of the nanoparticles. A Grant OLS 200 shaker was used for the dye adsorption. A Beckman J2-21 centrifuge was used for the ultrahigh speed centrifugation. A Perkin-Elmer Lambda 18 was used to determine the UV-vis absorption of the dye. Scanning electron microscopy (SEM) analyses were performed through a JOEL JSM 6335F; samples were placed on the surface of pre-washed silicon wafer for the investigation. The viscosities of the chitosan solution and emulsion were measured using a Ubbelohde dilute solution capillary viscometer at 25 ± 0.1 ^{o}C (Schott Gerate 537 10/I).

3.3 Results and discussion

3.3.1 Preparation and characterization of the nanoparticles

3.3.1.1 Preparation of the nanoparticles

According to the experimental parameters described in the literatures [32], an 8.4 mL of 5mg/mL TPP solution was dropped into 97.6 mL 1.54 mg/mL chitosan solution of 2.70 mg/mL acetic acid under violent mechanical stirring. But no obvious opalescent suspension was obtained. Then an additional volume (0.2mL/per time) of 5mg/mL TPP solution was dropped into the reaction system. The reaction system became opalescent, and aggregates appeared finally. The result is shown in **Table 3.1**.

The effect of stirring speeds was also studied. Three emulsion systems were prepared at same concentrations under different stirring speeds of 300rpm, 750rpm and 1000rpm. Slight differences were observed within fresh emulsions. But after storage of one week, the 300rpm one had a lot of precipitates while the 750rpm one had litter precipitates and the 1000rpm one did not have any precipitates. The result showed that the higher stirring speed is important for the stability of the emulsion. On the other hand, there was a sharp decrease of the viscosities after the chitosan solution turned into the emulsion. As shown in **Figure 3.2,** the result indicated that the viscosity of the emulsion was similar to DI water and the flowtime was almost half of that of chitosan solution, implying that most chitosan molecules changed the state from a long chain dissolved state into a particulate aggregation after the ionotropic gelation reaction.

We also studied the size change of the nanoparticles at different volumes of the 5mg/mL TPP solution (9mL, 9.2mL, and 9.5mL). As shown in **Figure 3.3**, the result indicated that the particle size increased positively to the volume of the TPP solution. The polydisperisty also increased at the same time, implying a wider size distribution of the particles in the emulsion. The additional TPP led to the growth of the nanoparticles into a bigger size which finally precipitated due to the breakout of stabilization balance.

Table 3.1 Physical states after adding different volumes of the TPP solution

Volumes (mL)	8, 8.2	8.4, 8.6, 8.8, 9, 9.2, 9.4	9.6, 9.8, 10
State	clear solution	emulsion	aggregates

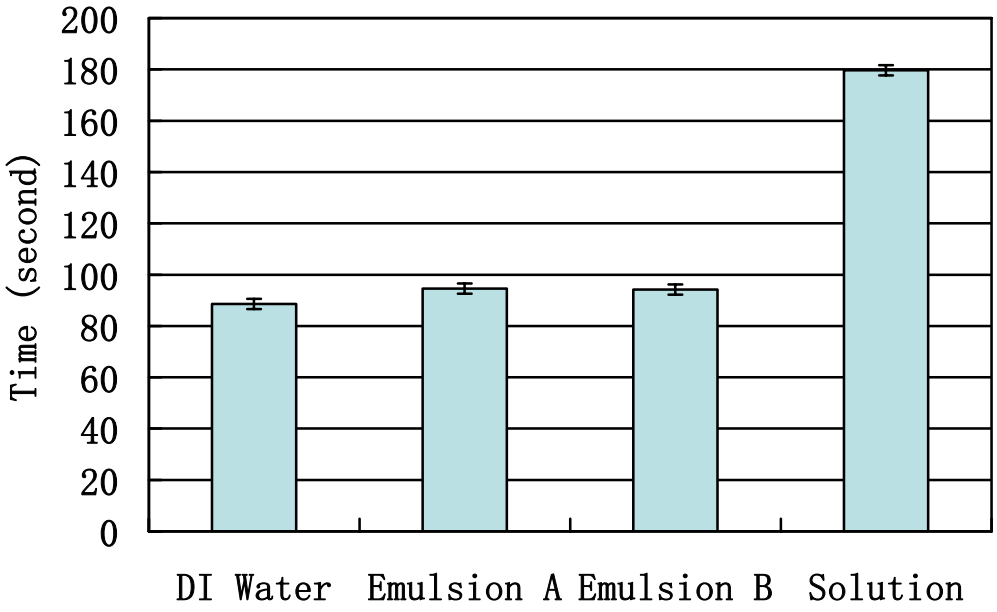

Emulsion A: stirred at 300 rpm Emulsion B: stirred at 750 rpm

Figure 3.2 The flow time of different systems

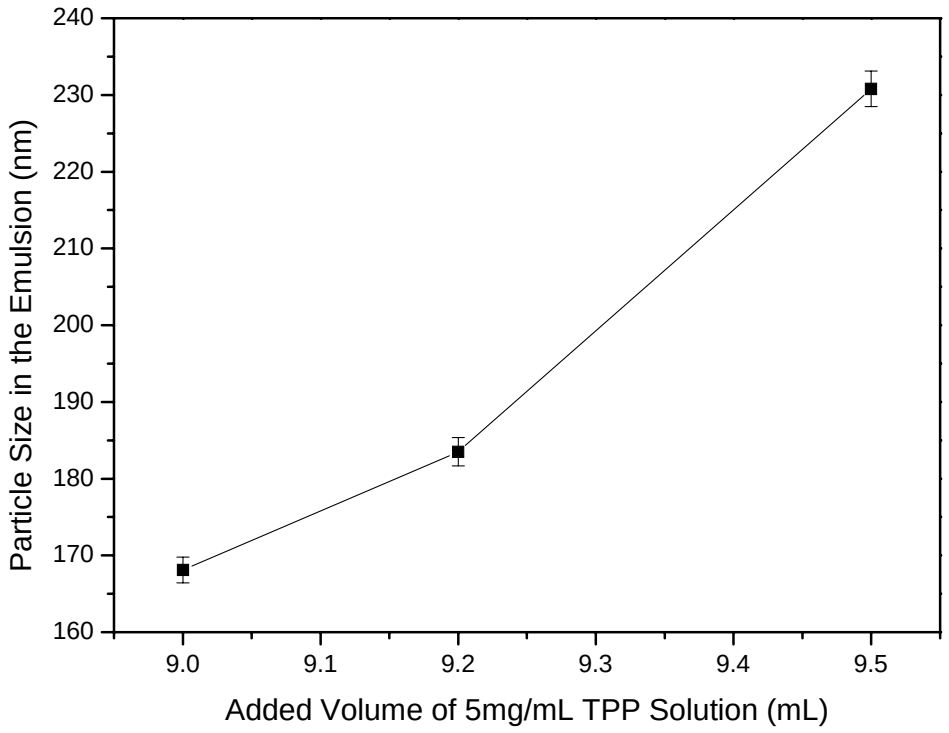

Figure 3.3 Particle sizes with adding different volume of TPP solution

3.3.1.2 Characterization of the nanoparticles

The nano-chitosan emulsion had an average size of around 180nm, which indicated that the particle size was narrow. **Figure 3.4** displays the narrow size contribution of the chitosan nanoparticles. Its zeta potential was +30mV. The positive charge of the chitosan nanoparticles suggested that the emulsions were stabilized by the hydrogen bonds between the amino groups and hydroxyl groups of chitosan and water molecules, in which water molecules acted as the provider of protons while the amino groups were the receiver [104-106]. **Figure 3.5 a** shows the spherical profile of the chitosan nanoparticles with sizes ranging from tens to hundreds nanometer. Actually, not all the chitosan molecules in the solution formed

nanoparticles. The supernatant after ultrahigh-speed centrifugation formed an opalescent emulsion again with a further additional TPP solution. Meanwhile, the attempt to turn all of the chitosan molecules into nanoparticles was difficult because the precipitates produced. The weight of the collected nanoparticles after centrifugation (1.2 mg/mL) was used as the weight of the nanoparticles in the emulsion (solid content) [107].

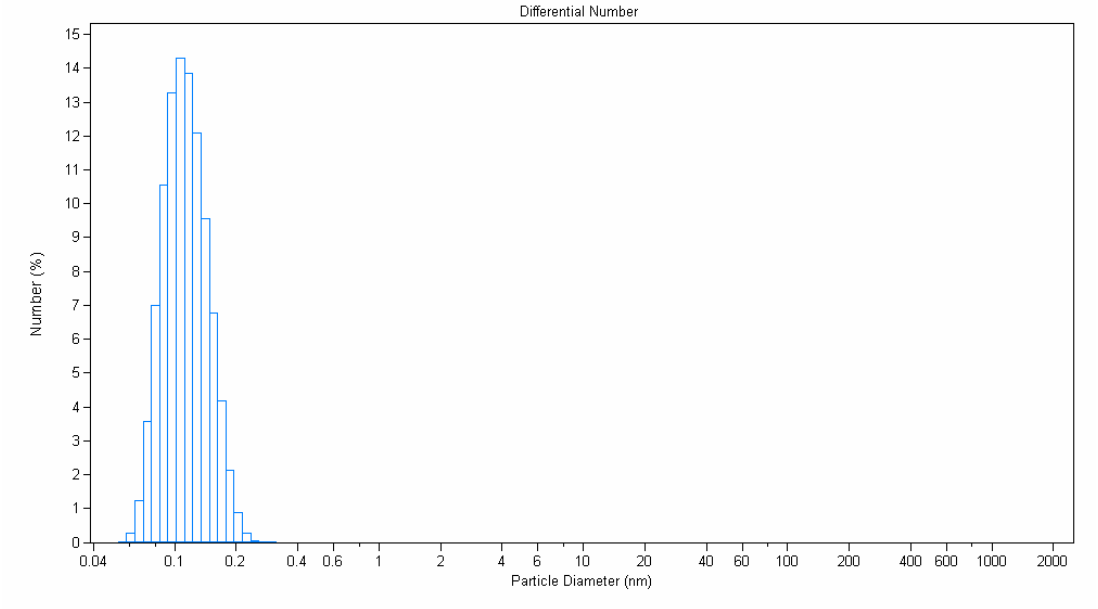

Figure 3.4 Laser scanning of chitosan nanoparticles

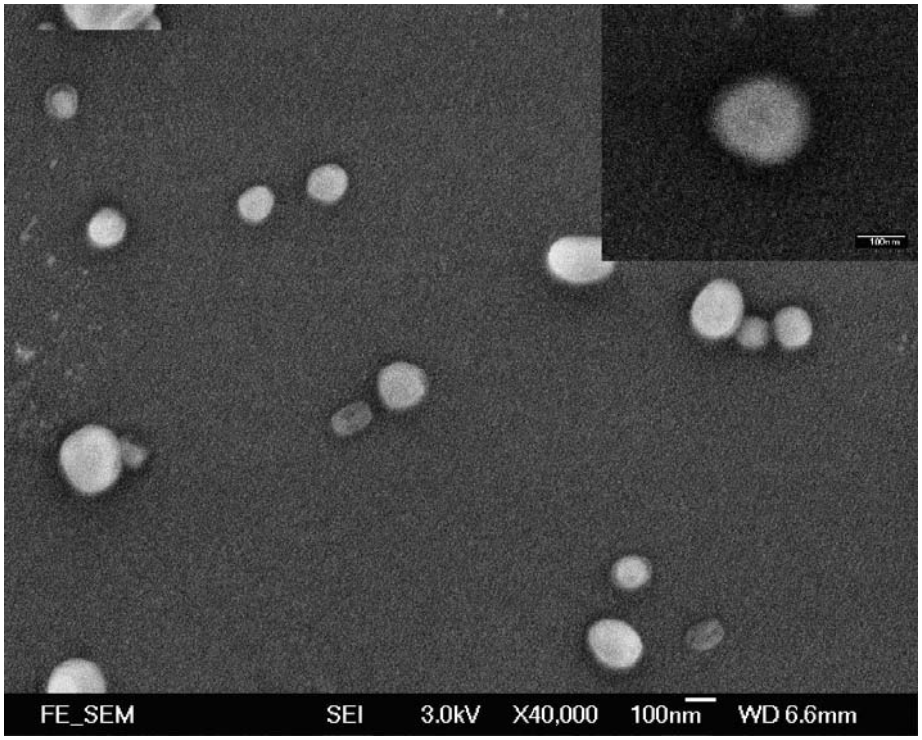

Figure 3.5 SEM micrographs of the chitosan nanoparticles

3.3.2 Results of the dye adsorption test

The nanoparticles quickly aggregated after interacting with the dye molecule and precipitates was formed. The possible mechanism of the adsorption process of chitosan and acid dye is electrostatic interactions between the anionic dye ions and the positive amino groups on the chitosan. In this study, anionic dye ions were believed to replace the hydrogen bonds between the chitosan nanoparticles and water with new electrostatic interactions, causing the aggregating of these nanoparticles, as illustrated in **Figure 3.6**. It was also observed that dilute sodium hydroxide solution could both de-adsorb the dye molecules and wash out TPP from the chitosan [101] while neutral water could not. On the other hand, no precipitate was observed in the mixture of a dye solution and a chitosan solution when TPP

was not present. The affinity between the nanoparticles and the chemicals used can be summarized: the order of attractive forces was TPP>H_3O^+>D-SO_3^->hydrogen bonds in acidic conditions; and OH^->TPP>D-SO_3^->H_2O in alkaline conditions.

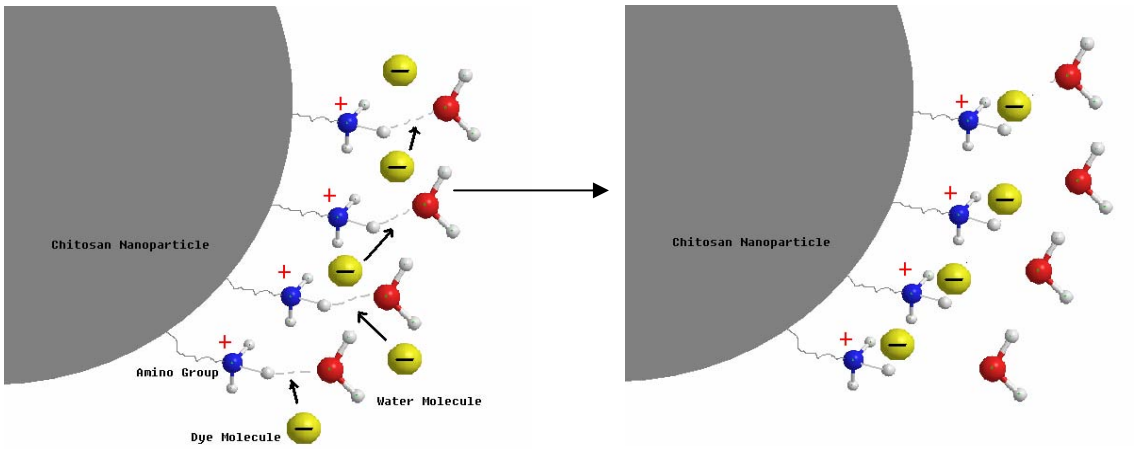

Figure 3.6 Possible adsorption process of acid green 27 onto the chitosan nanoparticles

Table 3.2 summarizes the adsorption results using 74% DD chitosan nanoparticles. The sorption was performed with eight concentrations of Acid Green 27. When the dye concentration was below 1.0 mg/mL, all the dyes were adsorbed by the chitosan. Because TPP has no contribution to the adsorption of dye, we calculated the solid-phase adsorbate concentration at equilibrium (Qe mg/g) with **Equations 1** and **2** using both the weight of nanoparticles in the emulsion (Qes) and the weight of chitosan in the nanoparticles (Qep) to investigate the adsorption ability of the nanoparticles and nano-scale chitosan in the nanoparticles. The weight of chitosan in the nanoparticles was calculated by reducing the weight of the nanoparticles with weight of TPP according to the original TPP concentration, which was 0.6mg/mL.

$$Qes = \frac{weight\ of\ adsorbed\ dye}{weight\ of\ nanparticles} = \frac{(Co - Ce) \times V_{the\ mixed\ solution}}{1.2 \times Vm} \text{ mg/g} \quad (1)$$

$$Qep = \frac{weight\ of\ adsorbed\ dye}{weight\ of\ chitosan\ in\ the\ nanoparticles} = \frac{(Co - Ce) \times V_{the\ mixed\ solution}}{0.6 \times Vm} \text{ mg/g} \quad (2)$$

whereas

Co is the original dye concentration in the mixing solution,

Ce is the dye concentration in the solution after centrifugation,

Vm is the used volume of the emulsion in sorption test.

Both Qes and Qep increased nonlinearly with the increase of Co and then reached a maximum. Equations 1 and 2 gave Qes and Qep with a big difference because TPP cannot be effectively in precipitating all the nanoparticles. Several comparing experiments were then performed, in which an extra TPP solution was added into the dye containing the mixed solution after shaking to deposit all chitosan, followed by centrifugation. The adsorption results are given in A2 to D2 of **Table 3.2,** which indicated no remarkable difference. It further proved that TPP had superior an attractive ability to chitosan in the acidic solution, and the dye molecules interacted primarily with the residual amino groups of chitosan after the gelation reaction.

Table 3.2 Adsorption results using 74% DD chitosan nanoparticles

Sample	Original dye concentration (Co), (mg/mL)	Final dye concentration (Ce), (mg/mL)	Qes (mg/g)	Qep (mg/g)
A	0.4	0.0000	555.6	1111.1
B	0.8	0.0000	1090.7	2222.2
C	1.0	0.0235 ± 0.0005	1331.3 ± 28.3	2712.5 ± 57.7
E	1.2	0.0588 ± 0.0009	1555.8 ± 23.8	3170.0 ± 48.5
F	1.4	0.2517 ± 0.0031	1565.5 ± 19.3	3189.7 ± 39.3
G	1.5	0.3438 ± 0.0033	1576.3 ± 15.1	3211.6 ± 30.8
H	1.8	0.6384 ± 0.0055	1583.6 ± 13.6	3226.7 ± 31.0
I	2.0	0.8354 ± 0.0072	1587.7 ± 13.7	3235.0 ± 27.9
A2	0.4	0	545.3	3333.3
B2	0.8	0	1090.7	6666. 7
C2	1.0	0.0227±0.0004	1332.4±23.5	2714.7±47.8
D2	2.0	0.8298±0.0069	1595.4±13.3	3250.6±27.1

3.3.3 Langmuir equilibrium isotherms

Adsorption isotherms are critical in optimizing the use of adsorbents because they describe how adsorbates interact with adsorbents. The correlation of equilibrium data, either by theoretical or empirical equations, is essential to the practical design and operation of adsorption systems. Research work by Wong et al. indicated that the Langmuir equation provided the best prediction for the adsorption of AG 25 in the entire concentration range [108], so it was adopted in this study because AG27 has a similar molecular structure to AG 25.

The Langmuir's theory describes the adsorption of gas molecules onto metal surfaces [109], when it can be successfully applied to other real sorption processes of monolayer adsorption. The Langmuir equation is based on the assumption of a structurally homogeneous adsorbent where all sorption sites were identical and energetically equivalent. Theoretically, the adsorbent has a finite capacity for the adsorbate. Therefore, a saturation value is reached beyond which no further sorption can take place. The saturated or monolayer capacity can be represented by the expression

$$Qe = \frac{K_L Ce}{1 + a_L Ce} \quad (\text{as } C_t \to \infty) \qquad (3)$$

whereas Qe is the solid-phase adsorbate concentration at equilibrium (mg/g),

Ce is the aqueous phase adsorbate concentration at equilibrium (mg/mL),

KL is the Langmuir isotherm constant (mL/g), and

aL is the Langmuir isotherm constant (mL/mg).

Therefore, plots of Ce/Qe versus Ce give a straight line of slope aL/KL and intercept 1/KL, where KL/aL gives the theoretical monolayer saturation capacity, Q_0. The adsorption data, Qes and Qep as summarized in **Table 3.2**, were analyzed with Equation 3. The linear plots of specific sorption Ce/Qe against the equilibrium concentration Ce are shown in **Figure 3.7**. The isotherms were found to be linear over the whole concentration range with high correlation coefficients which indicated that the dye-nano-chitosan sorption followed the Langmuir model.

Figure 3.8 summarizes the equilibrium capacities of AG 27 on 74% DD chitosan nanoparticles, showing that the monolayer saturation or maximum adsorption was reached. The Langmuir isotherm was found to provide a good prediction for the sorption in the study. As the dye purity was 65%, the Langmuir equilibrium monolayer capacities, Q_0, were 1033.4 mg/g and 2103.6 mg/g when derived from Qes and Qep using **Equations 1** and **2**. The two values had a big difference due to the large difference between Qes and Qep as discussed. The Q_0 of Acid Green 25 onto the chitosan (degree of deacetylation = 54%; particle sizes: 355-500 μm) was 645.1mg/g [108]. The nano-chitosan had a significantly higher capacity for the acid dye than that of the powdered chitosan (160% or 326% separately). Further work on the relationship between the surface area and the sorption capacity is being undertaken.

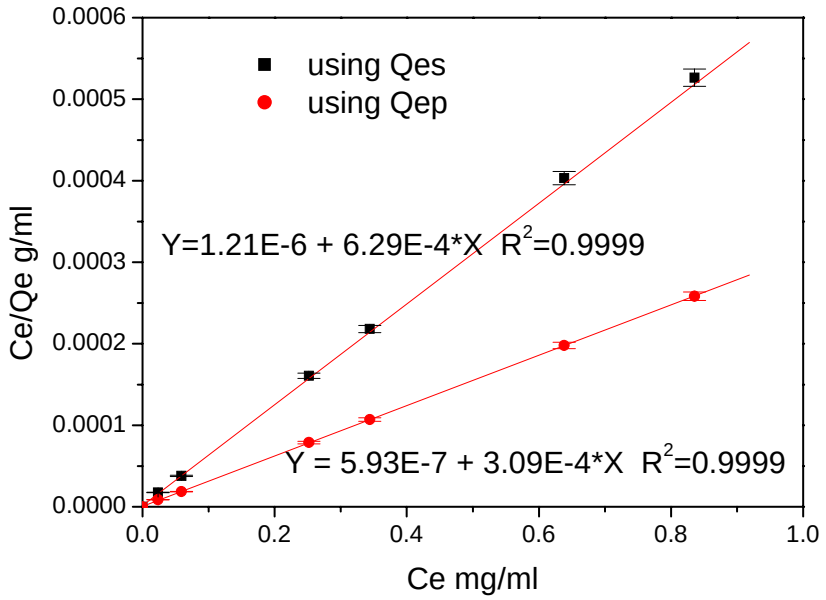

Figure 3.7 Isotherms for the sorption of Acid Green 27 onto the 74% DD chitosan nanoparticles at temperature = 25°C, pH =5

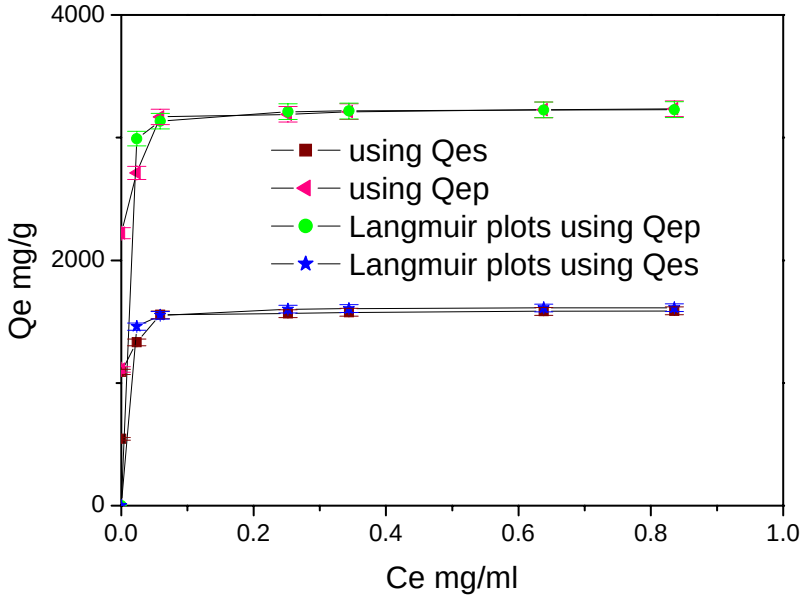

Figure 3.8 Langmuir isotherms of Acid Green 27 onto the 74% DD chitosan nanoparticles at temperature = 25 °C, pH = 5

3.4 Conclusions

The behavior of the chitosan nanoparticles as an adsorbent to remove Acid Green

27 from its aqueous solution was investigated. The affinity between the nano-chitosan and the chemicals used can be summarized: the order of attractive forces was TPP>H_3O^+>SO_3^-(in dye) > the hydrogen bonds in acidic conditions; and OH->TPP>SO_3^- (in dye) >H_2O in alkaline conditions. The equilibrium isotherm was measured to determine the capacities of the nano-chitosan for the dye and analyzed using the Langmuir equation. It was found that the sorption well fitted in the Langmuir model, especially when the dye concentration was high. The Langmuir monolayer adsorption capacities (Q_0) were calculated using the weight of the nanoparticles and the weight of chitosan in the nanoparticles respectively. The capacities were 1033.4 mg/g and 2103.6 mg/g. The values were significantly higher than that of the micron-sized chitosan. The study on nano-chitosan-dye sorption is worth further investigation to explore its high capacity advantage.

Chapter 4

Preparation of pure CSNPs

4.1 Research background

As described in **Section 2.1.3**, a lot of research work was performed on the preparation of chitosan nanoparticles. In summary, two methods are generally used, the ionotropic gelation method and the water-oil reversed-phase micro-emulsion method. There are still some limitations in the two methods, such as the difficulty in determining the particle content in the emulsion, the difficulty in removing additive chemicals from the system, and damages of organic solvents to protein.

On the other hand, ultrasound has become a widely used tool in the preparation of nano-materials [36,110], with its particular ability in breaking up aggregates and reducing the size and polydispersity of particles, and even breaking the chemical bonds through the ultrasound cavitation [111]. Breakdown of polymers into nanoparticles using ultrasound field was reported [112-114]. A similar attempt was also performed on chitosan. Tang et al. evaluated and correlated the effects of ultrasonication on the properties of chitosan nanoparticles from the ionotropic gelation method [36]. However, most applications of ultrasound on chitosan focused on the degradation of chitosan [115-121], and no method directly using ultrasound for nano-chitosan was reported.

We have developed a stable way to breakdown swollen chitosan solid into size-controlled nanoparticles in DI water without adding other assistant agents. By

this dissolving-precipitating-sonolysis method, a pure and stable emulsion containing 100% chitosan and water was achieved with an average particle size from 200nm to 500nm (determined using Zetasizer 3000HSA, a dynamic laser scan) at different conditions. The morphological character of the particle was studied by both SEM and AFM. The changes in molecule weights, particle sizes, degree of deacetylation and crystallinities prepared at different ultrasound intensities and durations were discussed.

4.2 Materials and experimental

4.2.1 Materials

Chitin was purchased from Sigma Co. Ltd. Four types of chitosan with different degree of deacetylation (DD) were prepared by treating the chitin with a 48% aqueous sodium hydroxide (NaOH) solution. Other chemicals were purchased from Aldrich Co. Ltd. and used as received.

4.2.2 Experimental

4.2.2.1 Prepare of chitosan with different DD

Referring to the method developed by Wang et al. [124], 2.5 g chitosan was dissolved in a dilute acetic acid (2% w/v), and then precipitated completely using an aqueous NaOH solution (5% w/v) to get swollen chitosan. Subsequently, the swollen chitosan was put into a 100mL three-neck bottle together with 50 mL 99.8% alcohol and 7.5 g solid NaOH. The obtained mixture was refluxed for one

hour under the protection of atmosphere of nitrogen gas. The treated chitosan was washed to neutral with DI water and soaked with methanol for one hour, and dried in vacuum at 50 ^{o}C for 48 hours. The sample was coded as CHITOSANA-1.

The reaction processes were repeated for one and two times respectively to get chitosan with higher DD, and they were named as CHITOSANA-2 and CHITOSANA-3 respectively.

4.2.2.2 Measurement of viscosity molecule weight (Mv)

The viscosity properties of the chitosan samples were determined by an Ubbelohde viscometer at 25 ^{o}C. A dilute 0.1 M acetic acid solution containing 0.2 M sodium chloride (NaCl) was used as a solvent. Each sample was filtrated by filter paper beforehand.

The Mv was calculated from the Mark-Houwink equation using the limiting viscosity,

$$[\eta]= Km*M^{\alpha}.$$

And the constants for the equation were determined for chitosan by Robert and Domszy [131] as Km = 1.81x10-3 $cm^3.g^{-1}$ and $\alpha = 0.93$.

4.2.2.3 Preparation of nanoparticles by using ultrasound processor

Firstly, chitosan was dissolved in a dilute aqueous acetic acid solution of 0.5 %

(w/v) under magnetic stirring. Aqueous ammonia was then dropped into the chitosan solution to precipitate the chitosan. The obtained gel-like swollen chitosan was washed to neutral with DI water, and was then transferred into a 25 mL volumetric flask. The total volume of liquid was added to 25 mL with DI water.

A Sonic VC120 ultrasound processor with a probe of 6 mm diameter was used. The ultrasound probe was put into the volumetric flask and was kept at 0.5 cm below the water level. Ultrasound treatments were conducted with different output intensities and durations under an ice-water bath. Finally, a milky emulsion was obtained as shown in **Figure 4.1**.

Typically 5 mL of prepared emulsion was used for the Mv measurement after the preparation. The emulsion was filtered using a 20-50 μm sintered glass filter before particle characterization. Some of the emulsions were centrifuged at 27200 G for 60 min at 4 ^{o}C; the obtained solids were freeze-dried for further DD measurements.

Figure 4.1 The milky emulsion of the pure chitosan nanoparticles

4.2.2.4 DD measurement

Infrared spectrometry method was used to determine the DD of the chitosan [120-124]. The samples were vacuum-dried at 50 ^{o}C for 48 hours. About 10 mg of each dried samples was mixed with 120 mg of potassium bromide (KBr) and was pressed into pellet under 10 ton pressures. The pellet was vacuum-dried at 50 ^{o}C for 24 hours again and placed into desiccator before the IR measurement (Nicolet Avatar 360 FT-IR).

The absorbances of amide I (1655 cm-1) and of the hydroxyl bond (3450cm-1)

were measured. The DD of samples were given by

$$DD = 100 - (A_{1655}/A_{3450}) \times 115.$$

Whereas, A1655 and A3450 were the absorbance at 1650 and 3450 cm-1 respectively.

4.2.2.5 Morphological characterization

The particle size and zeta potential of the emulsion were measured using a Zetasizer 3000HSA . Each sample was measured three times at an interval of 30 seconds. The average results were then calculated automatically by the instrument.

Typically one drop of the diluted emulsion was placed on the surface of a piece of washed silicon wafer, and then dried in ambient atmosphere, followed by vacuum-drying for 48 hours before the SEM and AFM measurements. The SEM measurement was performed by a JOEL JSM 6335F, and the AFM was performed by a SPI 4000. The thermal analysis was performed with a Perki Elmer DSC.

4.2.2.6 X-ray diffraction and calculation of crystallinities

X-ray diffraction measurements were conducted with a Philips Analytical X-Ray BV at the Cu Kα ray (λ=1.54Å) in the 2θ range of 5-70º. The spectra were recorded at 40 kV and 35mA at a scan rate of 0.03º per second.

The X-ray diffraction profiles were deconvoluted with Loess algorithm of the least-squares fit. The crystallinities were calculated by [125]

$$Xc = Fc / (Fc + Fa) \times 100\ \%$$

Here, Fc is the area of the crystalline region; Fa is the area of the amorphous region.

4.3 Results and discussion

4.3.1 Preparation of chitosan with different DD

Wang et al. [134] used 95% (w/v) alcohol to prepare of chitosan with different DD, and pointed out that, in the first 3 hours the rate of deacetylation increased quickly but subsequently became slower when molecule weight kept decreasing. Recognizing that the swollen chitosan already contained water, we used 99.8 % (w/v) alcohol directly and conducted the reactions repeatedly every one hour. As shown in **Figure 4.**2, the result indicate that the DD of chitosan increased from 58% to 98% proportionally to the repeating times when the linear decrease of the Mv was from 1000000 to 500000 respectively.

4.3.2 The stability of the nano-emulsion

The emulsions had zeta potentials of from +22 to +35 mV according to different DD, and pH values around 6.7. Many researchers [105,106,126-129] demonstrated the stable structure of the hydrogen bond between water molecules and the amino groups. In the structure water molecules acted as the provider of

hydrogen when amino groups are the receiver, as indicated in **Figure 4.3**. The positive charge of the chitosan nanoparticles suggested that the emulsions were stabilized by the hydrogen bond between the amino groups and hydroxyl groups of chitosan and water respectively. In the hydrogen bonds, amino groups were positively charged, which made the surface of the nanoparticles become positively charged too, as shown in **Figure 4.3**. The hydrogen bond was mentioned in **Chapter 3** previously, which was believed to act as a stabilizer in the emulsion from the gelation reaction between chitosan and TPP.

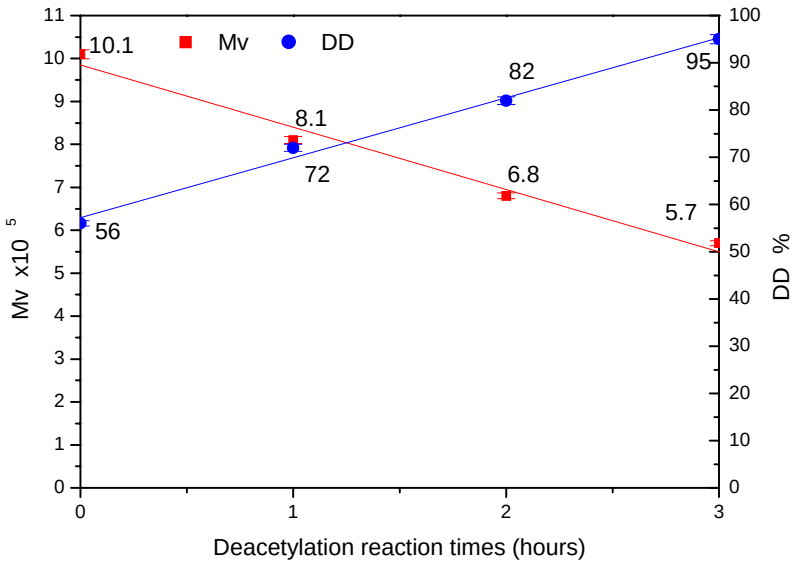

Figure 4.2 Deacetylation result

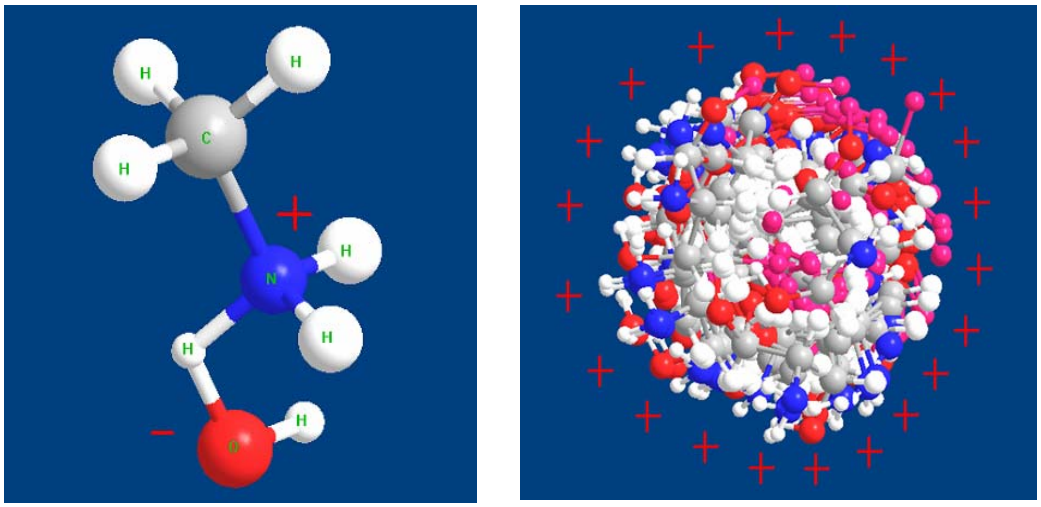

Figure 4.3 Illustration of the positive charge of the chitosan nanoparticle

When heated, precipitates appeared in the emulsion immediately at around 90 ^{o}C, which is believed to due to the break of the hydrogen bond at high temperature. The result of DSC measurement proved it. As shown in **Figure 4.4**, there is an endothermic peak from 75 ^{o}C to 90 ^{o}C, which should be responsible for the break of hydrogen bond.

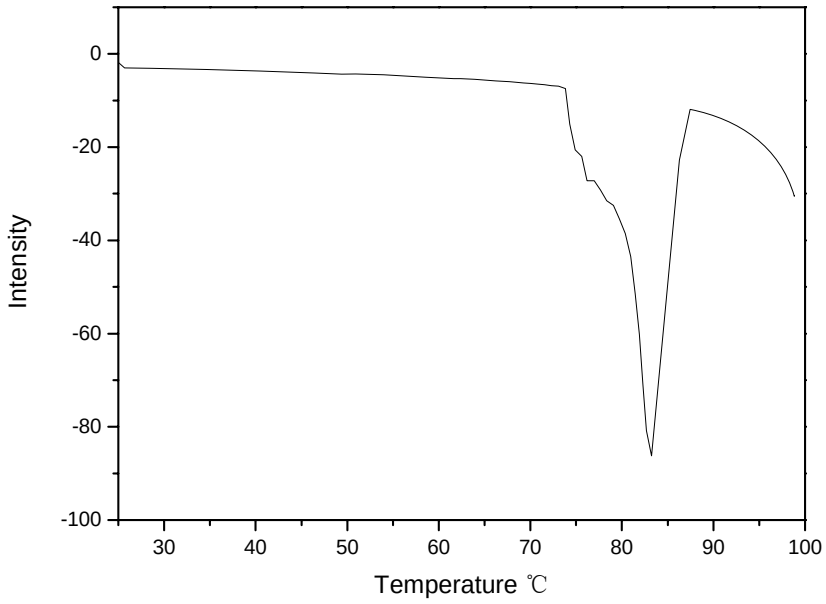

Figure 4.4 DSC of the emulsion

The crystal of chitosan was destroyed partially during the ultrasound treatments. As a result, the crystallinities of treated chitosan decreased. **Figure 4.5** shows the profiles of untreated and treated chitosan. Two major peaks were observed at 10º and 20º [131,132]. The intensities of the peaks decreased with the increase of the sonolysis time. The relationship between the crystallinities and the sonolysis time is shown in **Figure 4.6**. A sharply decrease was obtained at the beginning, and then the crystallinities seemed to reach a stable value. The crystallinities decreased from 78% to 54%, meaning 31% of the crystal area was destroyed. It suggested that effect mainly happened in the early part of the ultrasound treatment when the amorphous structure of the swollen chitosan was destroyed quickly; after that, the remained compact structure was too hard to break, the crystallinities became stable. Similar results were obtained in the investigation of particle size and Mv versus duration. The results were presented in **Table 4.1** and **Figure 4.7**.

Table 4.1 Effect of duration to the particle characters

Sample	Duration time	Particle size (nm)	Mv after treatment	DD after treatment
1	5 min	609±5	（9.4±0.36）×10^5 Da	63±2 %
2	10 min	507±6	（8.2±0.29）×10^5 Da	64±1 %
3	15 min	458±5	（7.1±0.27）×10^5 Da	62±3 %
4	20 min	413±8	（6.8±0.18）×10^5 Da	62±2 %
5	30 min	386±4	（5.8±0.24）×10^5 Da	60±1 %
6	40 min	334±5	（5.1±0.19）×10^5 Da	61±2 %

Note: Mv of control sample is 1200 kDa, and DD is 63%; treatment was performed with ultrasound output of 25 W.

As shown in **Figure 4.7**, an obvious size decrease happened at the beginning of sonolysis, and then it reached a minimum value. The result agreed to that of Tang, et al. who treated the nanoparticles obtained by adding a TPP solution into chitosan solution under stirring [36]. The Mv change was similarly to that of the size change. The result agreed to the observation in the depolymerization of chitosan solution by ultrasound as reported by Tsaih, et al. [133] They stated that, for chitosan with same DD, the molecular weight decrease was more pronounced during the earlier sonolysis, and then the decrease ratio became slower during the sonolysis later. The results explained change of crystallinities.

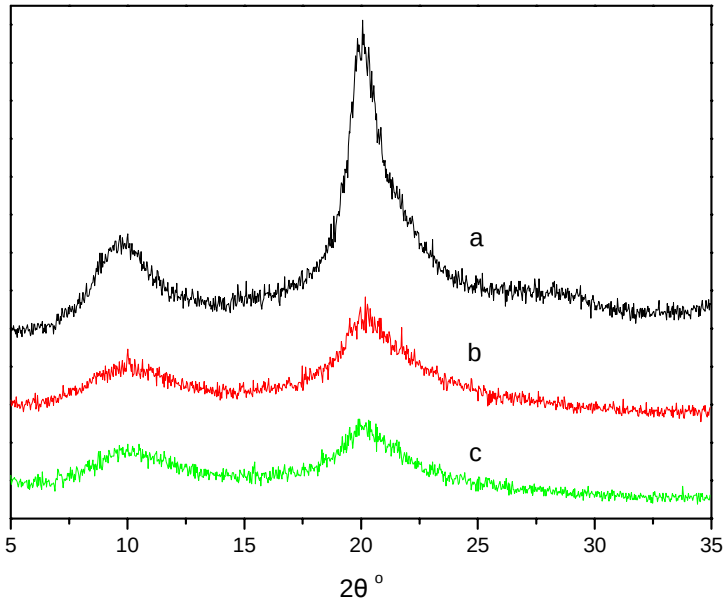

Figure 4.5 X-ray diffraction patterns of (a) initial chitosan (b) treated at 25W for 20min (c) treated at 25W for 40min

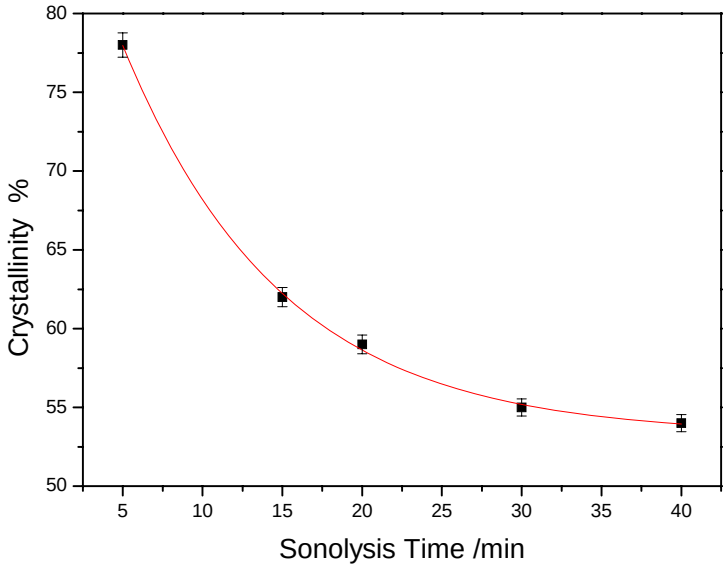

Figure 4.6 The relationship between the crystallinity and the sonolysis time

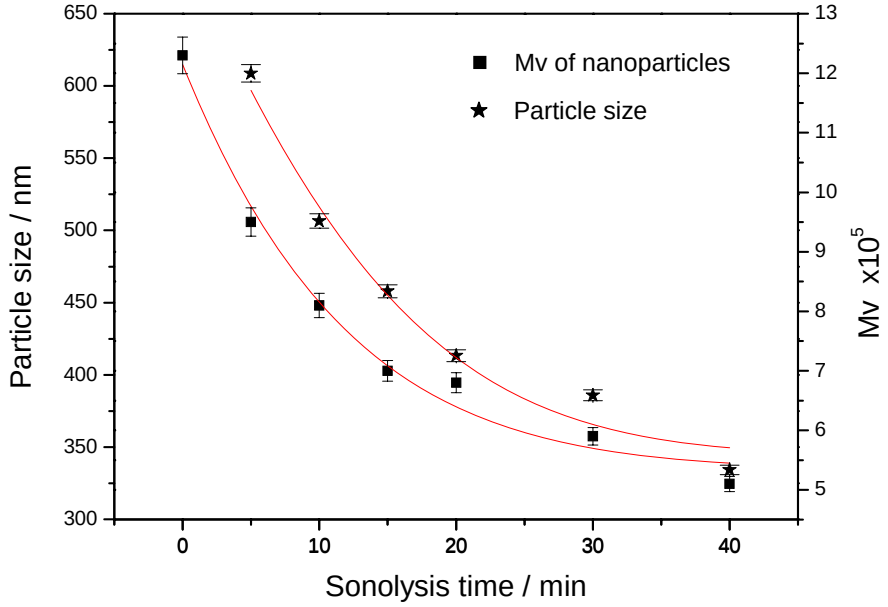

Figure 4.7 The relationship between the particle characters and sonolysis time

The DD of the nanoparticles did not change much during ultrasound treatment. The result was the same with that of depolymerization of chitosan solution [36,133]. Shyur reported that a chitosan solution treated with ultrasound radiation at 60 ^{o}C did not change its DD value as the solution contained no urea [133]. It is believed that the ultrasound wave did not to destroy the bond between amino group and acyl in pure water.

In the aspect of storage stability of the emulsion, no precipitates appeared in the emulsion after it had been stored for over two months. The results of the laser scanning showed that the particles size of chitosan has no obvious change. Thus, it can be said that the chitosan nano-emulsion had a good stability in the ambient condition.

4.3.3 Effect of ultrasound intensity to nanoparticles

Chitosan with Mv of 10×10^5 Da and DD of 56% was treated at four different ultrasound intensities. The results are summarized in **Table 4.2**.

Table 4.2 Effect of intensity to the emulsion

Sample	Output	Particle size (nm)	Mv after treatment
1	15W	368±5	$(7.2\pm0.27)\times10^5$ Da
2	20W	362±7	$(6.6\pm0.24)\times10^5$ Da
3	25W	326±7	$(6.4\pm\times0.25)\times10^5$ Da
4	27W	337±5	$(6.2\pm0.23)\times10^5$ Da
5	30W	331±4	$(6.1\pm0.17)\times10^5$ Da

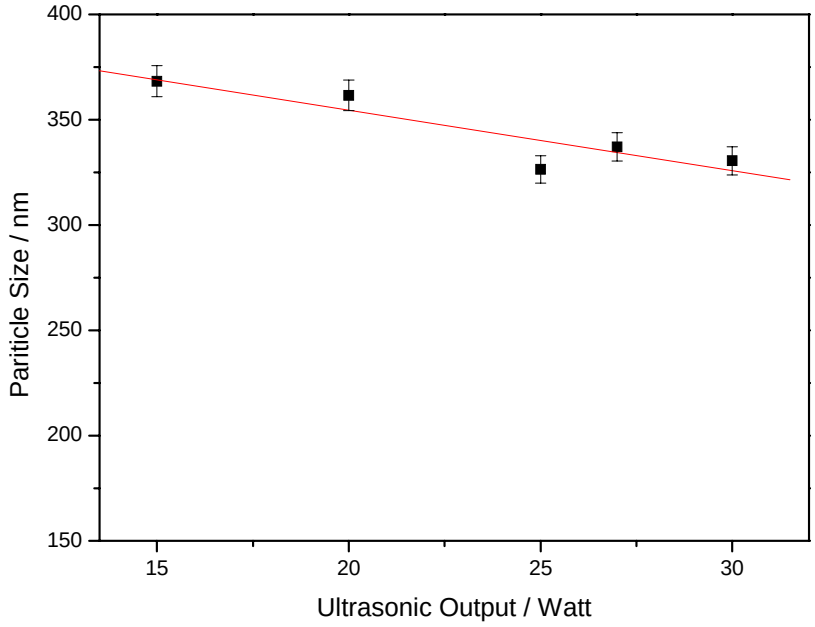

Figure 4.8 Change of particle size with different ultrasound intensities

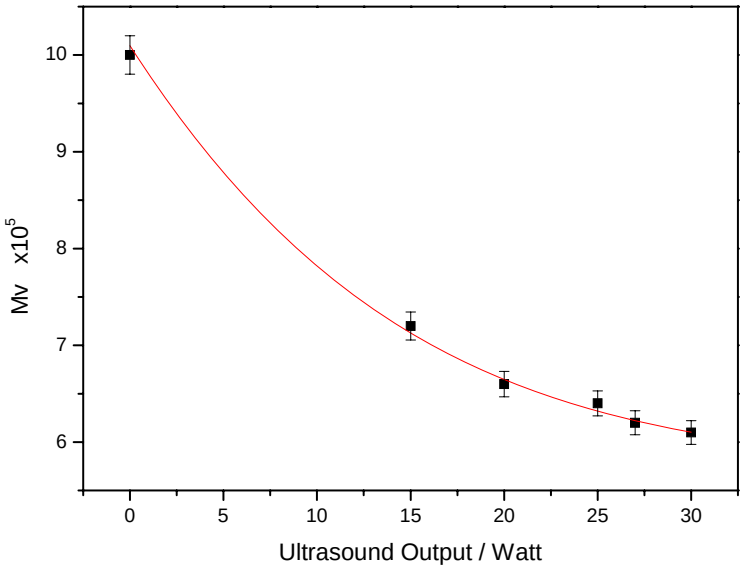

Figure 4.9 Effect of ultrasound on the molecular weight of chitosan

The particle size diminished with the increase of ultrasound intensity. However, the decrease was not as obvious as that of with sonolysis time, and size decrease of 10% was obtained, as **Figure 4.8** shows. It became difficult to break the particles into a much smaller size after the particle reached a certain size. On the other hand, the change of Mv versus the intensity was similar with that of to sonolysis time. The Mv decreasing rate became smaller when the ultrasound intensity was increased, as in **Figure 4.9**.

4.3.4 Effect of DD to nanoparticles

The effect of DD to particle size of chitosan was studied using the prepared samples with four different DD. The ultrasound treatment was performed at 25W for 20min each. The results are presented in **Table 4.3**.

Table 4.3 Effect of DD to the emulsion

Sample	DD	Particle size (nm)
1	56	326 ± 7
2	72	314 ± 6
3	82	324 ± 9
4	95	304 ± 8

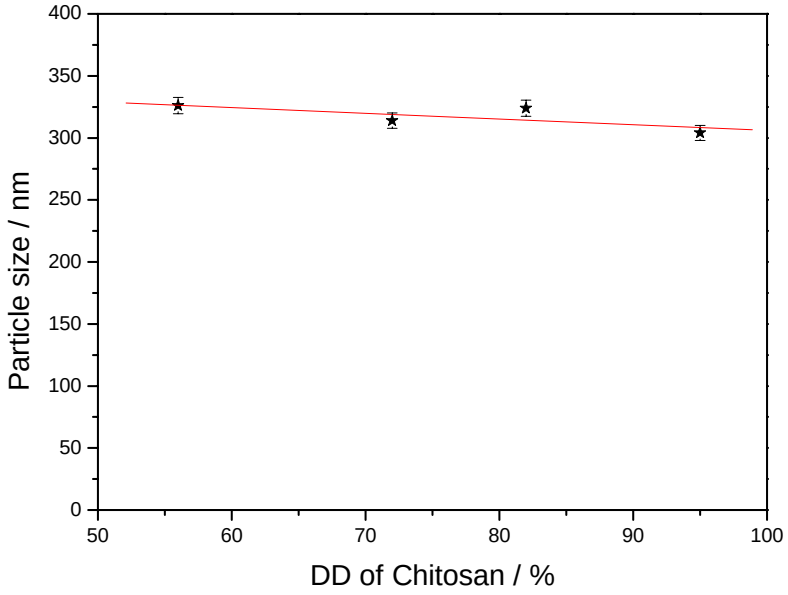

Figure 4.10 Change of particle characters with different DD

Figure 4.10 shows that there was no obvious relationship between the particle size and the DD of chitosan. Tsaih et al. [133] reported that the sonolysis depolymerizing reaction rate was increasing linearly with the increase of DD, implying that it was easier to depolymerize the chitosan in solution with high DD by ultrasound. Since the ultrasound treatment in our case also degraded the chitosan molecules, it seemed that chitosan with high DD should have smaller particle size. However, no obvious relationship between DD and the particle size was observed. Mv also decreased negatively to the increase of the DD but no clear relationship relate to DD was observed.

4.3.5 Morphological characterization of the CSNPs

As shown in **Figure 4.11 (a)** and **(b),** the particles were in irregular shapes, mainly

in the shape of triangles and rods. After filtering the emulsion using a 0.45 μm membrane, these residual particles were rectangular and had sizes from 100nm to 300nm. It is believed that the big particles were broken into smaller particles in various shapes in the early stage of the ultrasound treatment, and then the particles were more and more difficult to be broken up with the decrease of their sizes. Finally the particles became spherical shapes, as shown in **Figure 4.11 (c)**. The spherical shape was confirmed in the investigation of AFM and TEM, as showing **Figure 4.12** and **Figure 4.13**.

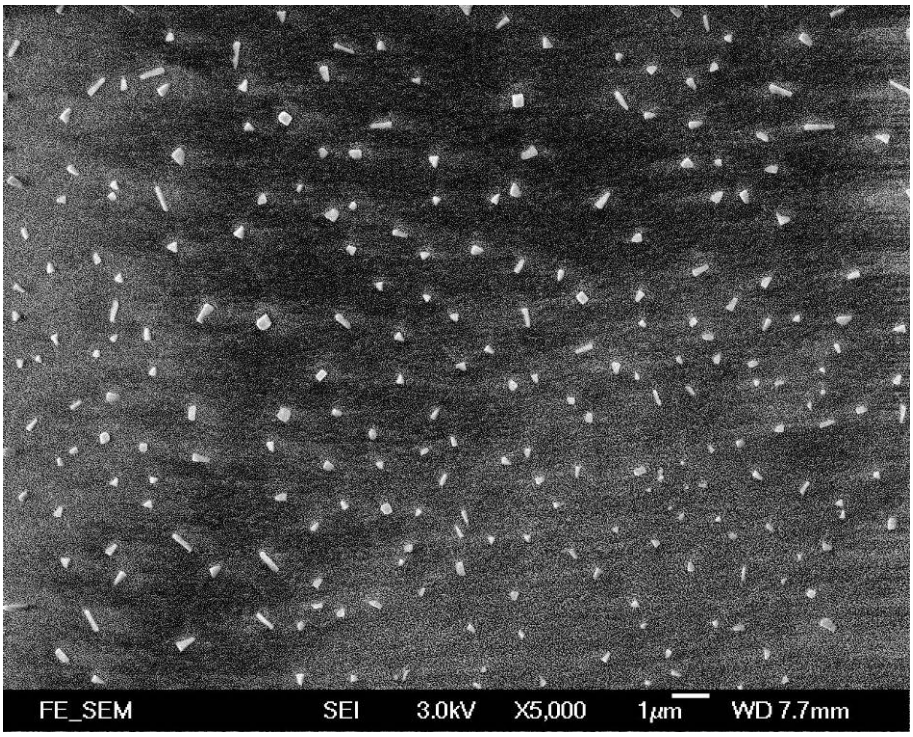

Figure 4.11 SEM micrograph of (a) CSNPs

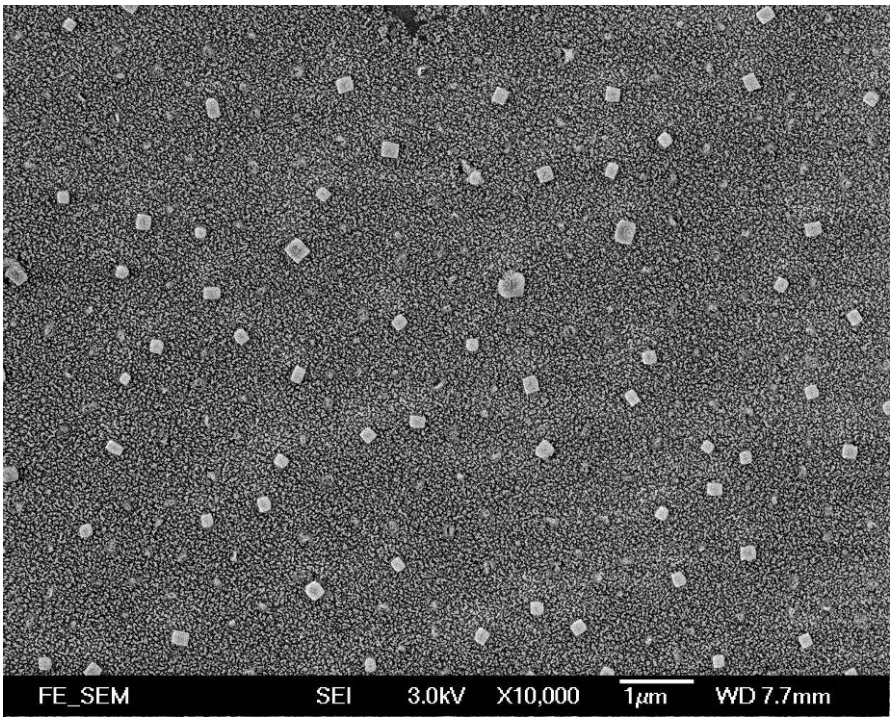

Figure 4.11 SEM micrograph of (b) CSNPs from filtrated emulsion with 0.45um membrane

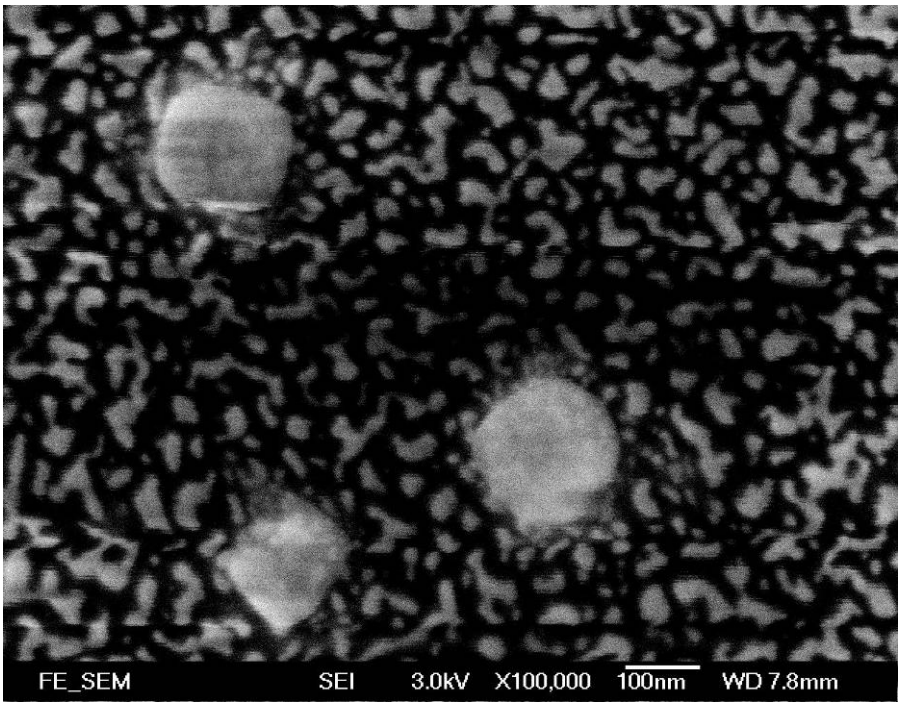

Figure 4.11 SEM micrographs of (c) CSNPs from filtrated emulsion with 0.45um membrane

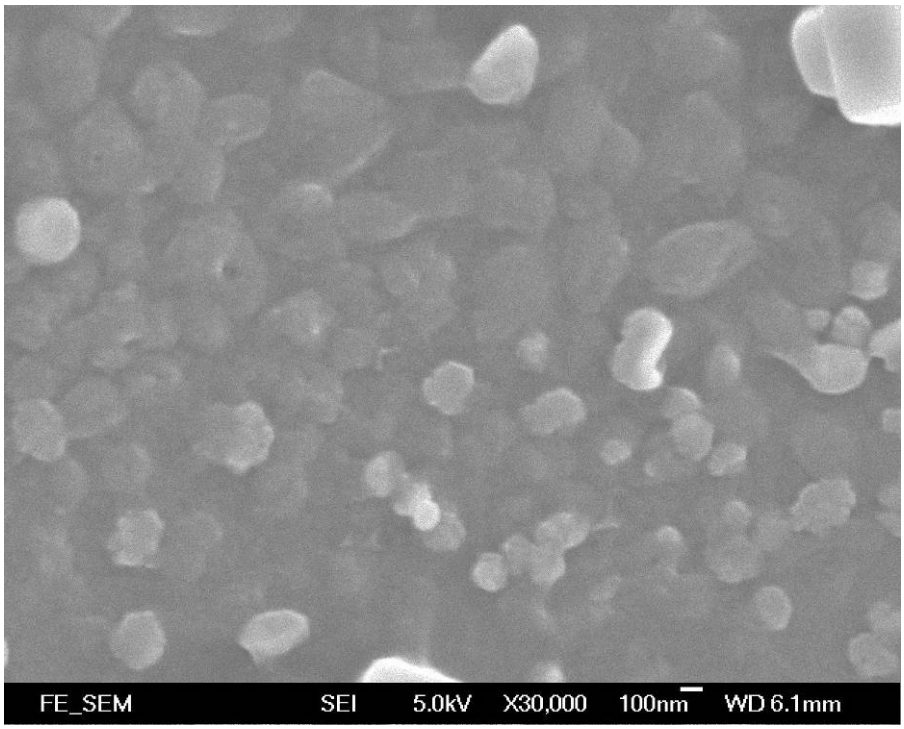

(d)

Figure 4.11 SEM micrographs of (d) CSNPs from emulsion at 0.3% (w/v) concentration

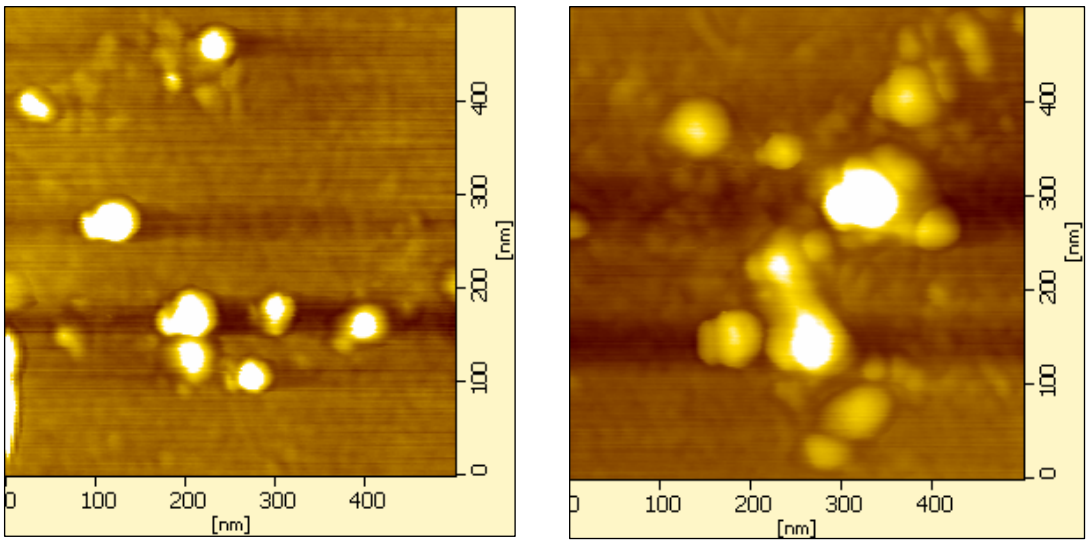

Figure 4.12 AFM micrographs of the CSNPs

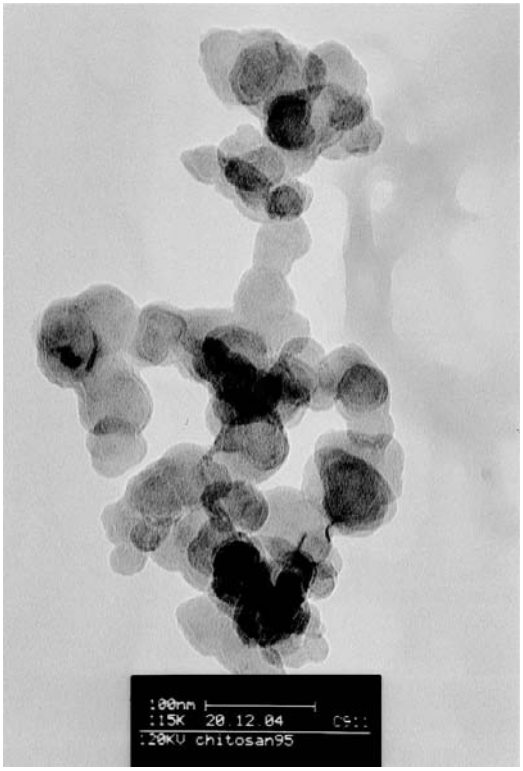

Figure 4.13 TEM micrograph of the CSNPs

These particles aggregated in the process of drying and formed a film with rough surfaces, as shown **Figure 4.11 (d)**. The rough surface was also observed in the AFM micrographies, as shown in **Figure 4.14**.

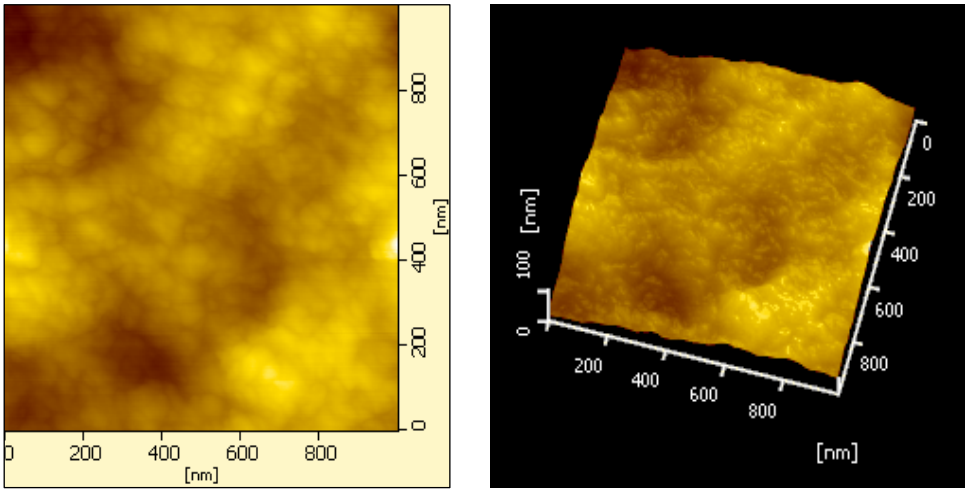

Figure 4.14 AFM micrographs of CSNPs

4.4 Conclusion

In this research, a new dissolving-precipitating-sonolysis method was developed for the preparation of the chitosan nanoparticles by using ultrasound treatment, through which emulsion of the chitosan nanoparticles with controllable sizes were prepared. The emulsion had a good stability because of the hydrogen bond between the amino groups and hydroxyl groups of water and chitosan molecules. The relationship of the nanoparticles and sonolysis duration, including the changes of particle size, crystallinity, molecule weight and DD, were studied. The results indicated that most changes happened in the beginning of the treatment, and were then faint in the later stage. The DD of chitosan had no obvious change during the ultrasound treatment.

The effects of duration, ultrasound intensity and chitosan DD to the particle size, Mv and crystallinities were studied. Crystallinities, particle size and Mv decreased with the increase of duration. At the same time, the rates were higher in the beginning of the treatment and became smaller. The effect of ultrasound intensity to Mv of chitosan was similar to that of duration time. Ultrasound intensity and DD of chitosan had a limiting effect on the particle size.

The dried chitosan nanoparticles were characterized by SEM, TEM and AFM. The shapes of the nanoparticles were spherical. Theses nanoparticles aggregated together after drying them and a rough film is formed.

Chapter 5

Antibacterial functionalization of cotton fabrics using the pure CSNPs

5.1 Research background

Coming into the new century, human beings have to face the hazard of many kinds of viruses, such as SARS, H_5N_2. So, it is natural that we require a safer and more hygienic living environment and our request becomes much stronger than before. As the daily expendable, textiles, especially clothes we dress everyday, could be a powerful shield keeping us from the threat of these viruses. Much research work was contributed to entitle the textiles an effective antibacterial property but many chemicals used could also be harmful to people as well as to the environment. A non-toxic and eco-friendly finishing agent for the antibacterial becomes an emerging topic for the researchers.

As mentioned in the ***Chapter 2***, chitosan has a good antibacterial activity against various bacteria and fungi. This unique polycationic property of chitosan facilitated its applications in a variety of fields, including food science, agriculture, medicine, pharmaceutics, and textiles. Based on the emulsion of the pure CSNPs we developed as described in ***Chapter 4***, this research work is conducted to disclose the potential applications of the nano-chitosan in the functional finishing of textiles for the antibacterial property, and figure out possible advantages of the nano-chitosan comparing with the traditional chitosan solution that may cause damage to the finished fabrics due to the acidic atmosphere as well as a tough handle. Since the emulsion of the pure CSNPs contains no additive chemicals, a green finishing process for antibacterial purpose can be desirable.

5.2 Materials and experimental

5.2.1 Materials

The emulsion of the CSNPs described in ***Chapter 4*** was used directly. Woven cotton fabrics, bleached and scoured, were obtained from commercial purchase. Other used chemicals were from Aldrich Chem. Co. Ltd. and used as received.

5.2.2 Experimental

5.2.2.1 Samples preparation

A two-dip-two-pad method was used. Cotton fabrics were soaked with the emulsion of 3 mg/mL for 3 minutes, and then padded with a pick-up weight (PUW) around 80%. The process was repeated again. The samples padded with the emulsion of 63% DD chitosan coded as 63CSE. For the parallel experiment using chitosan solution, acetic acid was added into another volume of the emulsion to obtain 3 mg/mL 63%DD chitosan solution of 0.5% (w/v) acetic acid. The samples padded with this solution were coded as 63CSC. All padded samples were dried at 100 ^{o}C for 3 minutes, cured at 150 ^{o}C for 3 minutes, and finally rinsed with tap water and dried again.

5.2.2.2 Characterization of mechanical properties of the finished fabrics

ASTM Test Method D 5035 1R-L was used. Six pieces of each sample were tested in both the warp direction and weft direction separately, and average values were

used. AATCC Test Method 66-2003 Option 2 was used. Four pieces of each sample were tested in the warp direction and weft direction separately, and average values were used. ASTM Test Method D 1424 was used. Three pieces of each sample were tested in warp direction and weft direction separately and average values were used. A subjective handle test was completed by touching the fabrics with hands directly. Objective handle tests were completed using instrumentations of Kato Tech Co. Ltd, Japan.

5.2.2.3 Antibacterial Test

The shaking method was used. The procedure is shown in Figure 5.1. Two kinds of bacteria, *E. coli.* and *S. aureus*, were used to assess each sample.

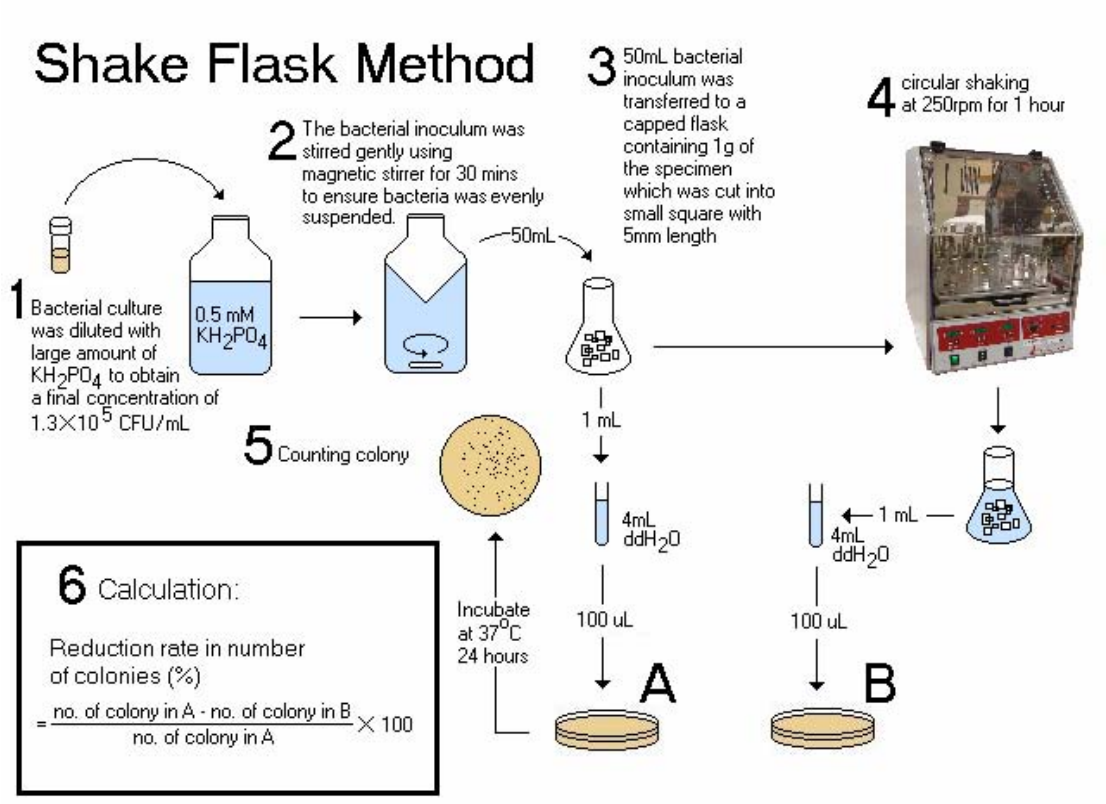

Figure 5.1 The process of antibacterial test

5.2.2.4 Other tests

AATCC Test Method 61-2003 was used with Options 1A and 2A for the washing durability test. The yellowness of the fabric was measured with a Datacolor Elrepho 2000 spectrophotometer according to ASTM E313 and ASTM D1925. The handle assessments were conducted including both the subjective assessment and objective assessment separately. The subjective assessment was performed by a group of five persons through touching the mark-free samples and giving out their handle feeling. The objective handle tests were completed using instrumentations of Kato Tech Co. LTD, Japan.

5.3 Results and discussion

5.3.1 Mechanical properties of the finished cotton fabrics

5.3.1.1 Mechanical strength tests

The tensile strength of the samples are summarized in **Table 5.1** and **Figures 5.2-5.4**.

Table 5.1 Result of break strength test

Sample	Displcment at Max.Load (mm)	Load at Max.Load (N)	%Strain at Max.Load (%)
Control-warp	14.127±0.441	355.433±21.923	18.836±0.587
63CSE-warp	14.522±0.658	320.400±21.174	19.362±0.878
63CSC-warp	13.607±0.415	299.783±14.084	18.142±0.553
Control-weft	10.575±0.477	218.750±7.440	14.100±0.636

Table 5.1 Result of break strength test (continued)

Sample	Displacement at Max.Load (mm)	Load at Max.Load (N)	%Strain at Max.Load (%)
63CSE-weft	9.137±0.361	215.033±9.737	12.182±0.481
63CSC-weft	9.352±0.282	208.117±14.136	12.469±0.376

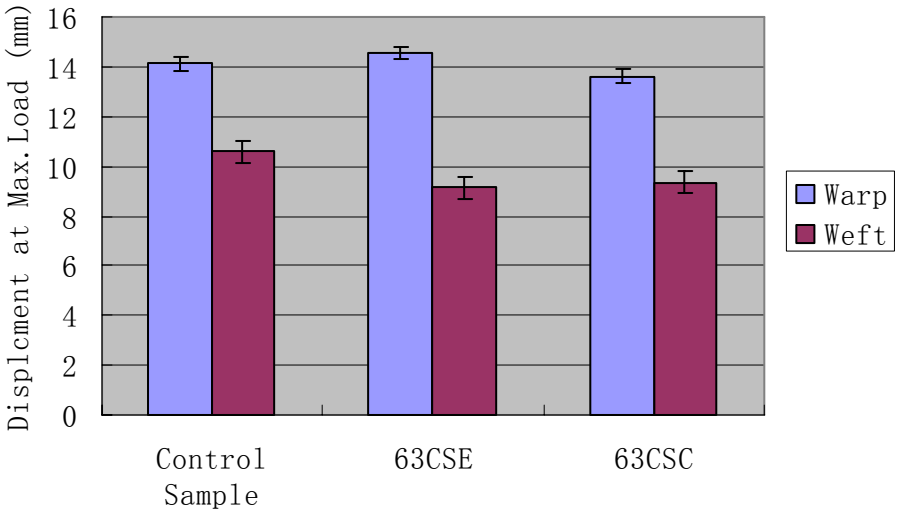

Figure 5.2 Displacements of Samples

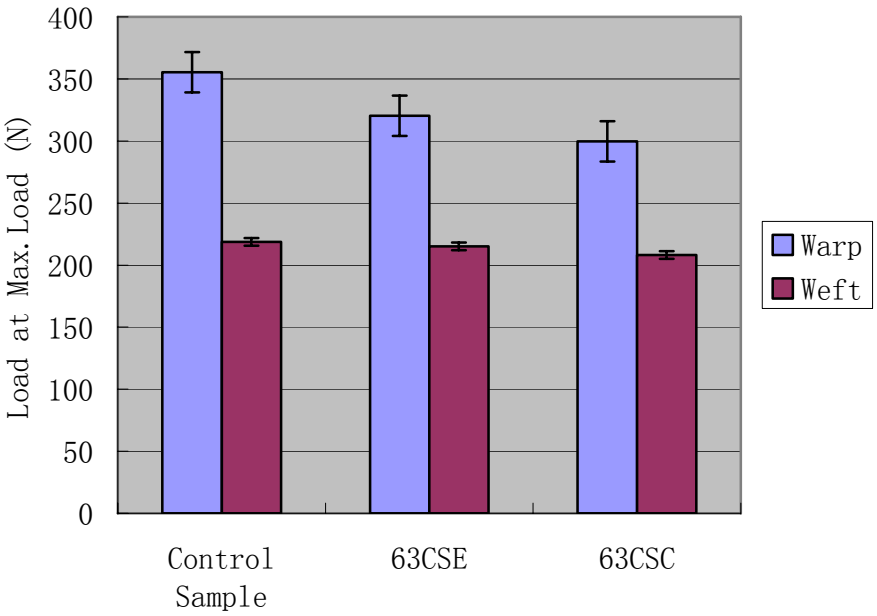

Figure 5.3 Max Load of Samples

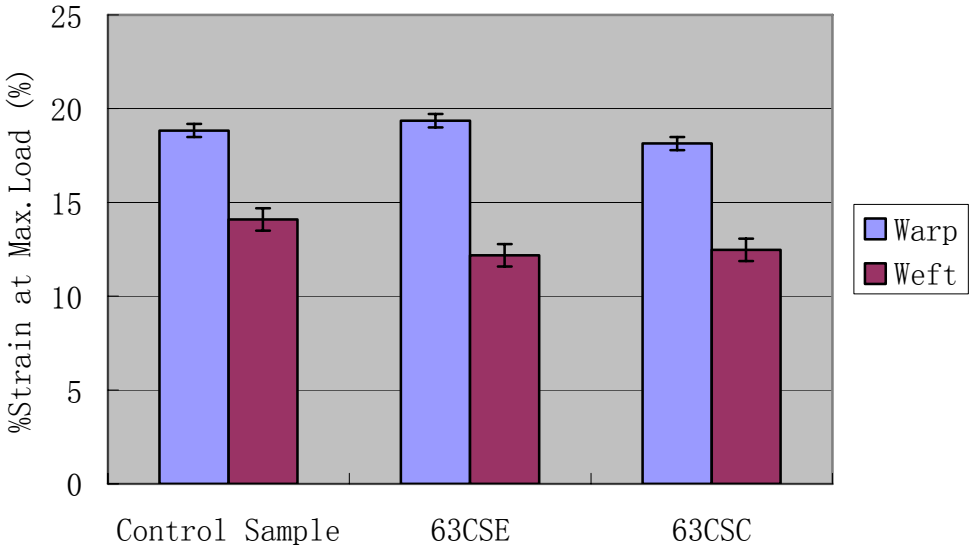

Figure 5.4 Strains of Samples

As shown in **Figures 5.2-5.4**, small changes were observed after finishing using either the emulsion or the solution, indicating damages were caused. In the warp direction the 63CSE seemed behaving better occasionally. The control sample was best in the weft direction. But these changes were not obvious, indicating that the finishing processes, no matter using the emulsion or the chitosan solution, caused slight damage to the fabrics. The samples finished with the chitosan solution had the worst score in the tests possibly because of the damage of the acidic condition from acetic acid.

Table 5.2 and **Figure 5.5** show the result of wrinkle recovery test.

Table 5.2 Results of winkle recovery tests

Sample	Warp (^{o}C)	Weft (^{o}C)
Control sample	80±3	80±3
63CSE	82±3	83±3
63CSC	81±2	88±4

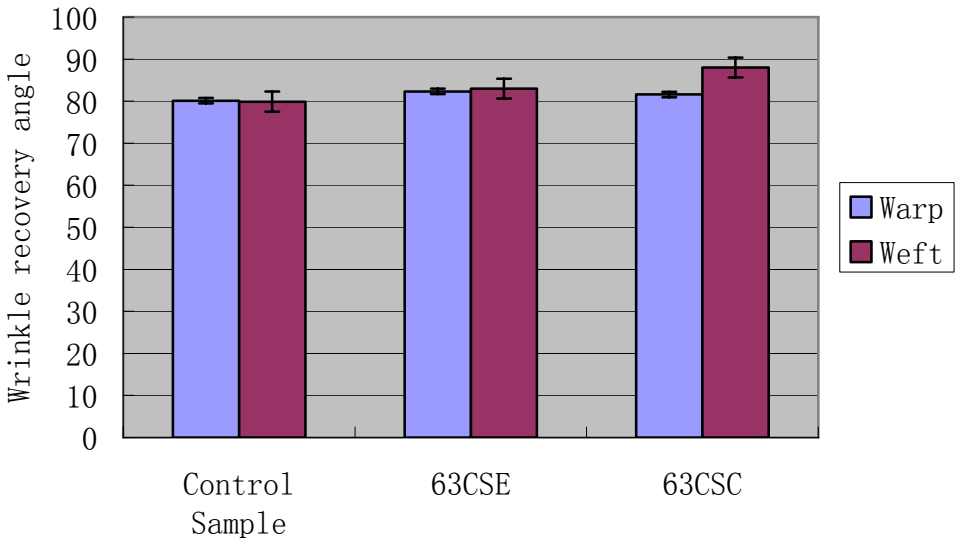

Figure 5.5 Wrinkle recovery angle of samples

The results shown in the above table and figure indicated that there was just little improvements in the anti-wrinkle property after the finishing process using the emulsion or the solution. The recovery angles varied within 10° while the solution-finished samples seemed to be performing better. Such low usages of chitosan in the emulsion and the solution may be the reason for the limited promotion on anti-wrinkle performance. According to the published papers, the use of chitosan for the durable press finishing was usually in a higher usage with the

assistant of crosslink agent such as dimethylol-dihydroxy-ethylene-urea (DMDHEU).

Table 5.3 and **Figure 5.6** show the results of tearing strength test. The damages to tearing strength caused during the finishing process, both using the emulsion or the solution, were more obvious. 63CSE and 63CSC showed no big difference in this property.

Table 5.3 Results of tearing strength tests (N)

Sample	Warp direction	Weft direction
Control sample	29.3±1.4	22.3±1.2
63CSE	22.5±1.5	19±0.9
63CSC	23.5±0.9	18.7±0.3

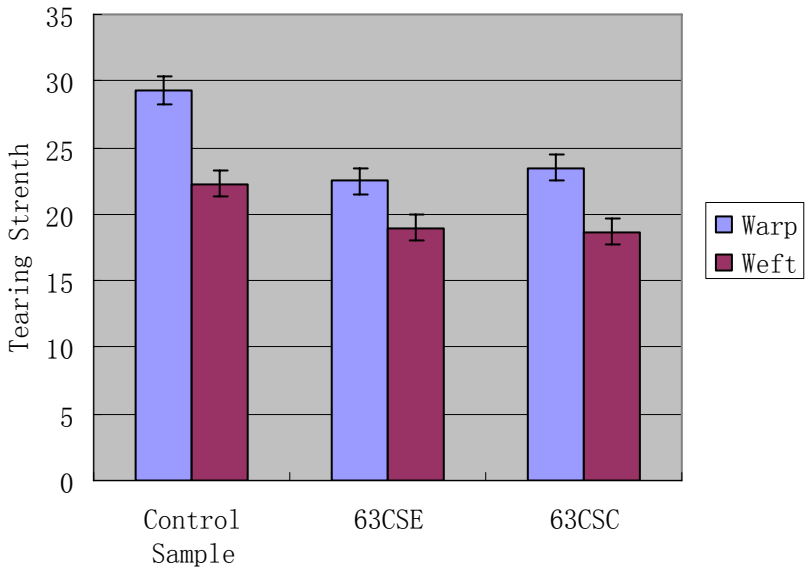

Figure 5.6 Tearing strength of samples

5.3.1.2 Handle assessment

In the subjective handle assessment, all of the five persons concluded that the control sample was the best, 63CSE was in the middle and 63CSC had the worst to handle. The objective handle assessments were performed in four aspects: tensile & shearing test, and surface test. **Figure 5.7** and **Figure 5.8** illustrated the results of the tests. In the tensile & shearing test, CSE63 kept in accordance with the control sample when CSC63 changed obviously. In the surface assessment, we did not observe any obvious difference among the three samples. A small dosage of chitosan in the emulsion and the solution meant that just a small amount of chitosan was coated onto the surface of the cotton fabrics, and kept the original surface property. The finishings, using the emulsion or the solution, slightly changed the handle properties of the original cotton fabrics when the solution-finished sample displayed as harder to handle than the other two.

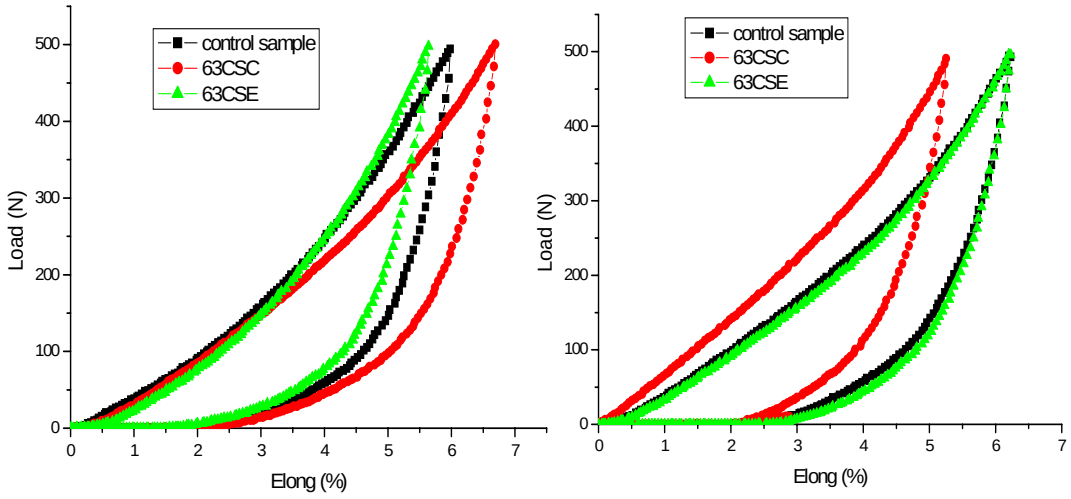

Warp direction Weft direction

Figure 5.7 Result of tensile test

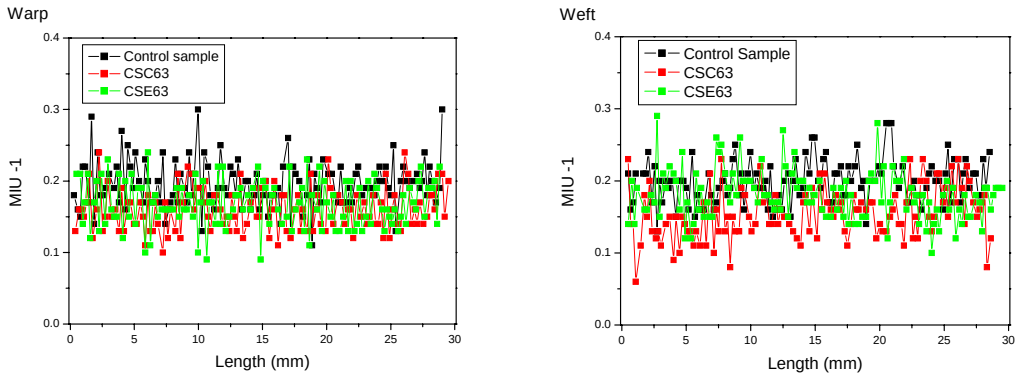

Figure 5.8 Coefficient of friction of chitosan-coated fabrics

5.3.2 Antibacterial activity of the finished cotton fabrics

Table 5.4 and **Figure 5.9** summarize the results of anti-bacterial tests performed at pH value of 5.

Table 5.4 Result of antibacterial tests

Sample	%reduction
Control sample	5.67 ± 1.1
63CSC	78.3 ± 2. 3
*63CSC	97.5 ± 3. 1
63CSE	98.1 ±1. 4

Note: After curing, *63CSC was treated with 1% $NaCO_3$ aqueous solution before tap water washing.

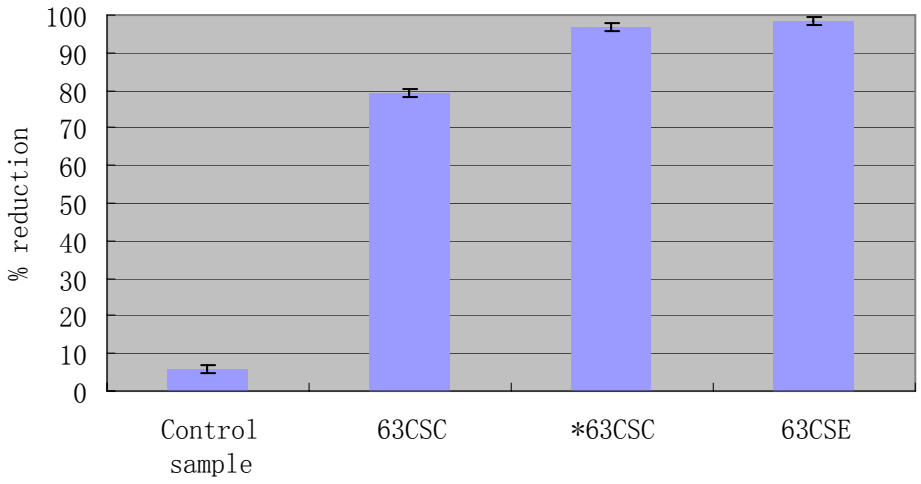

Figure 5.9 Results of antibacterial tests

Figure 5.9 indicates a remarkable enhancement of the antibacterial activity after the fabrics were finished with the emulsion or the solution, the bacteria reductions were 73% improved for 63CSC and 92% for 63CSE. But for 63CSC, there was acetic acid odor coming from the residual acetic acid in the solution. When being rinsed with tap water, the acetic acid could form a temporary acidic circumstance around the fabrics and dissolve chitosan away. So 63CSC in **Figure 5.9** displayed inferior antibacterial activity comparing the other two finished samples. After treating 63CSC with 0.5% $NaCO_3$ solution before tap water washing to get sample of *63CSC, the problem could be overcome. But before the alkaline treatment, 63CSE showed about 20% bacteria reduction higher than 63CSC.

The antibacterial activities of the cotton fabrics finished using the emulsion or the solution with different concentrations were studied. The results are shown in **Figure 5.10**. The antibacterial activities decreased at reduced uses of the chitosan.

Using of 0.01% chitosan content conducted a bacterial reduction of less than 40%. **Figure 5.10** also indicates that in all studied cases, though not remarkable, the emulsion-finished cotton fabrics displayed better antibacterial activities than the solution-finished samples.

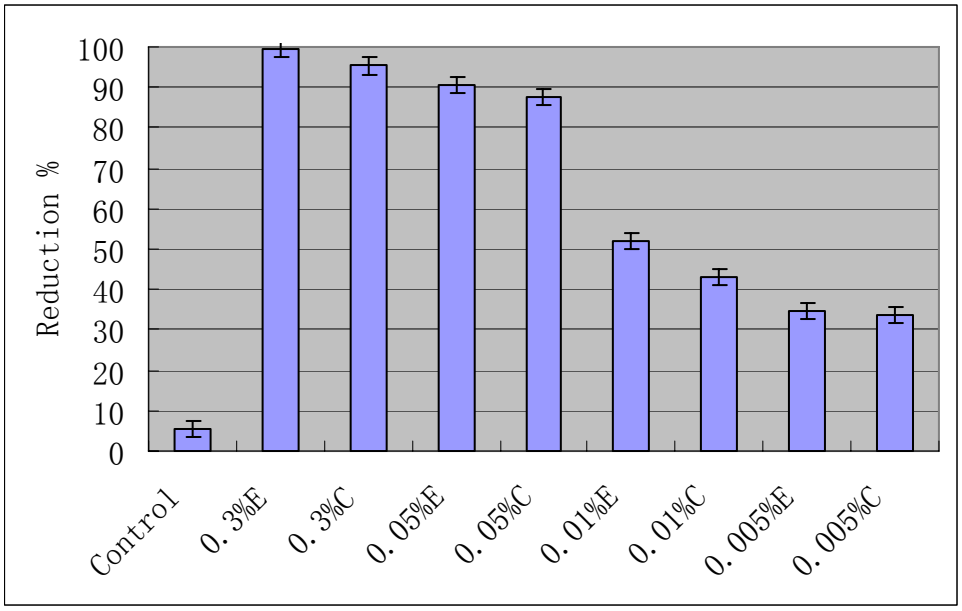

Note: E – emulsion, C – solution

Figure 5.10 Results of antibacterial tests with different chitosan usages

The effect of crosslink treatment after the emulsion-finishing process was also investigated. The results shown in **Figure 5.11** indicated the negative effect of the crosslink agent, DMDHEU in this case. DMDHEU consumed mainly with the amino groups of chitosan in the crosslink reaction but the amino groups were critical for the antibacterial activities, so that the cross-linked sample became inferior. On the aspect of the effect of pH value, antibacterial tests at pH value 7 were conducted and obtained similar results to these of pH 5, indicating that the finished samples still had efficient antibacterial activity in a neutral circumstance.

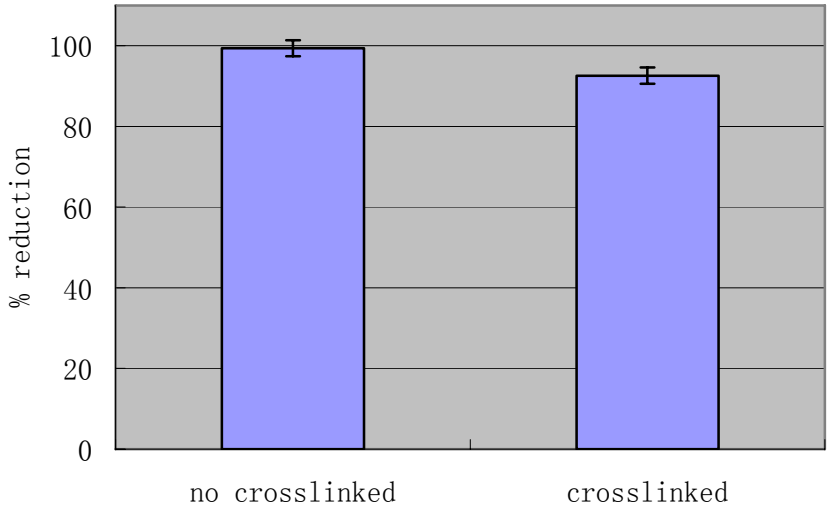

Figure 5.11 Bacteria reductions of samples with out and with crosslink treatment

Washing durability tests were conducted with 63CSE in the two assessment methods, as summarized in **Table 5.5** and **Figure 5.12**. In Method 1 more detergents were used when more steel balls were used in Method 2. The results from the two methods were similar. The bacteria reduction over 80% was obtained with the samples washed for 10 cycles that is equal to 50 washings. The results revealed good durability of the finished cotton fabrics to chemical corrosion and mechanical friction.

Table 5.5 Reduction for washing durability tests

Washing times / Method	10	30	50
Method 1	92.3 ±2.2	86.1 ±2.4	84.7 ±2.1
Method 2	95.1 ±1.6	81.2 ±1.9	84.0 ±1.1

Note: Method 1 is performed according to AATCC 61-2003 2A method; Method 2 is performed according to AATCC 61-2003 1A method.

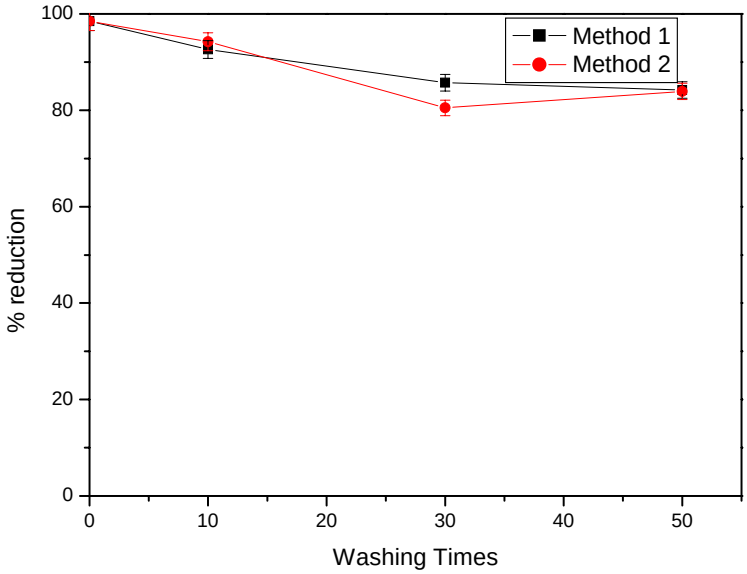

Figure 5.12 Bacteria reductions of samples with different washing times

5.4 Conclusions

In the aspects of mechanical properties, 63CSC and 63CSE were slight damaged during the finishing process. Break strength and tearing strength of the two samples decreased comparing to the control sample. According to the results of wrinkle recovery angle test, no remarkable promotion on anti-wrinkle property was achieved by the finishing. The emulsion-finished sample had better handle properties than the solution-finished one, and was inferior to the control sample.

In this research, the antibacterial ability of the cotton fabrics was enhanced remarkably after finished with either the emulsion or the solution while the emulsion-finished samples behaved better in different usages of chitosan, and the solution-finished samples needed additional treatments with sodium carbonate

solution to remove the residual acetic acid to avoid the losing of the chitosan when washed with tap water. The antibacterial activities decreased when reducing the usages of chitosan, using of 0.01% chitosan content conducted a bacterial reduction of less than 40%. After-treatment using crosslink agent, DMDHEU, could lead to a negative effect. Antibacterial tests with the emulsion-finished samples at neutral circumstance of pH 7 still gave good results.

As far as the washing durability of the emulsion finished samples, bacteria reduction of 80% was obtained with the samples even after being washed equal to standard home laundry of 50 times, indicating that the emulsion-finished samples held good durability to the chemical and mechanical corrosion.

Chapter 6

Antibacterial and deodorizing finishing of cotton fabrics using the nanoparticles of the chitosan/silver oxide composite

6.1 Research background

Silver is studied substantially due to its perfect antibacterial activity [135-137] and silver-based antibacterial materials attracts much attention because of their long-term biocidal activity, low volatility and the non-toxicity of the active silver ion to mammalian cells [138,139]. Many of these materials were introduced, which were prepared through either doping silver onto the host materials [140-143] or compositing it with other compounds [144-146]. Among them, new silver-based antibacterial polymers represent a great challenge for both the academic world and industry [145]. Meanwhile, to our knowledge, few efforts were done about aqueous silver-based polymer dispersive system, such as nanoparticulate silver-contained emulsion. A uniform and stable emulsion is believed to be advantageous in many fields, for instance, directly coating of biomaterials or medical textiles in the biologic, or therapeutically applications. But most of presented work has to use additional surfactants, reductants, emulsifiers or other assistant agents. These chemicals may cause undesirable side-effects.

As mentioned in the ***Introduction*** and ***Literature Review*** sections, chitosan is widely used as a nature biocide because of its excellent properties, such as antibacterial, non-toxic, biodegradable, biocompatible [147-151]. What's more important here is that the amino groups and hydroxyl groups of chitosan can form chelate complex with silver ions [152, 153]. This property provides a possibility to use chitosan as both reductant and surfactant in the preparation of nano-scale

silver-based materials from silver ions. The research work was done on the preparation of chitosan/silver nano-composites, which proved the ability of chitosan to reduce the silver ion into metallic silver [154-158]. However, most of these nano-composites were solid, such as fibers, powders and films, due to their poor stability in water.

In ***Chapter 5***, we studied the antibacterial activity of the emulsion of the pure chitosan nanoparticle with comparing that of the chitosan solution. The emulsion behaved better than the solution, but both of them required higher concentrations for a stable and efficient bacteria reduction, which led to the properties alteration of the original fabrics. The good stability of the emulsion benefiting from the hydrogen bonds between chitosan and water led us to believe that a stable silver emulsion could be achieved if the nanoparticulate silver was encapsulated into the chitosan nanoparticles. The combination of chitosan nanoparticles and silver oxide nanoparticles should succeed the efficient and long-term antibacterial activity of silver oxide and the stability of chitosan nanoparticles in the emulsion as well as the perfect biocompatible and eco-friendly property of the two materials.

6.2 Materials and experimental

Chitosan (degree of deacylation: 95%, molecule weight: 500 kDa) was purchased from Haidebei Ltd. China. Other used chemicals were chemical grade from Aldrich

Chem. Co. Ltd. and used as received.

6.2.1 Preparation of the chitosan/silver oxide nanoparticles

Typically, 5 ml 5 % (w/v) $AgNO_3$ solution was dropped into 150 ml 0.5% (w/v) chitosan solution of 0.3% (w/v) dilute acetic acid under magnetic stirring. After certain stirring duration (typically 4 hours), a 1% (w/v) sodium hydroxide solution was dropped into the silver-contained chitosan solution to produce black precipitates.

The precipitates were aged in pH of 11 for one hour, and subsequently rinsed to neutral with deionic water. A black emulsion was finally achieved with the rinsed precipitates through our new developed ultrasound method described in Chapter 4.

6.2.2 Morphology characterization

The emulsions were characterized by laser scanning through a Zetasizer 3000HSA; Scanning electron microscopy (SEM) analyses were performed through a JOEM JSM 6335F; samples were placed on the surface of pre-washed silicon wafer for the investigation. Transmission electron microscopy (TEM) analyses were performed through a Philips CM-20 TEM; some of the samples were stained using phosphotungstic acid (1% w/v) at pH 7. Atomic force microscopy (AFM) analyses were performed through a Seiko SPM-2.

6.2.3 Preparation of cotton samples

The finishing processes were performed through using the conventional pad-dry-cure method. Cotton fabrics were soaked with the finishing liquid for 3 minutes, subsequently padded with a 80% pick-up through a pair of padding rollers (Rapid Vertical Padder, Taiwan). The process was repeated twice. All the padded samples were dried at 100 ^{o}C for 3 minutes and cured at 150 ^{o}C for 3 minutes.

6.2.4 Antibacterial test and deodorization test

The Flask Shake Method (ASTM E2149-01) was used for the antibacterial test against E. coli and S. aureus, which was previously described in Chapter 5.

To prepare the artificial sweat for the deodorization tests, the following recipe was used:

sodium chloride (20g/L), ammonium chloride (17.5g/L), urea (5g/L), acetic acid (2.5g/L), lactic acid (15g/L),1-histidine monohydrochloride (0.25g/L). The pH was adjusted to 4.7 using 1.0M sodium hydroxy.

And the following recipe was used to prepare the nutrition broth:

“Lab-Lemco” powder (10g/L), sodium chloride (5g/L), Bacterialogical peptone (10g/L).

In the deodorization test, all the samples were padded after being immersed into the

artificial sweat for 3 min, and then put into sealed plastic bags separately with nutrition broth and human sweat. After that, all the samples were placed in the water bath at 37 ^{o}C for three days. A subjective method was used in the odor assessment, four persons were asked to smell the samples and give their comments.

The washing fastness tests were performed according to AACTT 63 option 1, which was also used in ***Chapter 5***.

6.3 Results and discussion

6.3.1 Growth of silver nanoparticles in the chitosan/$AgNO_3$ solution

Adding a $AgNO_3$ solution in to a chitosan solution changed the color of the chitosan/$AgNO_3$ solution phenomenally from colorless to brown slowly. **Figure 6.1** shows the UV–vis spectrum of the chitosan/ $AgNO_3$ solutions in different stirring time from 0 to 99 hours, in which two gradually increasing peaks were observed from 350 nm to 700 nm wavelengths. Silver nanoparticles absorbed radiation in the visible region of the electromagnetic spectrum due to the excitation of surface plasma vibrations, responding to the striking violet color of silver nanoparticles in various media [156-158]. The peak at 390 nm wavelength corresponded to the plasma in this study with increasing intensity of the peak, implying the size change of silver particles [154]. **Figure 6.2** shows SEM **(a)** and TEM **(b)** micrographs of

the chitosan/AgNO3 solution in a short stirring duration, in which silver nanoparticles about 20nm were observed. The other peak shifting from 500 nm to 600 nm wavelength was supposed to relative with the non-spherical morphology of the obtained particles. After a longer stirring duration, nano-scale hexagonal silver crystals were observed with size of around 200 nm, as shown in **Figure 6.3**. These nanoparticles kept growing until black precipitates appeared finally after a stirring duration of several days.

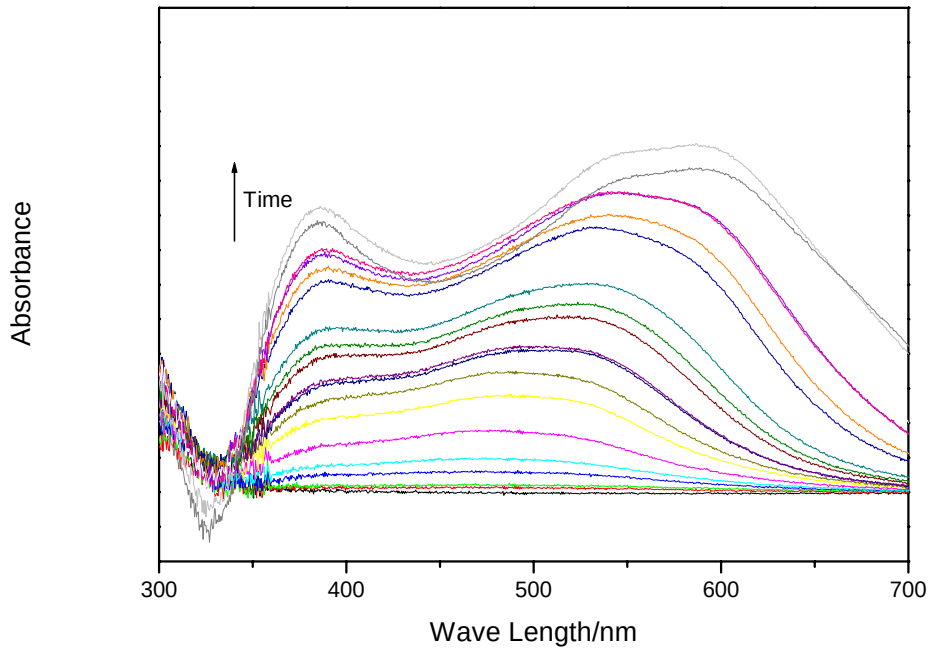

Figure 6.1 UV-vis spectrum of the chitosan/$AgNO_3$ solution at different stirring duration

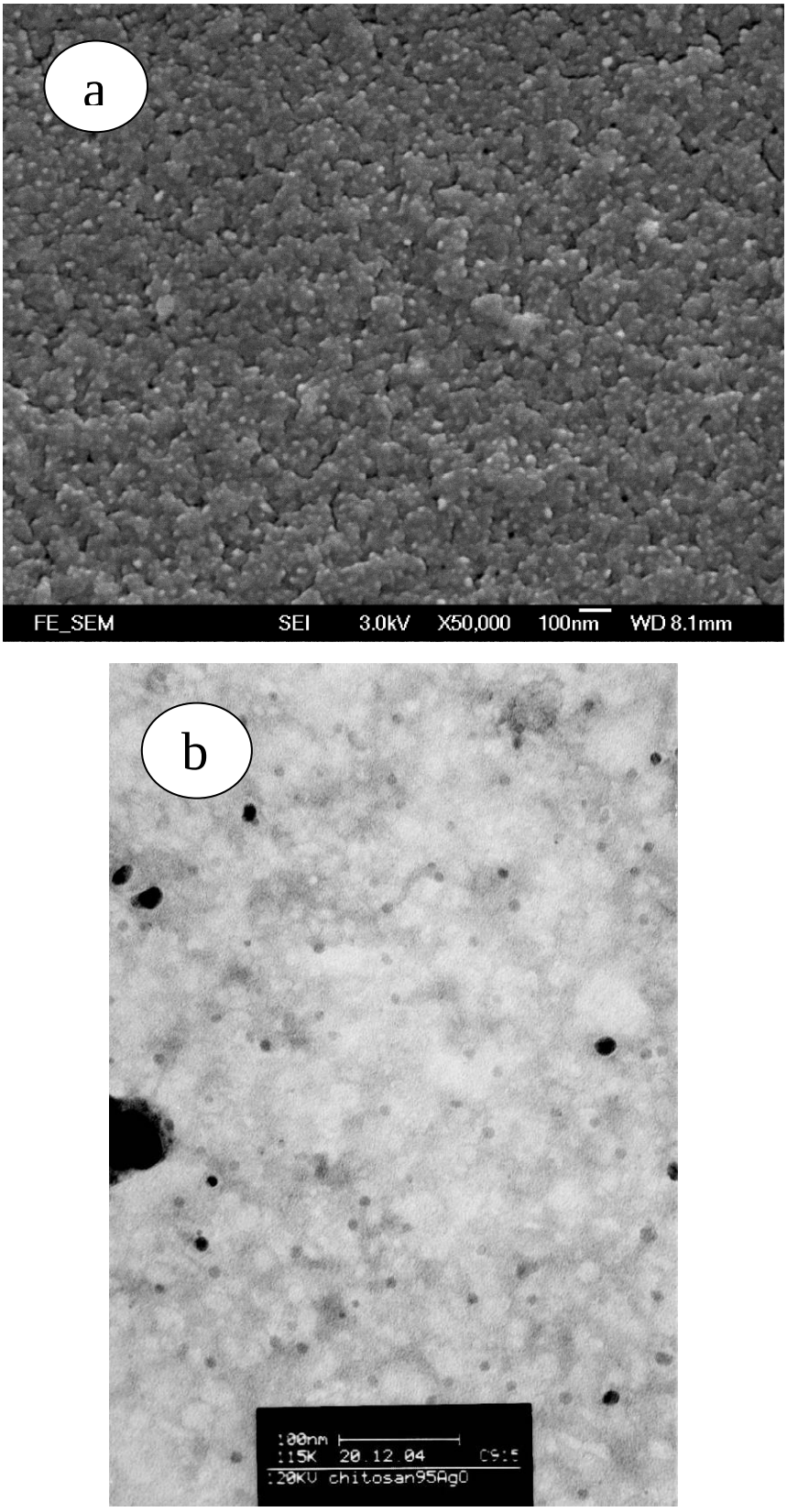

Figure 6.2 (a) SEM micrograph of the films from the mixed chitosan solution through freezedrying and (b) TEM micrograph of the chitosan/$AgNO_3$ solution after stirring of 5 hours

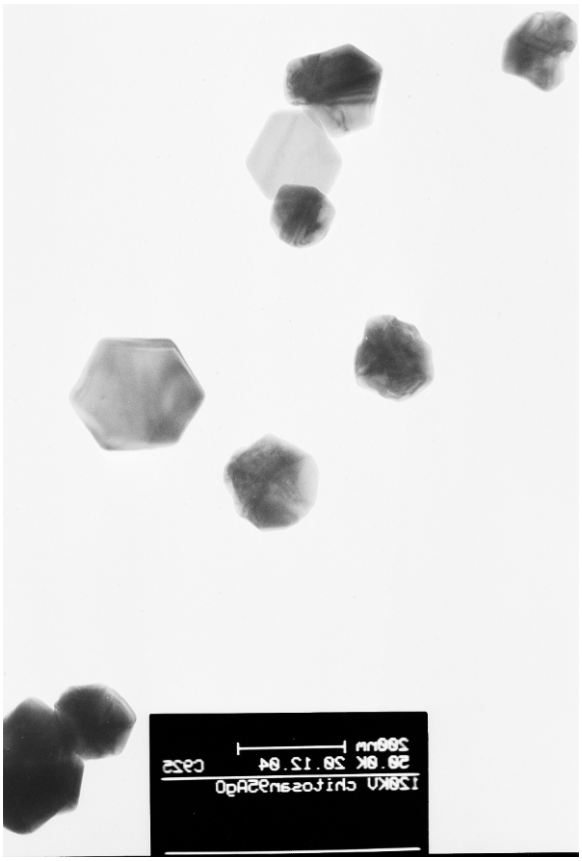

Figure 6.3 TEM micrograph of the silver crystal generated in the reactive solution after 30 hours

There are two main views on the interactions between chitosan and silver ions. The first school believes that, when silver nitrate is mixed with chitosan solution, silver ions can be bound to chitosan macromolecules probably via electrostatic interactions because the electron-rich oxygen atoms of polar hydroxyl and ether groups of chitosan are expected to interact with electropositive transition metal cations [157,161]. The other school argues that chitosan-metal ion complex formation occurs primarily through the amino groups of chitosan functioning as ligand [153]. **Figure 6.4** illustrates the IR spectra of the freeze-dried products of the

chitosan/AgNO3 solution after stirring duration of 5 hours (**Figure 6.4 (a)**) and pure chitosan (**Figure 6.4 (b)**). The differences between the two spectra focussed on 2800-3500cm^{-1}, 1500-1700cm^{-1}, 900-1100cm^{-1} and 700-400 cm^{-1}, which mainly corresponded to the stretching vibration and bending vibration of the amino group and hydroxyl group. The peaks of NH_2 and OH groups between 3000 cm^{-1} and 3500cm^{-1} had significant changes, indicating that the NH_2 and OH groups had certain interaction affecting their vibration characteristics. The 1680cm^{-1} peak of $CONH_2$ and 1600cm^{-1} peak of NH_2 shifted separately to 1640cm^{-1} and 1560cm^{-1}, which implied that the amino groups had a new interaction with the silver. New bonds observed in 700-400 cm^{-1} were assigned to the stretching vibration of N-Ag and O-Ag. Bonding with Ag(I) caused the substantial redistribution of different types of vibrations associating with the amino groups and hydroxyl groups.

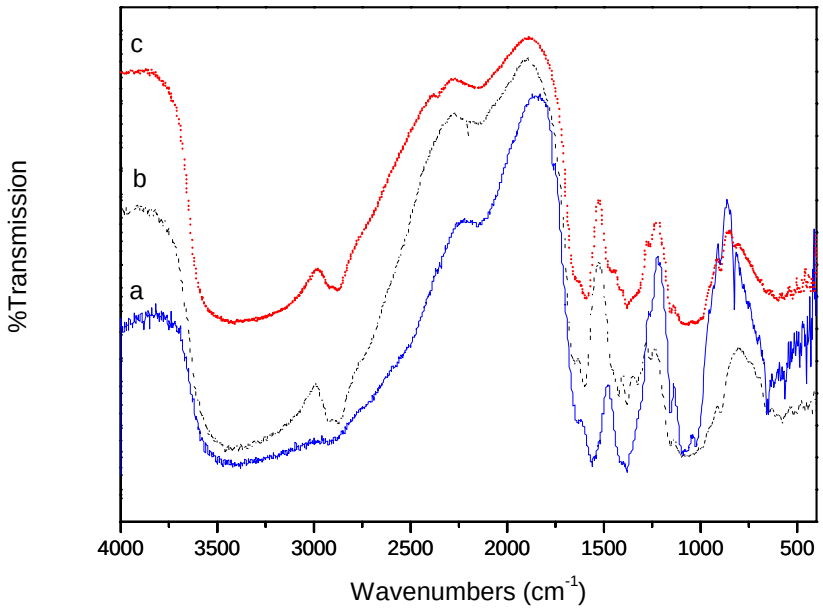

Figure 6.4 IR spectrums of (a) the freeze-dried products, (b) the pure chitosan and (c) the chitosan/silver oxide nanoparticles

On the other hand, **Figure 6.5 (a, b)** shows the XRD spectra of pure chitosan and the freeze-dried products of the chitosan/ $AgNO_3$ solution. There were mainly two strong peaks at about 10 and 20 degree for the pure chitosan due to the high degree of crystallinity [162,163], which disappeared in the spectrum of the latter. The disappearance of the peaks reflected loss of orderness in the chain alignment of chitosan, and new peaks were observed identifying silver and silver oxide [164-167]. When a host substance crystallizes with a solute additive, this substance can observe either a matrix lattice parameter alteration, or the formation of a new crystalline phase which is characterized by new bonds in the XRD pattern, and the latter occurs when the solute atoms occupy well-defined positions in the matrix lattice [153]. The above crystalline behaviour and the analyses of IR spectra revealed that the amino groups and hydroxy groups of chitosan were involved in the interactions between chitosan and silver.

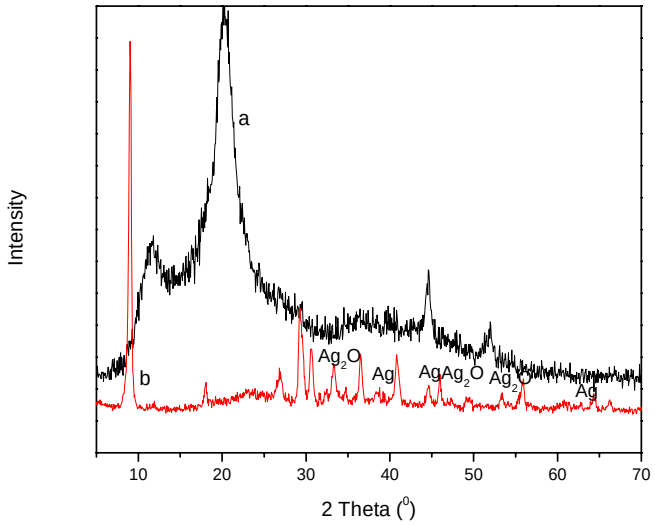

Figure 6.5 XRD spectra of (a) the chitosan and (b) the chitosan/silver complex

However, these complex interactions between silver and chitosan could not take the role of stabilizers for the generated nanoparticles. These particles kept growing and aggregating, finally deposited from the solution.

6.3.2 Preparation of chitosan/silver oxide nanoparticles

The peaks in **Figure 6.5 (b**) were not observed in the XRD spectrum of the black precipitates, and the crystalline peaks of chitosan appeared again companying peaks of silver oxide, as **Figure 6.6** shows. The alkaline treatment obviously destroyed the complex interactions between chitosan and silver, consequently freed the chemical groups of chitosan to form inter- and intra- hydrogen bonds that recovered the crystallinity of chitosan. Silver was oxidized into silver oxide simultaneously. The IR spectrum investigation also indicated the disappearance of the complex interactions. The spectrum of the precipitates was similar to that of pure chitosan, as **Figure 6.4 (c)** shows.

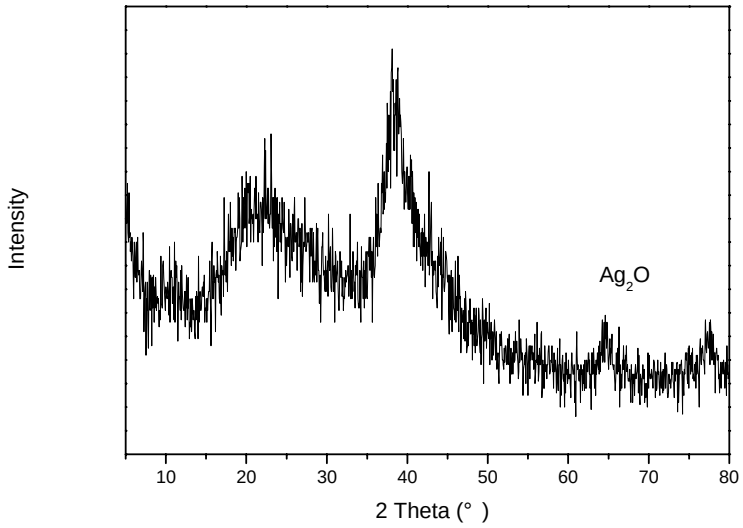

Figure 6.6 The XRD spectra of the chitosan/silver oxide nanoparticles

The achieved black emulsion from the black precipitates could stand for storage of over three months with no visible change. The result of laser scan indicated that the nanoparticles in the emulsion had an average size around 300nm with a zeta potential of +70 mV. The positive charge of the nanoparticles in the emulsion suggested the emulsions would be stabilized by the hydrogen bonds that were also observed in the emulsion of pure chitosan nanoparticles described ***in Chapter 4***. When heated to over 90 ^{o}C, the emulsion turned into aggregates immediately due to the break of the hydrogen bonds at a high temperature. On the other hand, a single peak at 440 nm wavelength shown in **Figure 6.7** should be the diffraction of the typical plasma vibration of silver.

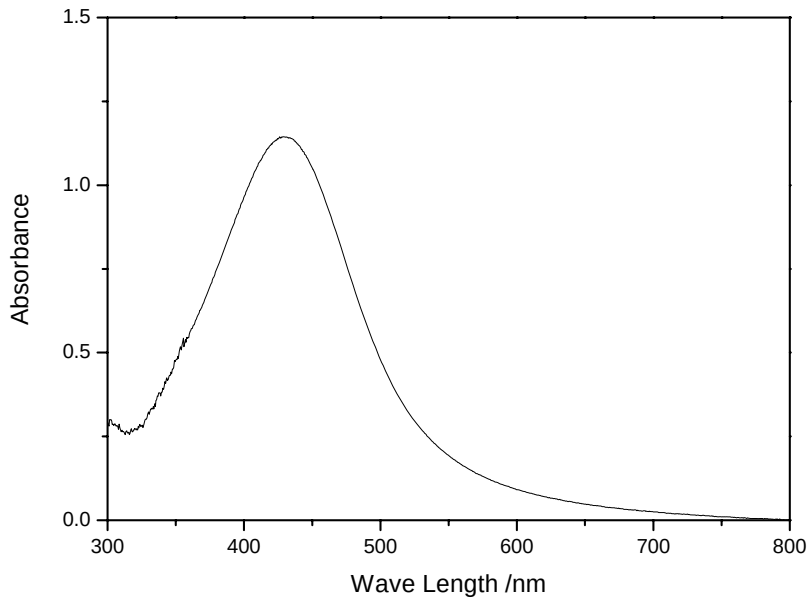

Figure 6.7 UV-vis spectra of the emulsion of the chitosan/silver oxide nanoparticles

Silver oxide nanoparticles were believed to be encapsulated into the chitosan nanoparticles, forming a nano-fabrication that was similar to that of dendrimer-metal nanoparticles system [171]. **Figure 6.8 (a)** illustrates the spherical profile of the chitosan/silver oxide nanoparticles of about 100 nm with a narrow size distribution. It was further confirmed through AFM microscopy, as **Figure 6.8 (b)** shows. The TEM microscopy in **Figure 6.9** disclosed the chitosan/silver oxide nanoparticles encapsulating the uniform silver oxide nanoparticles about 10-20nm, closely agreed to the results of the SEM and AFM microscopy. The result of the microscopic analysis proved successful immigration of silver oxide nanoparticles into the chitosan nanoparticles.

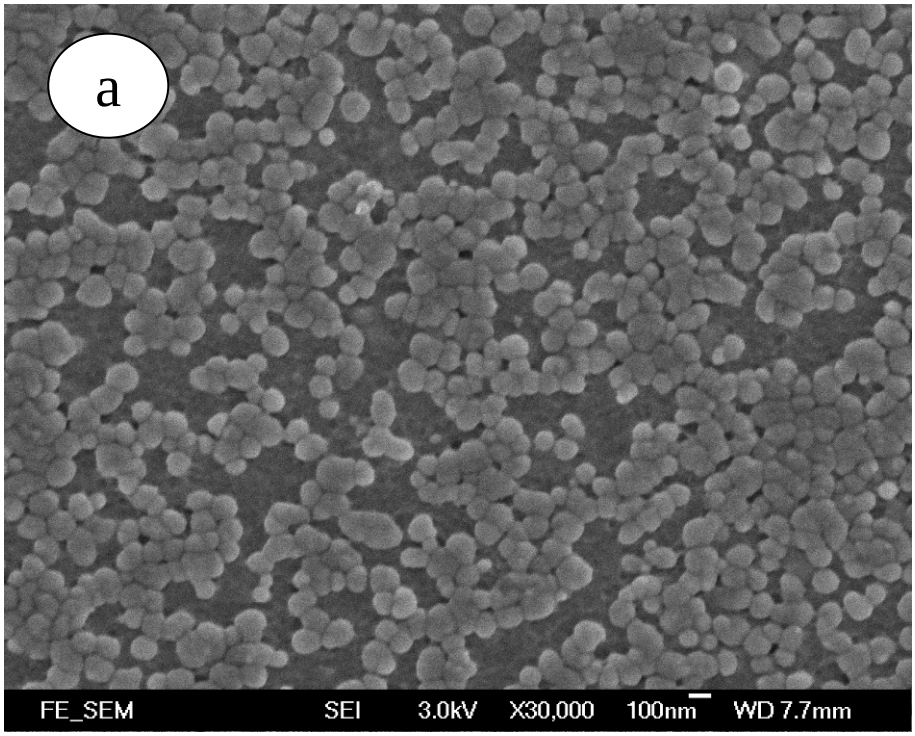

Figure 6.8 (a) SEM micrograph of the chitosan/silver oxide nanoparticles

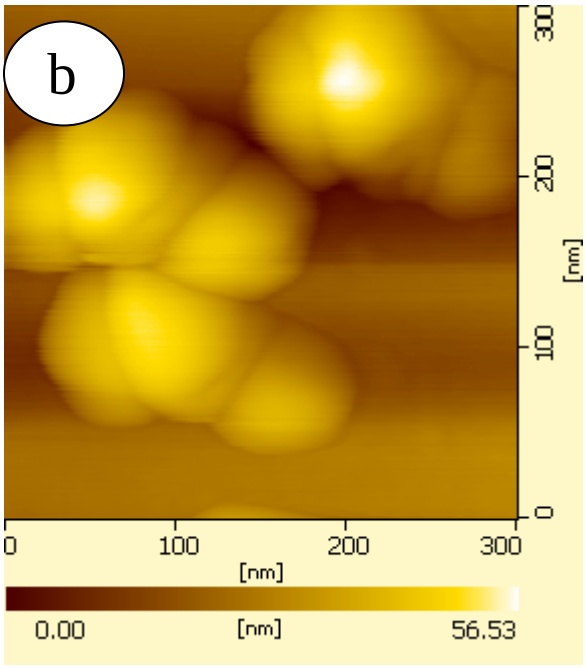

Figure 6.8 (b) AFM micrograph of the chitosan/silver oxide nanoparticles

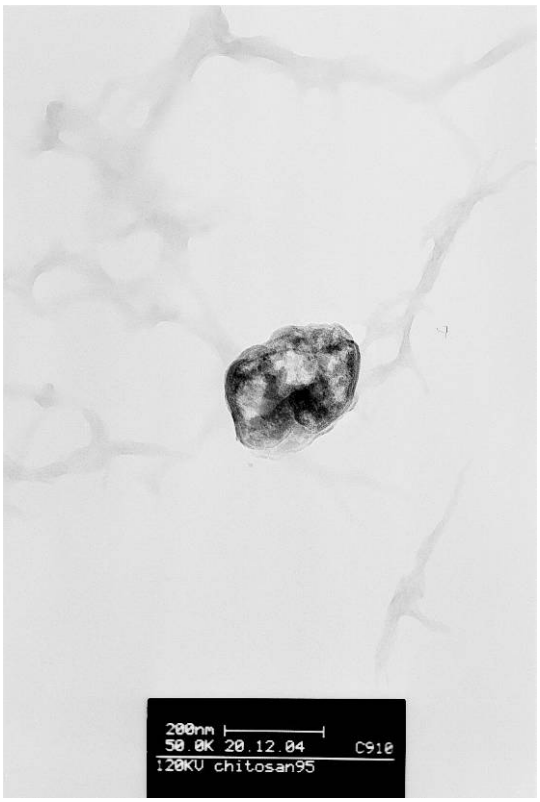

Figure 6.9 TEM micrograph of the chitosan/silver oxide nanoparticles stained using phosphotungstic acid (1%) at pH 7

As the precursor, the silver nanoparticles growing in the chitosan/ $AgNO_3$ solution were important for the uniformity of silver oxide nanoparticles. Both the chemical bonding and separating effects of chitosan molecules in the chitosan/ $AgNO_3$ solution played as size controllers for either the silver nanoparticles or the final silver oxide nanoparticles. A comparative experiment was done with immediately adding of sodium hydroxide solution after the $AgNO_3$ solution was mixed into the chitosan solution. The obtained emulsion turned into precipitates after several days. The results indicated that a proper growing time for the silver nanoparticles in the chitosan/ $AgNO_3$ solution was important for the stability of the final emulsion of the chitosan/silver oxide nanoparticles.

6.3.3 Morphology of treated cotton and its performance in antibacterial

As **Figure 6.10 (a)** shows, the nanoparticles built up a rough layer on the surface of cotton fibres, in which small silver oxide nanoparticles were supposed to disperse. In the microscopy with a higher resolution, as shown in **Figure 6.10 (b)**, the silver oxide nanoparticles could be identified. Five concentrations of the emulsion were applied to finish the cotton fabrics in the study, and the tests of the antibacterial tests are shown in **Figure 6.11**. All samples displayed high activity of antibacterial and 100 % bacteria reductions were obtained. In ***Chapter 5***, we studied the antibacterial activity of the cotton fabrics finished with a low concentration of the pure chitosan emulsion, and using of 0.01% chitosan content conducted a bacterial reduction of less than 40%. The results indicated that a trace of silver oxide enhanced the

antibacterial activity of the emulsion remarkably. **Figure 6.12** shows the antibacterial activities of the control sample, the sample finished with the emulsion of 6 ppm and the finished sample after 20 washings. The cotton fabric finished with the emulsion of chitosan-silver oxide nanoparticles had a 100 % bacterial reduction to S. aureus and E. coli respectively at pHs 5 or 7, and the bacterial reduction remained unchanged after 20 washings.

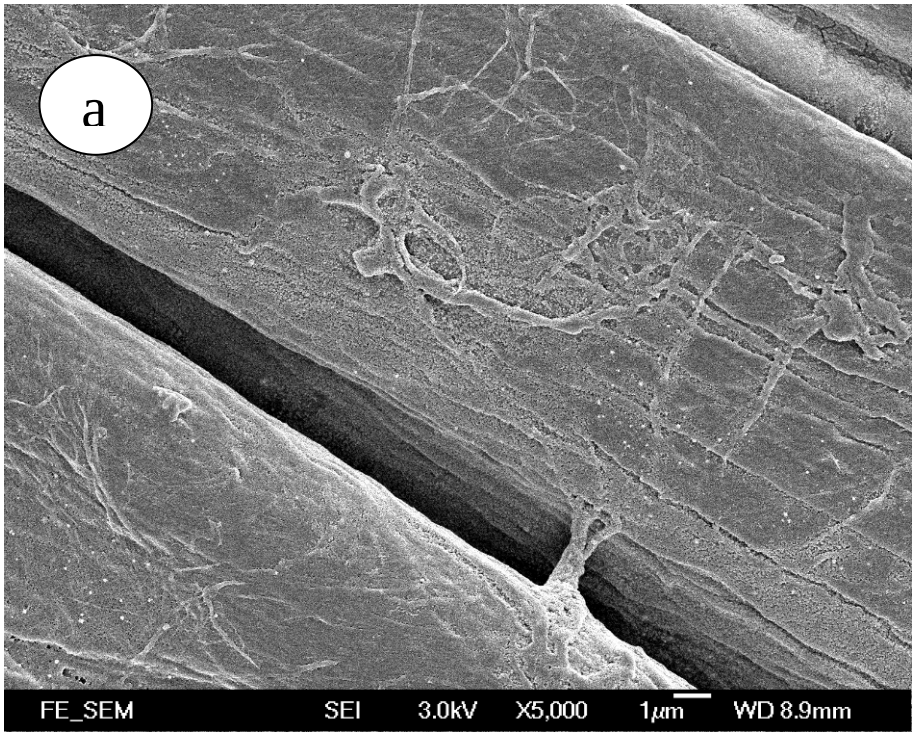

Figure 6.10 SEM micrograph of the surface of finished cotton fabrics

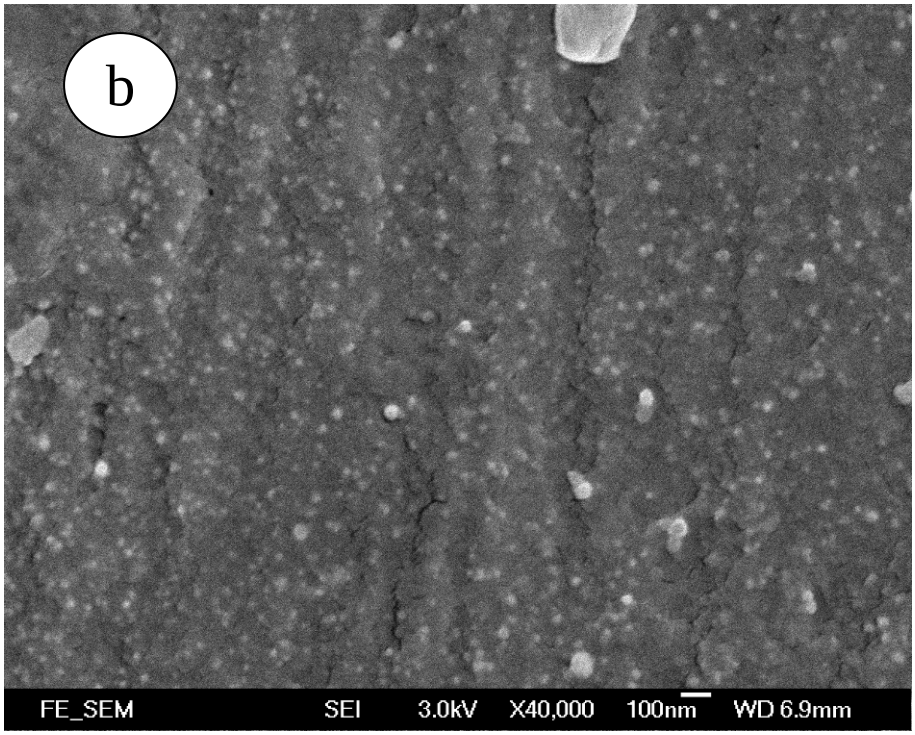

Figure 6.10 SEM micrograph of the surface of finished cotton fabrics

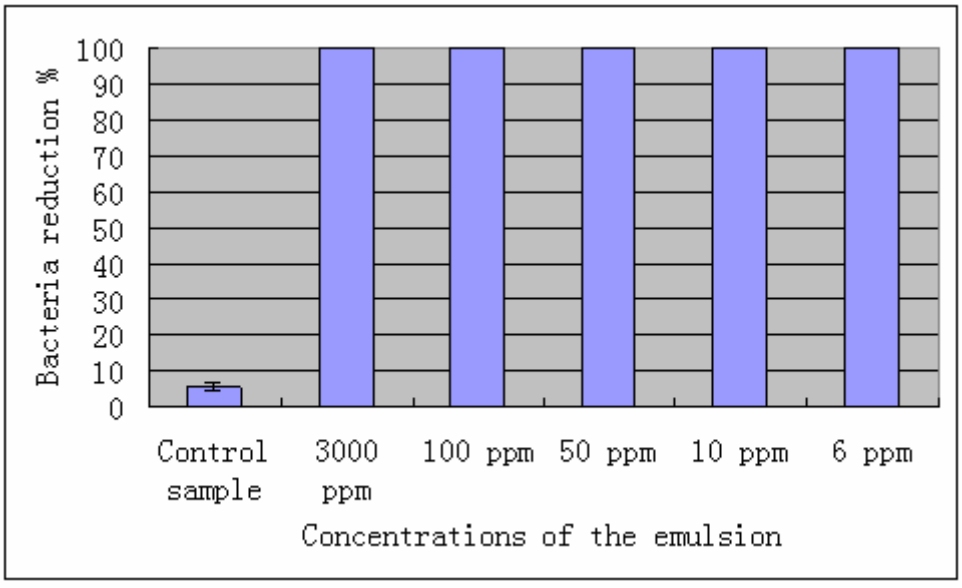

Figure 6.11 Results of antibacterial tests of cotton fabrics finished with different concentrations of the chitosan/silver oxide emulsion

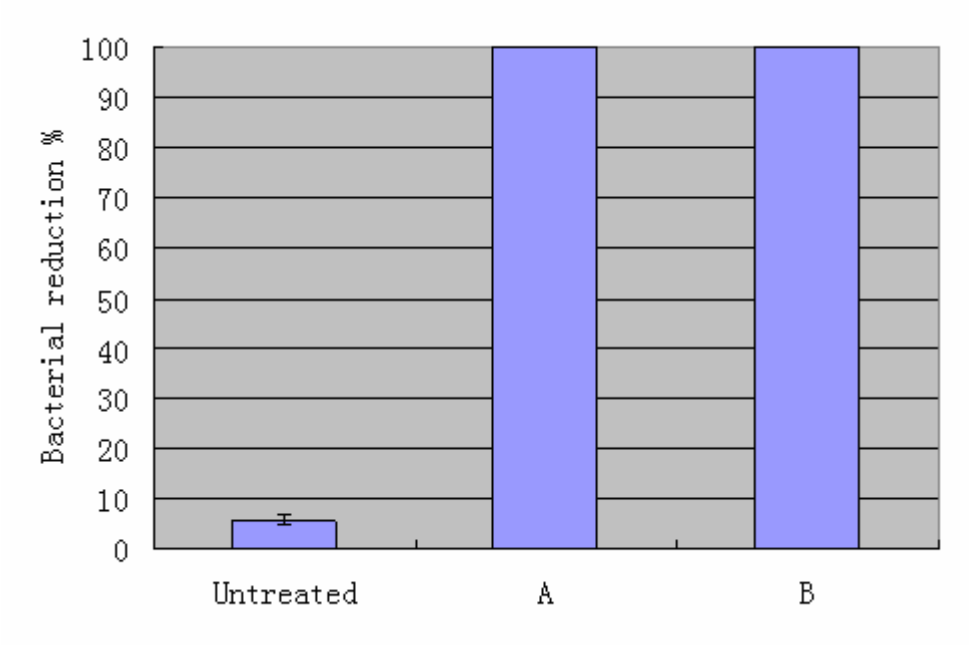

Figure 6.12 Comparison of bacteria reduction before and after treating cotton fabrics with the composite chitosan/silver oxide nanoparticles (Sample A), or the treated cotton fabrics after standard home laundry of 20 times (Sample B)

6.3.4 Freshness finishing of the cotton fabrics

Body odor is the term describing any unpleasant smell associated with a person's body while he or she may not be aware that the odor is offensive to others sometimes. A person has body odor due to all kinds of reasons and hyperhidrosis is a condition that causes an offensive body odor. Hyperhidrosis or excessive sweating is caused when nerves controlling the sweat glands become overactive or hyperactive.

A lot of research was contributed for the odor removal. In U.S. Pat. No. 3,857,732 activated carbon was used to remove odors, in which a conventional non-woven fabric had its fibers coated with a water insoluble composition that could include

activated carbon. Similarly, U.S. Pat. No. 5,744,236 disclosed a non-woven media of fibers made of polyamides, polyesters, or polyolefins, and activated carbon was entrapped within the hollow cavities of the fibers in the absence of an adhesive to thereby adsorb odor molecules.

On the other hand, a non-woven activated carbon fabric was shown in U.S. Pat. No. 4,565,727 for the use of protective clothing. The fabric was prepared by wet-laying the activated carbon with fibrillated acrylic fibers. Thereby, toxic compounds were adsorbed and water vapor (such as perspiration) permeates through the fabric. Of course, since water vapor permeates, the fabric was not removing water. A filter that not only removes odors but also absorbs water was described in U.S. Pat. No. 5,783,080 and U.S. Pat. No. 6302932.

An odor-removing composition may include a magnesium-containing salt mixed in water is described in U.S. Pat.5976193. In one embodiment, the odor-removing composition contains magnesium sulfate mixed in purified water. A unique filtration device can continuously remove odor contaminants from an air stream through the use of a wicking fiber material containing a selected chemical reagent package effective at removing a wide range of odors and having superior performance at higher humidity, as described in U.S. 5891221. The basic reagent package contains sodium permanganate in combination with sodium carbonate or sodium phosphate into which other reagents can be added for additional odor removal capabilities.

Meanwhile, though people generally associate body odor with sweating, sweating itself does not send off any offensive odor or smell. Our sweat consists of water and salts expelled by our sweat glands for the purpose of controlling our body temperature. It is the bacteria on the skin which mixes with the sweat and produces body odor that can sometimes be a sign of serious illness. Most of the contributed works are focused on the remove of the conducted body odors but little attention is given in preventing them from occurrence. Since the emulsion of the chitosan/silver oxide nanoparticles is proved to be high activity in antibacterial, it is feasible to suppress the bacteria growth in the sweat, consequently avoid the body odors.

In our research work, cotton fabrics were finished using the silver-contained emulsion, the pure chitosan emulsion and the gamma-cyclodextrin solution for a comparative investigation. **Table 6.1** summarizes the results of the investigation. As shown, control samples without human sweat did not have ammonia smell; neither did the gamma-cyclodextrin-finished sample. It proved that the bacteria in the human sweat were the true reason of the body odors. Both the silver-contained emulsion and the pure chitosan emulsion displayed activity of deodorization, as shown in the **Table 6.1** too, but a higher concentration of the pure chitosan emulsion was required. According to the results, a concentration lower than 1 mg/mL of the pure chitosan emulsion led to the ammonia smell. The silver-contained emulsion behaved best in this case.

Table 6.1 The results of comparative deodorizing test

Comment / Samples	A	B	C
Control sample without human sweat	Sweet smell	Sweet smell	Sweet smell
Control sample	Ammonia smell	Ammonia smell	Ammonia smell
Cotton finished with gamma-cyclodextrin (5 mg/mL)	Sweet smell	Sweet smell	Sweet smell
Cotton finished with the emulsion (2 mg/mL)	No smell	No smell	No smell
Cotton finished with the chitosan solution (0.3 mg/mL)	Ammonia smell	Ammonia smell	Ammonia smell
Cotton finished with the chitosan solution (0.6 mg/mL)	Slight Ammonia smell	Slight Ammonia smell	Slight Ammonia smell
Cotton treated with the chitosan solution (3 mg/mL)	No smell	No smell	No smell

Because the silver-contained emulsion behaved best in this case, more work was done to disclose deodorizing effect of the silver-contained emulsion. As shown in **Table 6.2**, cotton fabrics finished using the emulsion of 0.02 mg/mL still had efficient deodorizing activity while 0.002 mg/mL one behaved not bad. So we can say that the silver-contained emulsion could improve the cotton fabrics a remarkable deodorizing activity.

Table 6.2 Results of deodorizing tests with the silver-contained emulsion at different concentrations

Comment / Samples	A	B	C
Cotton finished with the emulsion (2 mg/mL)	No smell	No smell	No smell
Cotton treated with chitosan/silver (0.2mg/mL)	No smell	No smell	No smell
Cotton treated with chitosan/silver (0.02 mg/mL)	No smell	No smell	No smell
Cotton treated with chitosan/silver (0.002 mg/mL)	Slight ammonia smell	Slight ammonia smell	Slight ammonia smell

Concerning the durability of the finished cotton, the samples finished using silver-contained emulsion underwent further washing fastness tests. The samples were washed 20 times before deodorizing tests .The results are shown in **Table 6.3**. Comparing the results in **Table 2**, the samples finished with concentration of 0.02 mg/mL became inferior in the deodorizing activity when the 0.002 mg/mL one lost it almost completely. A concentration of over 0.02 mg/mL was preferred for a long term deodorizing activity with a good durability to water washing.

Table 6.3 Washing durability towards the deodorizing activity

Comment / Samples	A	B	C
Cotton treated with chitosan/silver (2mg/ml)	No smell	No smell	No smell
Cotton treated with chitosan/silver (0.2mg/ml)	No smell	No smell	No smell
Cotton treated with chitosan/silver (0.02mg/ml)	Slight ammonia smell	Slight ammonia smell	Slight ammonia smell
Cotton treated with chitosan/silver (0.002mg/ml)	Ammonia smell	Ammonia smell	Ammonia smell

6.3.5 Color change of the finished samples

The colour of silver is a widely-met problem in the applications of textile because treated cotton will become yellow when a higher concentration of silver is used. But in our research, the problem was overcome due to the trace usage of the silver. **Table 6.4** describes the test results of the yellow index of the sample finished with the emulsion of 0.2 mg/mL. The yellowness of the treated fabric was higher than that of the untreated but the change is small. In other words, the visual appearance

of the finished sample was similar to that of the unfinished.

Table 6.4 Yellowness index tests

Samples	Illum/obs.*	ASTM-E313	ASTM-D1925
Control sample	C/10	6.96±0.23	7.92±0. 22
	C/2	5.32±0. 19	6.65±0. 17
Finished sample	C/10	7.39±0. 25	8.50±0. 24
	C/2	5.71±0. 21	7.22±0. 19

Note: Illum: illuminant; obs.: observer

6.4 Conclusion

The formation of silver nanoparticles in the chitosan/$AgNO_3$ solution was studied. The results indicated that silver ions formed complicated chelating complex with chitosan, and hexagonal silver crystals were observed. The complex was unstable in the solution and turned into black precipitates finally. After a further alkaline treatment, silver nanoparticles were oxidized into silver oxide nanoparticles. The chemical interactions between silver and chitosan in the chelating complex were destroyed, and a fabrication of silver oxide nanoparticles in chitosan was obtained. An emulsion was achieved through an ultrasound method, which was consisted of positively charged composite chitosan/silver oxide nanoparticles with 10-20 nm silver oxide nanoparticles encapsulated. The emulsion had a good stability and could bear months of storage though no surfactant or other additive stabilizer was used.

After finished with the emulsion even at very low concentrations, the cotton

fabrics had an excellent antimicrobial property. The finished cotton fabrics also had an efficient deodorizing activity. Washing fastness tests were performed, proving the durable activities of antibacterial and deodorization of the cotton fabrics finished with the emulsion was good. The application of such low concentrations also avoided the colour problem of silver successfully and reserved the original characteristics of the treated cotton fabrics.

Chapter 7

Dyeability improvement of fabrics using the pure CSNPs

7.1 Research background

Large quantities of aqueous waste and dye effluents are discharged from the dyeing process with strong persistent color and high BOD loadings that are aesthetically and environmentally unacceptable in the textile industry [172]. Most of these dye wastes are harmful to the environment [173]. Dyeability improvement of textile fabrics through physical or chemical methods could be an efficient way to reduce the dosages of dyestuffs and other additives in the dyeing process and consequently alleviate the pollution to the environment. On the other hand, requirements of safety in the textile become great challenges for current researchers to explore a biocompatible and nontoxic process of textile finishing when most of the processes nowadays could be harmful to humans.

Chitosan can fit up to the above purpose because of its good biocompatibility, biodegradability, non-toxicity and functional chemical properties [174-181] as well as its cationic property from its protonated amino groups in an acidic condition making it easy to adsorb anionic dyes, such as direct dyes, acid dyes and reactive dyes [181]. The sorption of various dyes on chitosan fibers was studied, disclosing its high potentials of the adsorption of dyes [182-185]. This property is useful in the dyeing of protein fibers, such as wool and silk, because chitosan has very good affinity to them [186]. Endeavors to improve the dyeability of silk using chitosan were done [187-189], unclosing considerable potential of chitosan in this application. Whereas, surface modification of protein fabrics with chitosan

nanoparticles (CSNPs) seems seldom be reported while the latex coatings have been an active area of research for a long time [190-196]. Because the adsorption of dyes by chitosan mostly occurs in the interface by electrostatic interaction, huge surface area of nano-structure from the CSNPs will promise noteworthy advantage for improvement of dyeability of these fabrics.

This research was set up to disclose the potential applications of CSNPs as a kind of latex in surface modification for the nano-structure. Silk fabrics were chosen as a typical representative of protein fabrics because of its limited dyesites (*ca* 250 mmol/kg ammonium groups) than wool (*ca* 850 mmol/kg) [204]. A small number of dyesites was chosen for comparison of the dyeability of the fabrics before and after the surface modification using CSNPs. Furthermore, the smooth surface of the silk fabrics was much beneficial to the investigation of the surface changes. The silk fabrics were coated with the CSNPs through a pad-dry-cure finishing process. Dyeing of the finished silk fabrics was performed with three acid dyes and three reactive dyes accompanying with the morphology investigation of the silk surface through scanning electron microscopy (SEM), to figure out the relationship between the modality and the dyeability of the silk fabrics. The nylon fabrics (*ca* 30-50 mmol/kg NH2 groups) [204], as a typical artificial fabrics, were also used in the research to disclose potential applications of the CSNPs in the artificial fabrics.

7.2 Materials and experimental

7.2.1 Materials

Chitosan (95%DD, Mw 500 kDa) was purchased from Haidebei Co. Ltd. China. Scoured and degummed woven silk fabrics were purchased from Yue Hwa C.P.E. Ltd. Hong Kong. Lanaset series dyes (acid dyes) and Lanasol series dyes (reactive dyes) were from Ciba Specialty Chemicals Inc. Other used chemicals were from Aldrich Chem. Co. Ltd. and used as received.

7.2.2 Experimental

7.2.2.1 Finishing of silk with the emulsion of CSNPs

Aqueous emulsions of the chitosan nanoparticles were prepared with our newly developed method described in ***Chapter 4***. Nonionic detergent pre-washed silk fabrics were soaked for 15 minutes in the emulsions with different concentrations separately: 0.01%, 0.05%, 0.1% and 0.3% (w/v). The padding processes were then completed with pick up weight of around 80%. Finally, the silk fabrics were dried at 80 ^{o}C for 3 min and cured at 150 ^{o}C for 3 min. Comparing experiments were performed with chitosan solutions of 0.5% (w/v) dilute acetic acid in four concentrations relative to these of the emulsions.

The chitosan contents in the silk fabrics were determined through extracting the finished fabrics with 1% (w/v) dilute acetic acid at 25 ^{o}C for 24 hours under shaking.

The chitosan concentrations were calculated through UV-vis absorption method with a standard calibration curve obtained from standard chitosan solutions.

7.2.2.2 Physical assessment of finished fabrics

ASTM Test Method D 5035 1R-L was used for the break strength tests. Six pieces of each sample were tested in the warp direction and weft direction separately, and average values were used. ASTM Test Method D 1424 was used for the tearing strength tests. Three pieces of each sample were tested in the warp direction and weft direction separately and average values were used. The subjective handle test was completed by five persons through touching the fabrics with hands directly. Objective handle tests were completed using a handle tester of Kato Tech Co. LTD, Japan. The yellowness of the fabric was measured with a Datacolor Elrepho 2000 spectrophotometer according to ASTM E313 and ASTM D1925.

7.2.2.3 Dyeing processes

A pad-dry-steam method was used. Silk fabrics, both unfinished and finished, were padded with the dye solution through an one-dip-one-pad process, the fabrics were then dried at 90 ^{o}C for 3 min and steamed at 110 ^{o}C for 15 min in the atmosphere of 100% humidity. The dyed silk fabrics were washed with nonionic detergent (0.1% w/v) and rinsed with tap water, and then dried before colorization assessment. The recipes of dye solutions are listed in **Table 7.1**. The pH values of the dye solutions were adjusted to 6.5 with acetic acid for acid dye solutions, and 8.5 for reactive dye

solutions with sodium carbonate respectively.

Table 7.1 The recipes of dye solutions

Dyes	DyeConcen.	Na_2SO_4	Triton X-100	Ciba Abegal Set
Lanaset	30,50,80 g/L	----	1 g/L	10 g/L
Lanasol	10,30,50 g/L	20 g/L	----	----

DyeConcen. : dye concentration

For the exhaustion dyeing process, a liquor ratio of 50:1 and dye solutions of 2.5g/L were used. The silk fabrics were dyed at 80^{o}C for 45 min under shaking, then washed with dilute nonionic detergent (0.1%) and rinsed with tap water, finally dried in air. For the dyeing of nylon fabrics, liquor ratios of 40:1 and 20:1were used with dyeing depths of 2%, 5%, 10% and 40% respectively.

7.2.2.4 Assessment of dyeing results

The color yields (K/S value) were computed by the Kubelka & Munk equation. The color fastness to rubbing was according to AATCC Test Method 8-2004. The color fastness to washing was determined according to Test A1S of EN ISO 105-C06: 1997.

7.3 Results and discussion

7.3.1 Micro morphology of the finished silk fabrics

The pH of the emulsion was near neutral, which was much preferred for the carboxyl groups in the protein fiber to be ionized into $–COO^-$. The ratio of ionization could be 99% with pH value beyond 5 [205]. Once the silk fabrics were soaked into the emulsion, these anions were supposed to adsorb onto the positively charged CSNPs through electrostatic interactions. The CSNPs aggregated on the surface and finally formed a rough layer on the surface of silk after drying. **Figure 7.1** shows the coating structure of chitosan on the fiber.

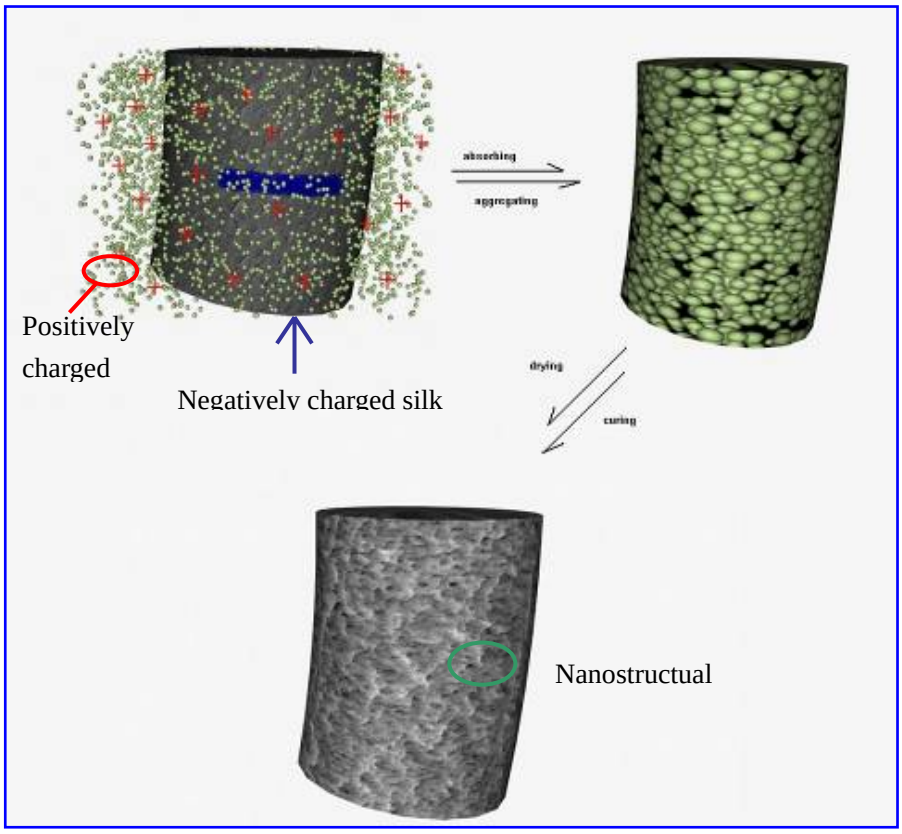

Figure 7.1 Illustration of the coating process of the chitosan nanoparticles on the silk surface

The SEM of the surface of the emulsion-finished silk fabrics agreed with the above assumption. A tubular and porous nano-structure was observed on the surface, as shown in **Figure 7.2 (c)**. The CSNPs in the emulsion accumulated onto the surface of silk, aggregated together during drying and finally formed a rough film, promising a huge surface area that could be useful in the dyeing process. The surface of the chitosan solution-finished silk fiber was as smooth as that of unfinished silk fiber, as shown in **Figure 7.2 (a, b)**.

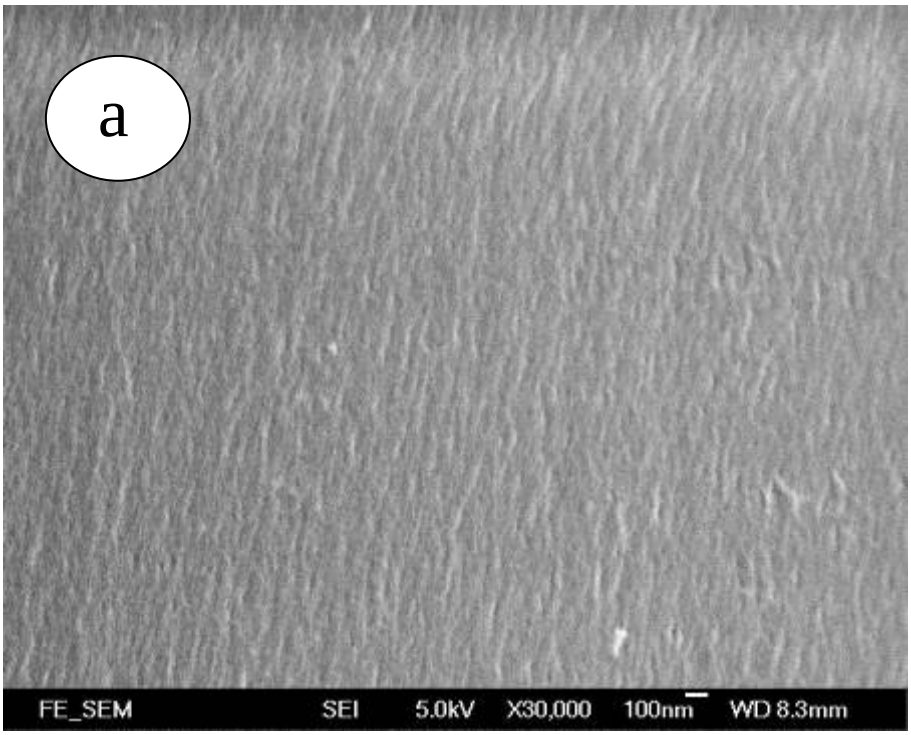

Figure 7.2 SEM micrograph of Untreated silk

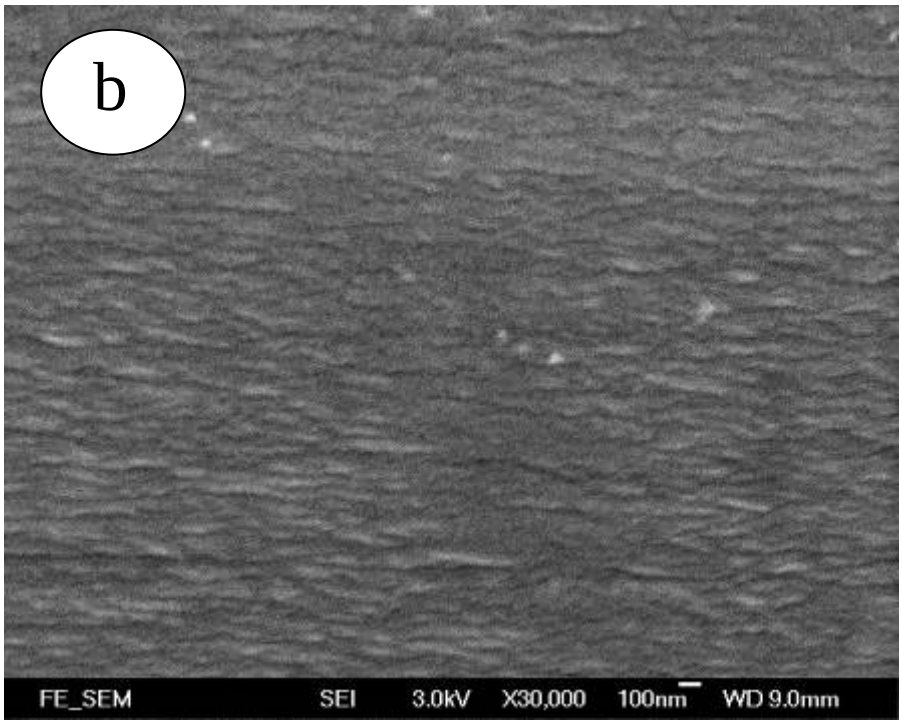

Figure 7.2 SEM micrograph of silk treated by chitosan solution

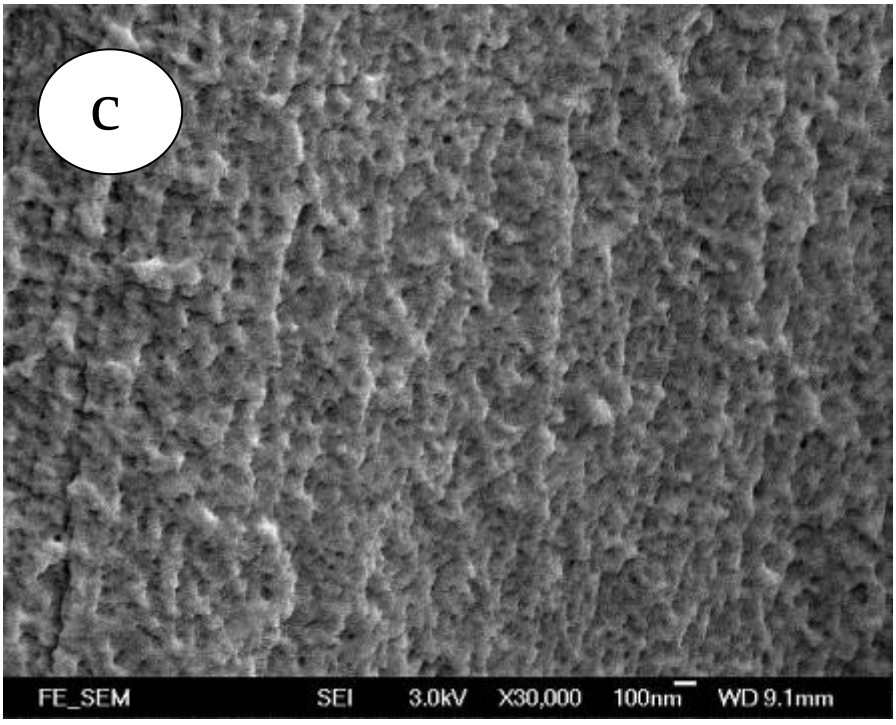

Figure 7.2 SEM micrograph of silk surface treated by CS emulsion

The cross-sections of solution-treated silk and emulsion-treated silk were further studied, as **Figure 7.3** shows. Both the solution and the emulsion formed thin layers on the surface, but the layer formed by the emulsion is thicker than that from the chitosan solution. As a kind of protein fibers, silk was believed to bind with chitosan mainly due to ionic interactions similar to the interaction between wool and chitosan [202], such as the interaction between free amino groups of chitosan and the carboxyl groups of silk. The pH of the emulsion was more suitable than the acidic chitosan solution for the carboxyl groups to confer negative charges and consequently attracted more chitosan to form a thicker film. This explanation was proved through investigating the content of chitosan on the finished silk fabrics. For the emulsion-finished silk fabrics, the chitosan content was 66 mg/g (chitosan/silk) while that of solution-finished silk fabrics was 42 mg/g.

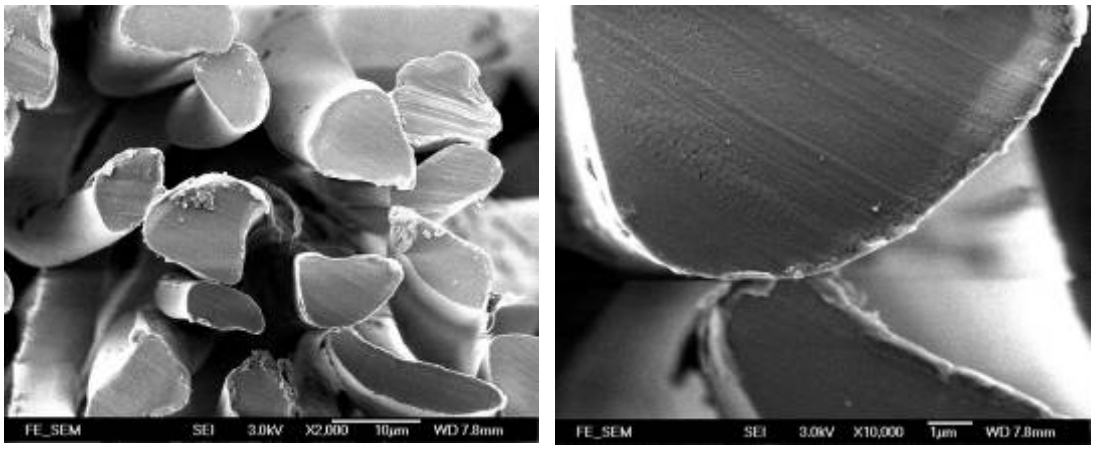

Figure7.3 SEM micrographs of cross section of silk:

Cross-section of the solution-finished silk

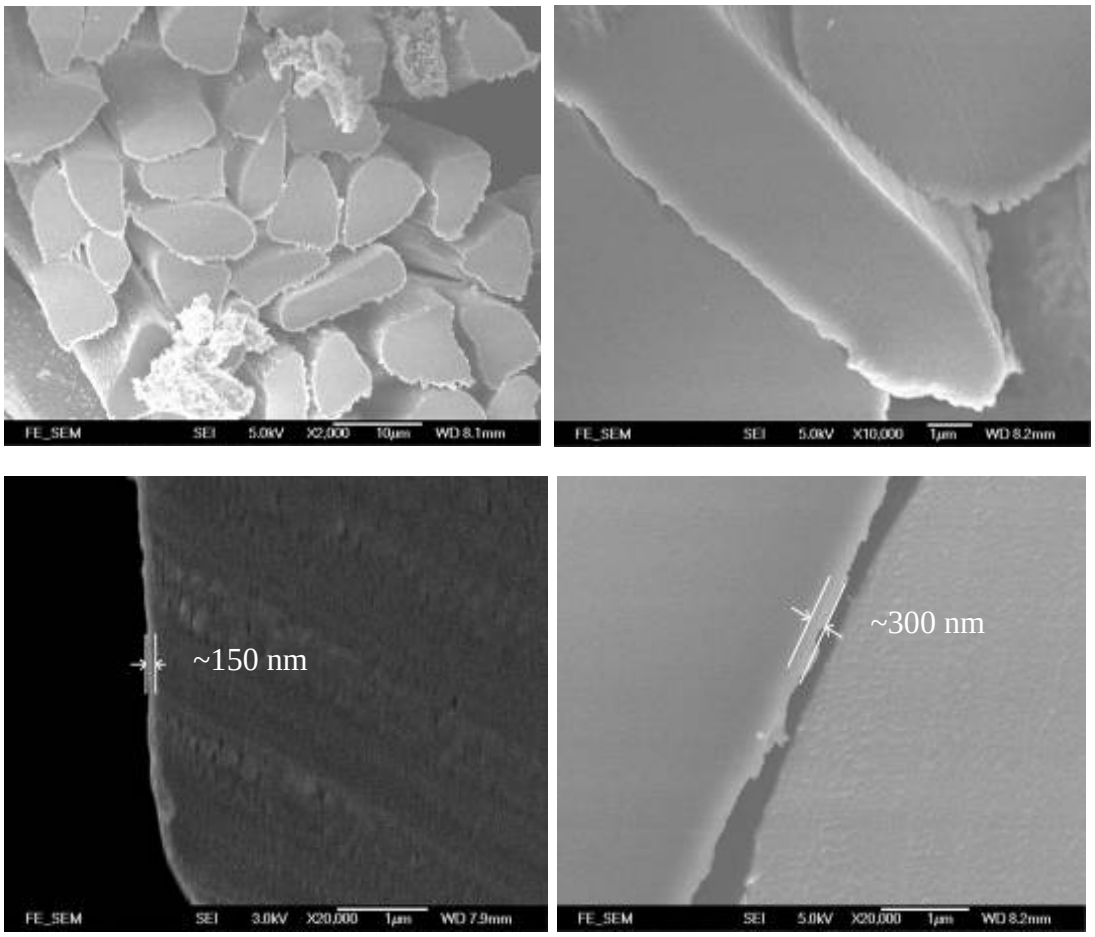

Figure7.3 SEM micrographs of cross section of silk
(left: solution-finished, right: emulsion-finished)

7.3.2 The formation of the nano-structural layers with different chitosan concentrations

Studies were performed on the formation of the chitosan layer from different concentrations of the emulsion. **Figure 7.4** displays the surfaces of the silk fibers finished with the emulsions at concentrations of 0.01%, 0.05% and 0.1%, in which different structures were observed. Three kinds of inter-particle forces were accepted to govern the packing of latex films during solvent evaporation, including flotation forces, lateral capillary forces and convection forces [191-196]. The flotation forces were supposed to mainly decide the appearance of the layer in this

study. Comparing the chitosan layer in **Figure 7.2 (c)**, the tubular nano-structure became more and more obvious with the increase of chitosan concentration from 0.01% to 0.3%. The higher particle density brought on limitation to the flotation of these particles during drying, which was preferred to form fine nano-structure instead of smooth film.

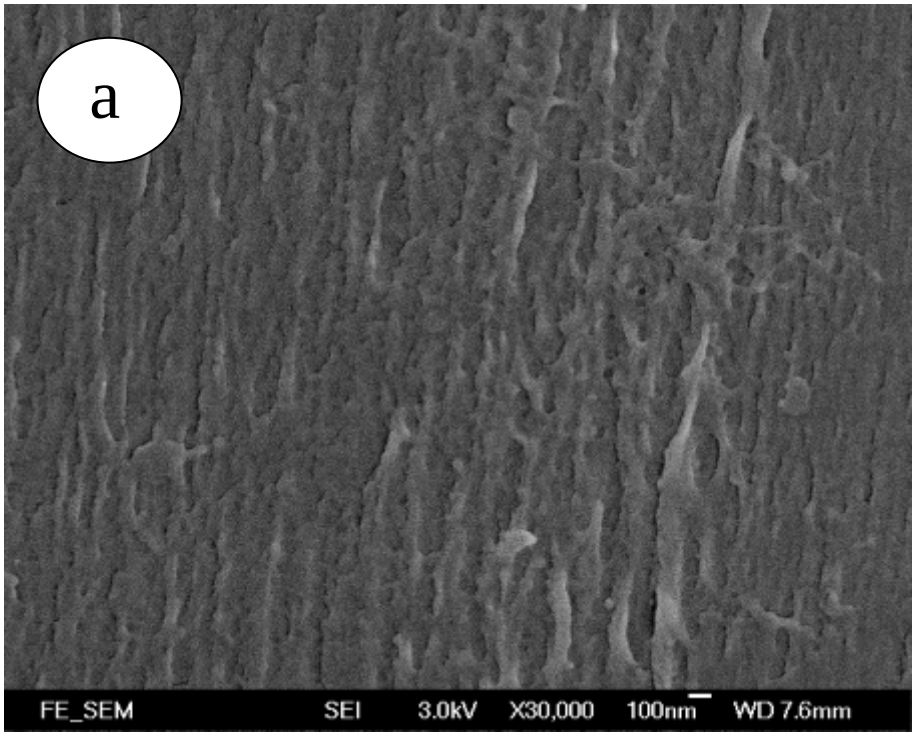

Figure 7.4 SEM micrograph of surfaces of the silk fabrics finished

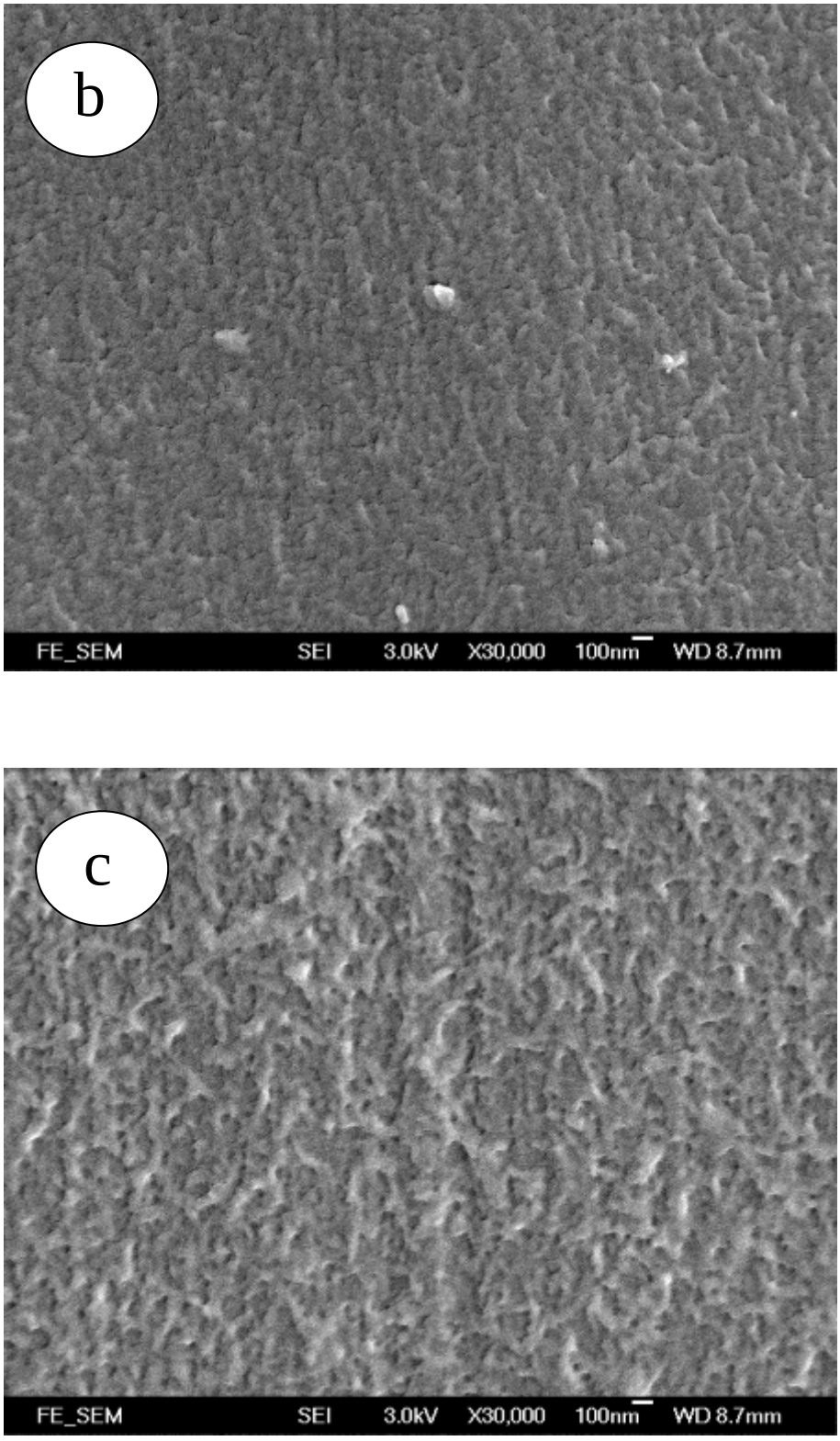

Figure 7.4 SEM micrographs of surfaces of the silk fabrics finished using 0.01% (a), 0.05% (b) and 0.1% (c) emulsion of CSNPs and dried at 100^{o}C

7.3.2 Physical assessment of finished silk fabrics

7.3.2.1 Handle assessments

In the subjective handle assessment, four persons were asked to assess the anonymous samples. Same conclusions were conducted that the control sample had the best handle while the emulsion-finished one was better than that of the solution-finished. In the objective assessment four aspects, tensile & shearing test, pure bending test, compression test and surface test, were performed, and overall assessments according to different using were conducted, and the results are shown in **Figure 7.5**, indicating that the emulsion-finished sample obtained the highest score. The control sample was too soft to care while the solution-finished one had a tough handle. **Table 7.2** describes the result of surface assessment. The control sample obtained the highest friction coefficients. Finishing using the chitosan solution or emulsion smoothed the fabrics surface and gave smaller coefficients while these of the emulsion-finished samples were bigger due to the relative rough structure mentioned above.

Table 7.2 Coefficients of friction measurements

	Control sample	Solution-finished sample	Emulsion-finished sample
Warp	0.193±0.031 MIU-1	0.165±0.059 MIU-1	0.180±0.041 MIU-1
Weft	0.208±0.019 MIU-1	0.156±0.014 MIU-1	0.160±0.018 MIU-1

Control **Solution-finished** **Emulsion-finished**

Women's thin dress fabrics (summer)

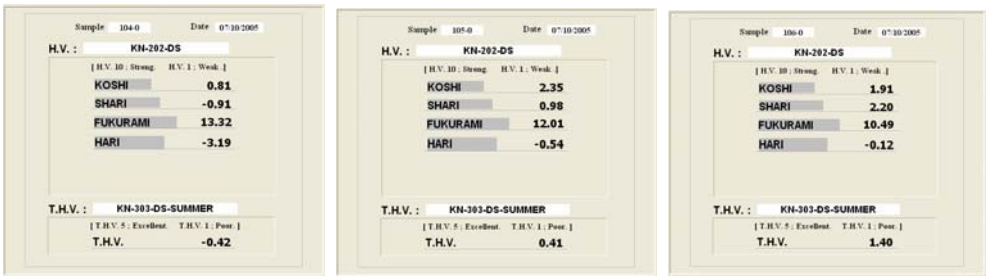

Control **Solution-finished** **Emulsion-finished**

Men's dress shirt (summer)

Control **Solution-finished** **Emulsion-finished**

Women's thin dress fabrics (filament)

Figure 7.5 Objective handle assessments of the silk fabrics

7.3.2.2 Physical strength

Figure 7.6 summarizes the results of physical tests. No obvious change was found among the three samples. The treatments using the solution or the emulsion did not cause obvious alteration of the original physical properties of the silk fabrics.

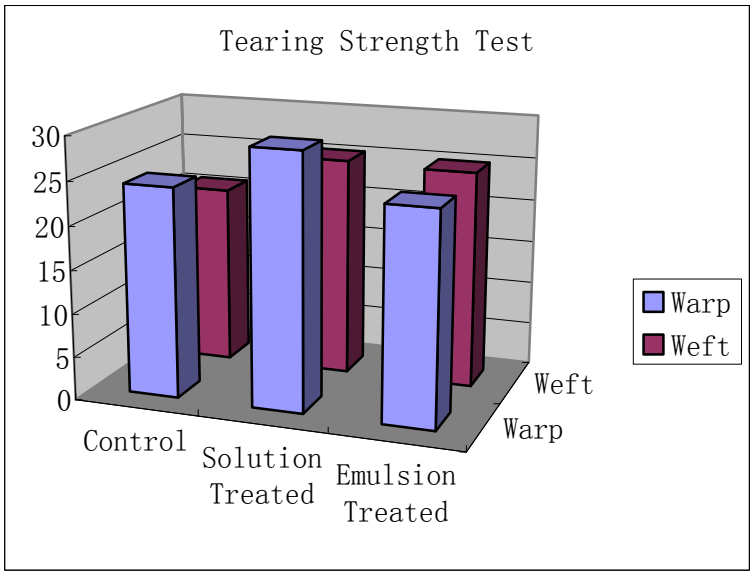

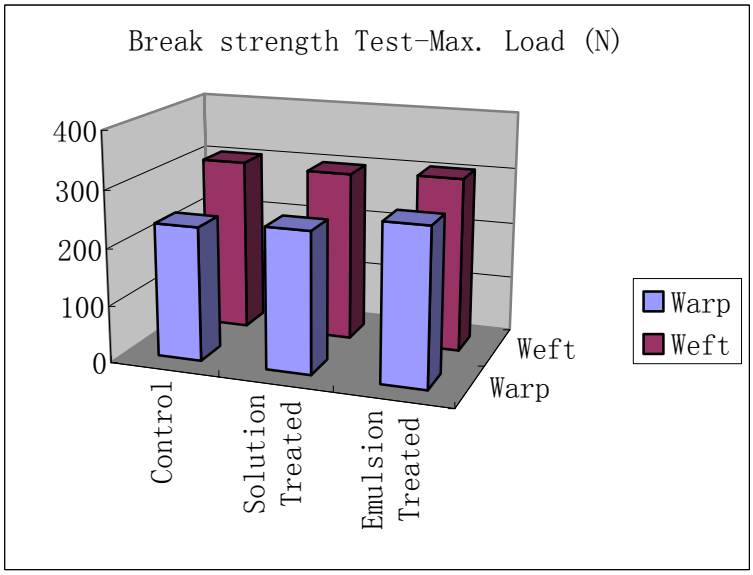

Figure 7.6 Physical tests of the silk fabrics

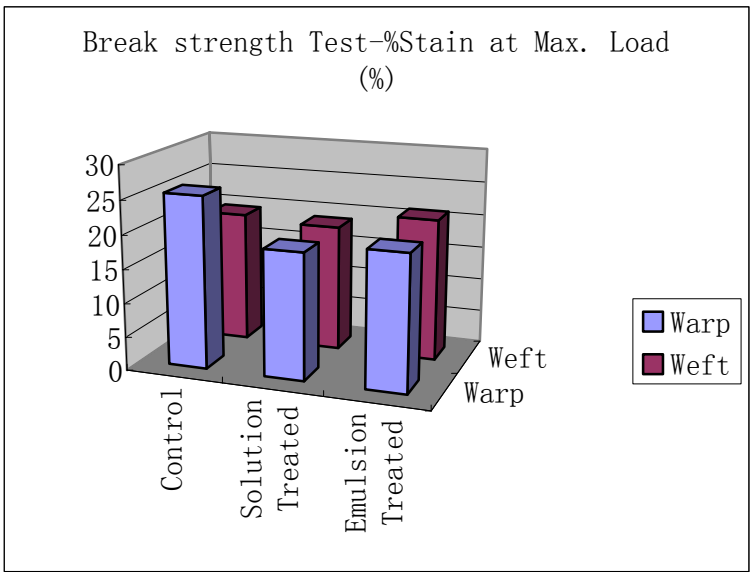

Figure 7.6 Physical tests of the silk fabrics

7.3.2.3 Color change

The color change of the finished samples, the solution-finished one and the emulsion-finished one, were assessed using the yellowness index and whiteness index as parameters. The results are summarized in **Table 7.3** and **Table 7.4**, indicating that no obvious color alteration occurs during the finishing process as well as there was no eyeable color change in the subjective assessment. The treatments did not cause obvious alteration of the original color properties of the silk fabrics.

Table 7.3 Results of yellowness index tests

	Illums/obs	%Z	TAPPITS525
Control	D65/10	67.2±3.38	75.1±3.75
Solution Treated	D65/10	67.4±4.06	75.9±4.11
Emulsion Treated	D65/10	67.3±3.99	75.6±3.89

Table 7.4 Results of whiteness index tests

		ASTM_E313	ASTM_D1925
Control	C/10	5.83±0.23	6.38±0.26
	C/2	4.2±0.16	5.12±0.20
Solution Treated	C/10	6.11±0.31	6.71±0.34
	C/2	4.37±0.19	5.41±0.23
Emulsion Treated	C/10	6.95±0.32	7.62±0.36
	C/2	5.19±0.25	6.25±0.31

7.3.3 Color assessment of the dyed silk fabrics

The solutions of acid dyes and reactive dyes caused different changes to the nano-structual surfaces. The low pH value of the acid dye solution made the chitosan layer becoming smoother (**Figure 7.7 a**) when the reactive dyes dyed surface had no obvious change (**Figure 7.7 b**). The result indicated that an acidic circumstance could cause damage to the formed nano-structure of the chitosan layer.

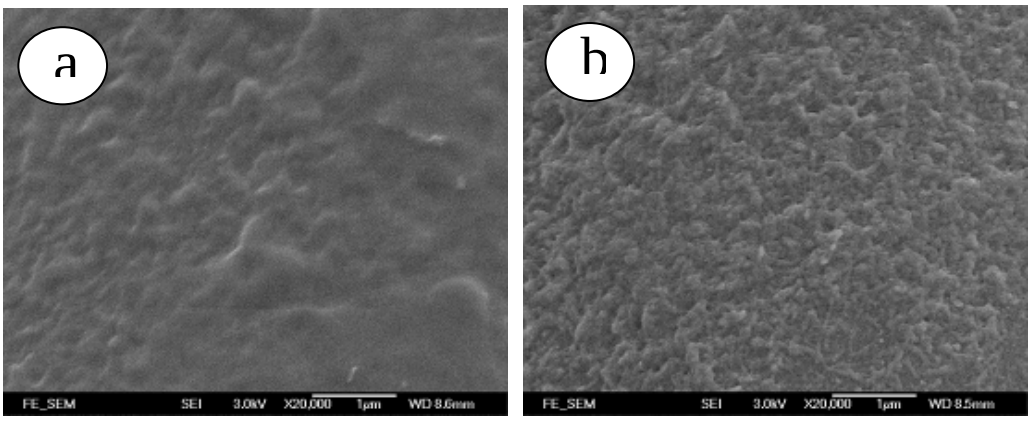

Figure 7.7 Different textures caused by the bathings

Table 7.5 describes the K/S values of dyed silk fabrics with 30 g/L dye solutions. The dyeability of the emulsion-finished silk fabrics was improved remarkably comparing to these of the unfinished silk, and it was also much better than those of the solution-finished silk fabrics when the K/S values could be over 100% higher in some occasions, as shown in **Figure 7.8** and **Figure 7.9**. When using chitosan concentration of 0.3%, **Table 7.6** shows that the K/S values of the emulsion-finished samples were over 100% higher than those of control samples and the solution-finished samples, even 200% higher in same cases. For the emulsion-finished silk fabrics, the formed nano-structure promised a huge surface area, providing more dye sites for dyes as well as a thicker film can adsorb more dye molecules.

On the other hand, the dyeability of the finished silk fabrics using the acid dyes was enhanced more remarkably than that of using reactive dyes. Concluding from the data in **Table 7.5**, the acid dyes generally achieved bigger increasing percentage of K/S values than the reactive dyes when 0.3% chitosan concentration was used.

Chitosan is very attractive to the anionic dyes through the electrostatic attraction because of its cationic property in acidic environments [181]. At lower pH values, more amino groups of chitosan were protonated to capture anionic dye molecules, which was difficult to happen in the alkaline solutions of the reactive dyes [94, 186,]. Consequently, more acid dyes were adsorbed by the finished silk fabrics.

Table 7.5 K/S values of the dyed silk fabrics with 30 g/L solutions of the acid dye and reactive dye through padding-drying-steaming method

Con. / Dyes	Contr.	0.01%		0.05%		0.1%		0.3%	
		S	E	S	E	S	E	S	E
Lanaset Black B	1.99 ± 0.13	2.15 ± 0.16	2.33 ± 0.15	2.18 ± 0.23	3.05 ± 0.28	2.17 ± 0.17	3.26 ± 0.30	2.28 ± 0.13	4.71 ± 0.25
Lanaset Blue 2R	2.81 ± 0.20	2.73 ±0.17	2.998 ± 0.16	2.98 ± 0.20	4.71 ± 0.31	3.21 ± 0.21	4.11 ± 0.25	3.25 ± 0.18	5.95 ± 0.29
Lanaset Red G	2.42 ± 0.17	2.40 ± 0.15	2.82 ± 0.21	2.35 ± 0.13	3.21 ± 0.23	2.54 ± 0.22	5.45 ± 0.32	2.82 ± 0.23	6.18 ± 0.40
Lanasol Scarlet 3G	8.70 ± 0.49	6.65 ± 0.32	9.42 ± 0.51	6.20 ± 0.29	9.67 ± 0.49	7.25 ± 0.37	11.51 ± 0.55	8.19 ± 0.39	13.76 ± 0.53
Lanasol Yellow 4G	6.80 ± 0.41	6.91 ± 0.43	7.78 ± 0.45	6.64 ± 0.39	7.76 ± 0.51	6.62 ± 0.36	7.96 ± 0.48	6.82 ± 0.45	8.36 ± 0.52
Lanosol Navy B-01	5.79 ± 0.31	5.33 ± 0.52	8.22 ± 48	5.62 ± 0.41	8.27 ± 0.50	5.75 ± 0.33	9.45 ± 0.52	6.36 ± 0.39	10.31 ± 0.55

Note: Con. concentration of chitosan; Contr. control sample; S: the solution-finished silk; E: the emulsion-finished silk.

Table 7.6 Increase of K/S values of the emulsion-finished samples comparing to these of the other two samples

Dyestuffs / Samples	Lanaset Black B	Lanaset Blue 2R	Lanaset Red G	Lanasol Scarlet 3G	Lanasol Yellow 4G	Lanosol Navy B-01
Control sample	236.7%	211.7%	255.4%	158.2%	122.9%	178.1%
Solution-finished sample	206.6%	183.1%	219.1%	168.0%	122.6%	162.1%

Note: The data of with chitosan concentration of 0.3% in **Table 7.5** was used.

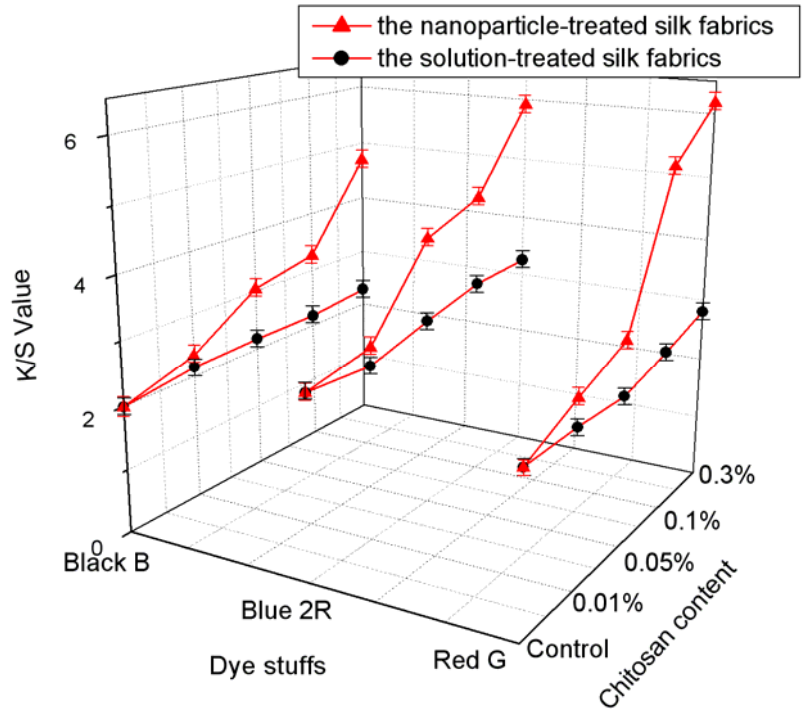

Figure 7.8 Illustrative of K/S value of the acid dyes dyed silk fabrics finished with different chitosan contents through padding-drying-steaming method

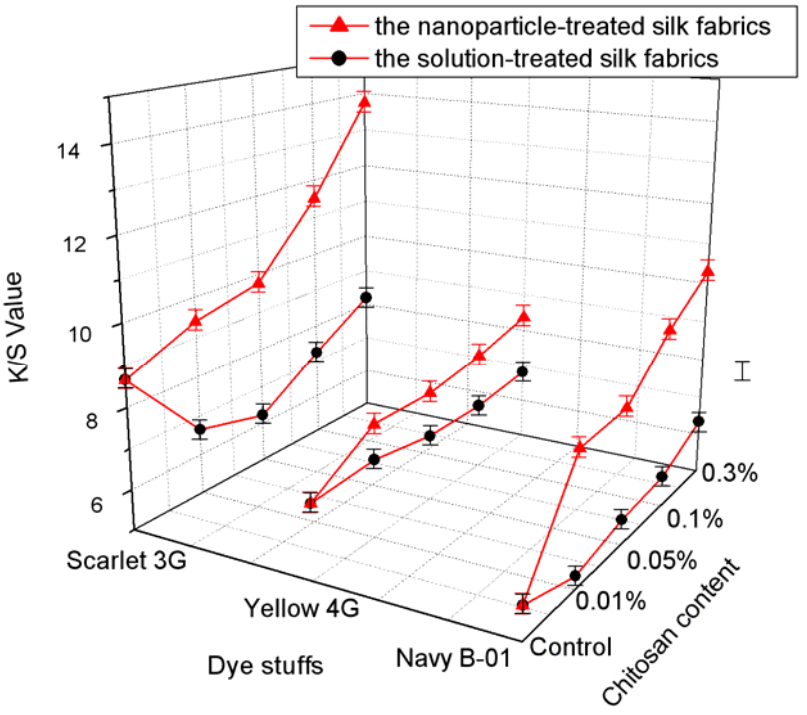

Figure 7.9 Illustrative of K/S value of the reactive dyes dyed silk fabrics with different chitosan contents through padding-drying-steaming method

7.3.4 Color fastness assessment of dyed silk fabrics

The dry rubbing fastness of the chitosan-finished silk was similar to that of the unfinished silk. The grey scale assessments of the staining for all of the finished silk were at 4 to 4-5 in spite of the big difference in K/S values, which indicated that all dyed silk fabrics commanded good fastness to dry rubbing. Difference appeared between the acid dyes and reactive dyes in the washing fastness assessments. **Table 7.7** summarizes the results of the washing fastness assessments of the emulsion-finished silk dyed at concentration of 30 g/L through the padding-drying-steaming method. For the silk dyed by acid dyes, color varying degree was from 1 to 2, indicating that most dye molecules were washed away from the silk. Because the acid dye molecules just interacted with the silk through anionic sulphonic groups electrostatically, water could destroy the interactions and dissolve them again. Meanwhile, color varying degree of 3-4 a ware obtained for the silk dyed by Lanasol Scarlet 3G and Lanasol NavyB-01. The reactive dyes could form covalent bonds with the silk fabrics besides the electrostatic interaction, which caused the better washing fastness. The above assessments of color fastness suggested that the loss of color was due to the poor affinity of dye molecules to the silk fabrics instead of the damage of the nano-structural chitosan layer, reflected the good fastness of the chitosan layer to the silk surface.

Table 7.7 Washing fastening of emulsion-finished silk dyed at concentration of 30 g/L through fast padding-steaming method

Con. / Dye	Unfinished silk	0.05%	0.3%
Lanaset Black B	1-2	1	1
Lanaset Blue 2R	2	2	1
Lanaset Red G	2	1-2	2
Lanasol Scarlet 3G	3-4	2-3	3-4
Lanasol Yellow 4GN	2	1-2	1-2
Lanasol Navy B-01	3	2-3	3-4

Note: Con. concentration of chitosan.

7.3.5 Dyeing of finished nylon fabrics

The emulsion was also applied to finish nylon fabrics. Four primary colors of acid dye were used. The results are summarized in **Table 7.8** and showed in **Figure 7.10**. In low concentrations of the dye bathing, the control samples even displayed better than the emulsion-finished samples occasionally. Though the results were a little different, higher usages of the dye stuffs generally achieved better dyeability improvements. Reason for the phenomenon was waiting for further work. The chitosan layer had better adsorption ability to the dye molecules than nylon. It is difficult for the dye molecules to penetrate the layer and go into the nylon fiber in a lower concentration of dye bathing, so that similar K/S values were obtained for the control samples and the finished samples. With higher concentration of the dye, the chitosan layer was saturated, and more dye molecules went into the inside nylon fabrics through the layer. Similar results were observed in the dyeing of the silk fabrics in the previous section. Bur further evidence to support this deduction is scarce due to the limitation of the analysis methods.

Table 7.8 Dyeing results of the nylon fabrics through exhausting method

Dye / Usage / Dye names	2%		10%		40%		40%B	
	Con	E	Con	E	Con	E	Con	E
Lanaset Black B	20.1 ± 0.41	17.4 ± 0.32	25.9 ± 0.4	26.1 ± 0.42	27.7 ± 0.52	28.3 ± 0.51	28.2 ± 0.55	28.9 ± 0.49
Lanaset Blue 2R	8.60 ± 0.20	9.14 ± 0.19	16.7 ± 0.29	20.0 ± 0.39	21.5 ± 0.29	26.20 ± 0.45	23.4 ± 0.44	29.6 ± 0.49
Lanaset Red G	17.4 ± 0.33	18.0 ± 0.31	24.1 ± 0.46	22.8 ± 0.40	27.8 ± 0.50	28.6 ± 0.55	29.3 ± 0.49	30.4 ± 0.61
Lanaset Yellow 4G	10.0 ± 0.17	9.8 ± 0.12	15.8 ± 0.29	17.4 ± 0.29	17.1 ± 0.32	20.3 ± 0.37	17.5 ± 0.35	21.3 ± 0.39

Note: Con-control samples; E-emulsion finished samples; Liquor ratio 1:50; 40%B Liquor ratio 1:20.

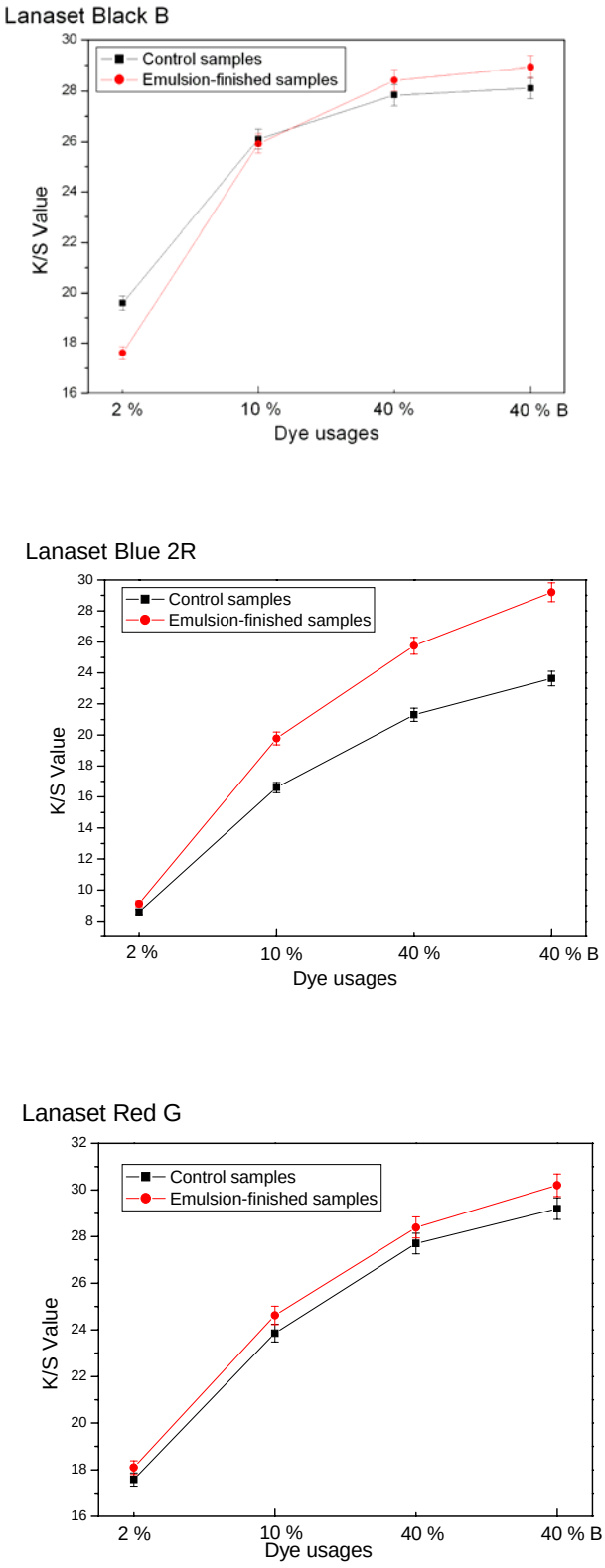

Figure 7.10 Illustraton of the dyeing results of nylon fabrics (to be continued)

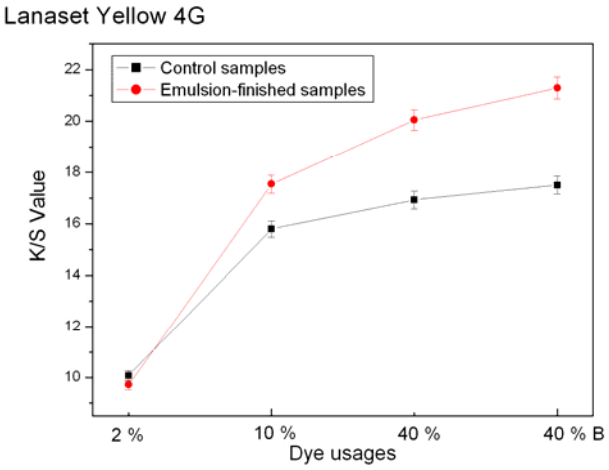

Figure 7.10 Illustration of the dyeing results of nylon fabrics

Meanwhile, we traced the changes of the dye concentration after dyeing process with dyeing condition of 40% deep and 20:1 liquor ratio. The results are shown in **Table 7.9**, indicating that all of the emulsion-finished samples had a higher dye consumption comparing to the control samples. In the case of Lanaset Yellow 4G, the dye capacity of each gram of fabrics is 3.7 times higher than that of control sample. The results agreed to that of the K/S value. The additional chitosan layer made the finished fabrics adsorb more dye molecules and achieve higher K/S value. The color fastness of the dyed nylon fabrics was also investigated, and summarized in **Table 7.10**. In the exhaustion dyeing process, the fibers had enough time to interact with the dye molecules as well as the dye molecules could penetrate into the fiber deeply, so that good colorfastness of water washing was achieved.

Table 7.9 Dye consumption in the dyeing process of nylon

	Dye concentration after dyeing mg/ml		Δ Concentration mg/ml		Percentage of consumed dye %		Dye capacity of each gram of fabrics mg/g	
	Con	E	Con	E	Con	E	Con	E
Lanaset Black B	13.6±0.3	13.3±0.3	6.4±0.3	6.7±0.3	32.0±1.5	33.5±1.5	128±6	134±6
Lanaset Blue 2R	17.5±0.4	16.4±0.3	2.5±0.4	3.6±0.3	12.5±2.0	18.0±1.5	50.0±8	72.0±6
Lanaset Red G	15.0±0.2	14.6±0.2	5.0±0.2	5.4±0.2	25.0±1.0	27.0±1.0	100±4	108±4
Lanaset Yellow 4G	19.7±0.1	18.6±0.2	0.3±0.1	1.4±0.2	1.5±0.5	7.0±1.0	6±2	28±4

Note: Con-control samples; E-emulsion-finished samples. Dyeing conditions: 40% of dye usage, Liquid ratio of 1:20

Table 7.10 Result of color fastness assessment of the dyed nylon fabrics

	Control sample	Emulsion-finished sample
Lanaset Black B	4-5	5
Lanaset Blue 2R	4-5	4
Lanaset Red G	4	4-5
Lanaset Yellow 4G	4	4

7.4 Conclusion

Nano-structual chitosan layer was formed on the surface of silk fabrics through the coating of the CSNPs onto the surface, whose structure could be affected by the CSNPs concentration. A higher concentration was preferred for a loose and thicker nano-structure of the layer that provided a huge surface area. Benefiting from the nano-structure, the dyeability of finished silk fabrics was improved remarkably by

the layer comparing to the unfinished and chitosan-solution-finished silk fabrics. Studies on the rubbing fastness and washing fastness of the finished silk fabrics after dyeing process revealed good adherence of the layer on the surface of finished silk fiber.

Also, the CSNPs were applied to improve the dyeability of nylon fabrics using a traditional exhausting dye method, the finished nylon fabrics had higher K/S values than the control samples when a higher dye concentration was used. Good color fastness to washing was obtained for both the control samples and the finished samples.

In Conclusion, the CSNPs could improve the dyeability of silk and nylon, which could have desirable potential on textile finishing in the textile dyeing industry. But there were still some shortages, such as the inferior wet fastness of the fast-dyed silk and the unstable dyeing resulted in the nylon dyeing. They are discussed in ***Chapter 8***.

Chapter 8

Conclusion and future work

In this thesis, the research work was focused on mainly three aspects of the applications of chitosan in nano-scale. Firstly, a new method for the preparation of the emulsion of the chitosan nanoparticles was developed based on the application of ultrasound, including the preparation of the pure chitosan nanoparticles and the composite chitosan/silver oxide nanoparticles. Secondly, the prepared nanoparticles were studied in the application of textile antibacterial and deodorizing finishing. At last, research work was done to study the interaction between the chitosan nanoparticles and the acid dye molecules, and to apply the emulsion of the pure chitosan nanoparticles to improve the dyeability of silk fabrics and nylon fabrics.

In this chapter conclusion and future work were summarized according to the three aspects of the research separately.

8.1 The preparation of the chitosan nanoparticles

8.1.1 Conclusion

A new method for the preparation of an aqueous emulsion of the chitosan nanoparticles was developed based on a dissolving-precipitating-sonolysis process. Several relative parameters (treatment duration, ultrasound intensity, DD, molecular weight (Mv) and crystallinities) were studied for the purpose of size control of the nanoparticles. We found that, crystallinities, particle sizes and Mv decreased with the increase of treatment duration and ultrasound intensity, and the

DD of chitosan had no obvious change during the ultrasound treatment. The dried chitosan nanoparticles were characterized by SEM and AFM, discovering the spherical profiles of the obtained nanoparticles. The emulsion was stabilized depending on the hydrogen bonds among amino groups and hydroxyl groups of chitosan and water molecules, and had good thermo-stabilization at room temperature.

8.1.2 Future work

The stability and aggregating behavior of the nanoparticles in the emulsion were still waiting to be studied, especially the change according to the change of the pH value and storage time. On the other hand, more work was waiting to be done on the exact size control in the preparation process as well as on the effect of ionic strength to the stability of the emulsion.

8.2 Antibacterial and deodorizing application

8.2.1 Conclusion

Firstly, the antibacterial activity of the cotton samples finished using chitosan, including the chitosan nanoparticles and the chitosan solution, was studied. The mechanical properties (break strength and tearing strength) of the emulsion-finished and the solution-finished samples were a slightly damaged in the finishing process, while no remarkable promotion on anti-wrinkle property was achieved according to the results of wrinkle recovery angle test. The subjective and

objective handle assessments indicated that the handle properties of the emulsion-finished sample were better than the solution-finished sample, and inferior to the control sample. Antibacterial ability of the cotton fabrics were enhanced remarkably after finished with either the emulsion or the solution of the chitosan, and the emulsion-finished samples behaved better than the solution-finished samples. The emulsion-finished samples gave out bacterial reduction of over 90% even at a neutral condition. Bacterial reduction of 80% was obtained with the emulsion-finished samples washed equal to standard home laundry of 50 times, indicating good washing fastness.

Secondly, for higher efficient antibacterial activity of the finished cotton, the nanoparticles of silver oxide were encapsulated into the pure chitosan nanoparticles to obtain a nano-composite. The growth of silver nanoparticles in the chitosan/$AgNO_3$ solution was studied, indicating that silver ions formed complicated chelating complexes with chitosan that acted as reductant, and hexagonal silver crystals were observed. But the complex was unstable in the solution and turned into black precipitates finally. Further alkali treatment oxidized silver nanoparticles into silver oxide nanoparticles, and a fabrication of silver oxide nanoparticles in the chitosan nanoparticles was obtained. The emulsion of the chitosan/silver oxide nanoparticles was consisted of positively charged composite chitosan/silver oxide nanoparticles with 10-20 nm silver oxide nanoparticles encapsulated. The emulsion had good stability and could bear

months of storage though no surfactant or other additive stabilizer was used. Cotton fabrics were entitled excellent antibacterial property companying. The finished cotton fabrics also had efficient deodorizing activity. Washing fastness assessments were performed, proving the durable activities of antibacterial and deodorization of the cotton fabrics finished using the emulsion. The application of such low concentrations also avoided the colour problem of silver successfully and reserved the original characteristics of treated cotton fabrics.

8.2.2 Future work

Since the emulsion of the pure chitosan nanoparticles can impact the finished sample considerate antibacterial activity with preserving original properties of the fabrics, more work could be done on the application of the emulsion to finish some high quality textiles that requires a critical finishing process, especially such as a neutral environment to avoid any damage to the quality. Beyond the field of the textile finishing, the nanoparticles can be used to coat onto some biological devices for antibacterial purposes, or directly applied as a neutral biocide agent. Furthermore, the nanoparticles is a good host to immigrate other functional group because of the chemical activity of the amino groups in the chitosan molecules as well as its good affinity to the textile materials. So that more work can be done to develop the potential of the nanoparticles as a host for more functions of the finished textile.

Concerning the composite chitosan/silver oxide nanoparticles, the key work

awaiting to be done is the investigation of the color change of the finished samples during long term storage because that, low usage of silver avoid colorization in the finishing process, but possible change color change of finished textile caused by certain change of silver on the textile is still not studied. On the other hand, the stability of the emulsion of the composite, especially the stability when mixed with other agents for multi-functional finishing, was waiting to be enhanced.

8.3 Dye-related research

8.3.1 Conclusion

First, the behavior of the chitosan-TPP nanoparticles as an adsorbent to remove Acid Green 27 from its aqueous solution was investigated, figuring out that the adsorbing ability was significantly higher than that of the micron-sized chitosan. The equilibrium isotherm was measured and analyzed using the Langmuir equation to determine the capacities of the nanoparticles for the dye. It was found that the sorption well fitted in the Langmuir model, especially when the dye concentration was high. The Langmuir monolayer adsorption capacities (Q_0) were calculated using the weight of the nanoparticles and the weight of chitosan in the nanoparticles, which are 1051.8 mg/g and 2103.6 mg/g respectively. The affinity between the nanoparticles and the chemicals used could be summarized: the order of attractive forces was TPP>H_3O^+>SO_3^-(in dye) > the hydrogen bonds in acidic conditions; and OH->TPP>SO_3^- (in dye) >H_2O in alkaline conditions.

Secondly, the emulsion of the pure chitosan nanoparticles (CSNPs) was applied to finishing silk fabrics for the purpose of dyeability enhancement. Nano-structual chitosan layer was formed on the surface of silk fabrics through the coating of the CSNPs onto the surface, whose modality could be affected by the CSNPs concentration and drying temperature. Benefiting from the nano-structure, the dyeability of finished silk fabrics was improved remarkably by the layer comparing to the unfinished and chitosan-solution-finished silk fabrics. Studies on the rubbing fastening and washing fastening of the finished silk fabrics after dyeing process reveal good adherence of the layer on the surface of finished silk fiber. The improvement in the dyeability of the silk fabrics exhibited desirable perspective of the CSNPs for the dyeability enhancement of protein fabrics through simple process.

The CSNPs were also applied to improve the dyeability of nylon fabrics in the research. Studied through a traditional exhausting dye method, the finished nylon fabrics behave better than the control samples obviously when higher dye concentration is used. Good color fastness to water washing was obtained with either the control samples or the finished samples.

In conclusion, the CSNPs could improve the dyeability of some of the protein or artificial fibers efficiently, which could explore a new biocompatible and eco-friendly strategy for textile finishing in the textile dyeing industry.

8.3.2 Future work

Detail work about the adsorption of the pure chitosan nanoparticles to the acid dye molecules is not done yet while the chitosan-TPP nanoparticles display efficient adsorption capability toward to acid dye. Since the adsorption mechanisms are the same, the pure chitosan nanoparticles are believed to have higher adsorption capability than the chitosan-TPP nanoparticles because TPP is inactive in the adsorption. So that, more work is deserved to be done on study of the adsorption behavior of the pure chitosan nanoparticles toward kinds of dye molecules. Furthermore, considering the reuse of the nanoparticles in the real application, a proper recycle process should be researched. Possible approach now is the coating of the nanoparticles onto easy-renewed host materials, such as cotton and other cellulose fabrics.

On the aspect of dyeability enhancement, several parameters in the process, including the particle size, concentration, finishing temperature, dyeing process, were awaiting for more investigation. Since the remarkable enhancement comes from huge surface area of the nano-structure layer formed by the chitosan nanoparticles, more work should be done to optimize the process condition for a desired nano-structure, and to try to control the morphology of the nano-structure layer. The effect of the dyeing process to the dyeability enhancement should be also investigated. The color fastness of the fabrics dyed through the fast dyeing process is inferior. Additive chemicals and proper experimental condition should

be studied for improving the color durability. On the other hand, uneven color deep is observed with some of the emulsion-finished samples. Maybe this is due to the uneven dispersing of the CSNPs on the fiber surface under the condition of fast dry, or caused by the shortage of the dyeing process. These shortages are waiting for further work.

References

[1] Sang-Hoon Lim, Samuel M. Hudson, *Journal of Macromolecular Science, Part C- PolymerReviews*, 2003, 43, 223.

[2] Hudson S.M ., Smith C., *Polysaccharide: chitin and chitosan: Chemistry and technology of their use as structural materials. In Biopolymers from Renewable Resources*, Springer-Verlag: New York, 1998, p96.

[3] Roberts G.A.F., *Chitin Chemistry*, Macmillan Press Ltd., London,1992.

[4] Li Q., Dunn E.T., Grandmaison E.W., Goosen M.F.A., *Applications and properties of chitosan. In Applications of Chitin and Chitosan*, Technomic Publishing Company,Inc.: Lancaster, PA, 1997, p3.

[5] Muzzarelli R., Jeuniaux C., Gooday G.W, *Chitin in Nature and Technology*, Plenum Press: New York, 1986.

[6] Brine C.J., Sandford P.A., Zikakis J.P., *Advances in Chitin and Chitosan*, Elsevier Science Publishers Ltd.: London, New York, 1992.

[7] Domard Roberts G.A.F., Varum K.M., *Advances in that Chitin Science Vol. II*, Jacques Andre Publisher: Lyon, France,1997.

[8] Peter M .G., Domard A., Muzzarelli R.A.A ., *Advances in Chitin Science Vol. IV*, Universitat Potsdam: Potsdam, Germany, 2000.

[9] Sannan T., Kurita K., Ogura K., Iwakura Y., *Polymer*, 1978, 19, 458.

[10] Moore G.K., Roberts G.A.F., *International Journal of Biological Macromolecules*, 1980, 2, 115.

[11] Miya M., Iwamoto R., Yoshikawa S., *International Journal of Biological Macromolecules*, 1980, 2, 323.

[12] Domszy J.G., Roberts G.A.F., *Makromol. Chem.*, 1985, 186, 1671.

[13] Baxter A., Dillon M., Taylor K.D.A., Roberts A .F., *International Journal of Biological Macromolecules*, 1992, 14, 66.

[14] Aiba S., *International Journal of Biological Macromolecules*, 1986, 8, 173.

[15] Domard A., *International Journal of Biological Macromolecules*, 1987, 9, 333.

[16] Hirai A., Odani H., Nakajima A., *Polymer Bulletin*, 1991, 26, 87.

[17] Varum K.M., et al., *Carbohydrate Research*, 1991, 221, 17.

[18] Raymond L., et al., *Carbohydrate Research*, 1993, 246, 331.

[19] Hayes E.R., Davies D.H., *Characterization of chitosan II. The determination of the degree of acetylation of chitosan and chitin.* In Proceedings of the First International Conference on Chitin/Chitosan, Muzzarelli R.A.A ., Pariser E.R., Eds.; MIT Sea Grant Program, Massachusetts Institute of Technology: Cambridge, MA, 1978, 406.

[20] Lim S.H., *Synthesis and characterization of a fiber-reactive and water-soluble chitosan derivative with enhanced antimicrobial activity,* M.S. Thesis, North Carolina State University, 1999.

[21] Terayama H., *Journal of Polymer Science*, 1952, 8, 243.

[22] Wang A., Yu X., *Fine Chemicals*, 1998, 15, 17.

[23] Rathke T., Hudson S., *J. Macromol. Sci. R. M. C.*, 1994, 34, 375.

[24] Hudson S.M., Jenkins D.W., *Chitin and chitosan. Encyclopedia of Polymer Science and Technology, 3rd Ed.*, (on line version, www.interscience.wiley.com) Wiley Interscience, 2001.

[25] Kurita K., Sannan T., Iwakura Y., *Makromol. Chem.*, 1977, 178, 3197.

[26] Kurita K., et al., *Chemistry Letter*, 1989, 1597.

[27] Kurita K., Kamiya M., Nishimura S., *Carbohydrate Polymer*, 1991, 16, 83.

[28] Nudga L.A., Plisko E.A., *Zhurnal Obshchei Khimii*, 1973, 43, 2752.

[29] Hirano S., Osaka T., *Agric. Biol. Chem.*, 1983, 47, 1389.

[30] Moore G.K., Roberts G.A.F., *International Journal of Biological Macromolecules*, 1981, 3, 337.

[31] Nishimura S.I., et al., *Chemistry Letter*, 1990, 243.

[32] Calvo P., Remunan C., et al., *Journal of Applied Polymer Science*, 1997, 63, 125.

[33] Rocio Fernandez-Urrusuno, et al., *Pharmaceutical Research*, 1999, 16, 1576.

[34] Janes K. A., Alonso M. J., *Journal of Applied Polymer Science*, 2003, 88, 2769.

[35] Li F., Luo F., *Fine Chemicals*, 2003, 20, 197.

[36] Tang E. S. K., M. Huang L.Y. Lim, *International Journal of Pharmaceutics*, 2003, 265, 103.

[37] Tao C.C., et al., *Macromolecular Bioscience*, 2004, 4, 416.

[38] Tanima Banerjee, et al., *International Journal of Pharmaceutics*, 2002, 243, 93.

[39] Ye W., Xin H. John, Li P., et al., *Journal of Applied Polymer Science*, 2006, 102, 1787.

[40] Wang X., Du Y., Ding S., et al., *Journal of Physical Chemistry B*, 2006, 110, 1566.

[41] Yea W., Leung M. F., Xin H. John, *Polymer*, 2005, 46, 10538.

[42] Chen L., Subirade M., *Biomaterials*, 2005, 26, 6041.

[43] Ehab Taqieddin, Mansoor Amiji, *Biomaterials*, 2004, 25, 1937.

[44] Cheng D., Xia H., Sze On Chan Hardy, *Langmuir*, 2004, 20, 9909.

[45] Hu Y., Jiang X., et al., *Biomaterials*, 2002, 23, 3193.

[46] Hirano S., *Agric. Biol. Chem.*, 1989, 53, 3065.

[47] Panineau A.M., et al., *Food Biotechnology*, 1991, 5, 45.

[48] Sudardshan N.R., et al., *Food Biotechnology*, 1992, 6, 257.

[49] Wang G.H., *Journal of Food Protection*, 1992, 55, 916.

[50] Fang S.W., et al., *Journal of Food Protection*, 1994, 46, 136.

[51] Hwang J.K., et al., *Bactericidal activity of chitosan on E. coli.* In Advances in Chitin Science; Chen R.H., Chen H.C.

[52] Tsai G.J., Su W.H., *Journal of Food Protection*, 1999, 62, 239.

[53] Jeon Y.J., Kim S.K., *Carbohydrate Polymer*, 2000, 41, 133.

[54] Liu X.F., et al., *Journal of Applied Polymer Science*, 2001, 79, 1324.

[55] Jeon Y.J., et al., *Carbohydrate Polymer*, 2001, 44, 71.

[56] Choi B.K., et al., *International Journal of Antimicrobial Agents*, 2001, 18, 553.

[57] Helander I.M., et al., *International Journal of Food Microbiolog*, 2001, 71, 235.

[58] Tokura S., et al., *Macromolecular Symposia*, 1997, 120, 1.

[59] Tanigawa T., et al., *Advances in Chitin and Chitosan*, Elsevier Science Publishers Ltd.: London,New York, 1992, p206.

[60] Young D.H., et al., *Plant Physiology*, 1982, 70, 1449.

[61] Young D.H., et al; *Plant Physiology*, 1983, 73, 698.

[62] Hadwiger L.A., et al., *Chitin in Nature and Technology*; Plenum Press: New York, 1986, p209.

[63] Yalpani, M., et al., *Advances in Chitin and Chitosan*, Elsevier Science Publishers Ltd.: London, New York, 1992, p543.

[64] Qi L., et al., *Carbohydrate Research*, 2004, 339, 2693.

[65] Vigo T.L., *Handbook of Fiber Science and Technology; Vol. II, Chemical Processing of Fibers and Fabrics, Functional Finishes Part A*, Marcel Dekker: New York, 1983, p367.

[66] Yoo D.I., et al., *Advances in Chitin Science Vol. II*, Jacques Andre Publisher: Lyon, France, 1997, p763.

[67] Shin Y., et al., *Journal of Applied Polymer Science*, 2001, 80, 2495.

[68] Yoo D.I., et al., *Journal of Applied Polymer Science*, 1999, 74, 2911.

[69] Shin Y., et al.; *Advances in Chitin Science Vol. II*, Jacques Andre Publisher:Lyon, France, 1997, p771.

[70] Chung Y.S., et al., *Textile Research Journal*, 1998, 68, 772.

[71] Rippon J.A., *J. Soc. Dyers Colour*, 1984, 100, 298.

[72] Canal J.M., et al., *Int. Dyer*, 1998, 183, 16.

[73] Annadurai G., Krishnan M.R.V., *Iranian Polymer Journal*, 1997, 6, 169.

[74] Vandevivere P.C., Bianchi R., Verstraete W.J., *Chem Technol Biotechnol*, 1998, 72, 289.

[75] Lin S.H., Lin C.M., *Water Research*, 1993, 27, 1743.

[76] Ganesh R., Boardman G.D., Michelsen D., *Water Research*, 1994, 28, 1367.

[77] Walker G.M., Weatherley L.R., *Water Research*, 1997, 31, 2093.

[78] Chu W., Tsui S.M., *Chemosphere*, 1999, 39, 1667.

[79] El-Geundi M.S., *Water Research*, 1991, 25, 271.

[80] Grau P., *Water Science and Technology*, 1991, 24, 97.

[81] Lucarelli L., Nadtochenko V., Kiwi J., *Langmuir*, 2000, 16, 1102.

[82] Poots V.J.P., McKay G., Healy J.J., *Water Research*, 1976, 10, 1061.

[83] Ho Y.S., McKay G., *Chemical Engineering Journal*, 1998, 70, 115.

[84] McKay G., Elgeundi M., Nassar M.M., *Water Research*, 1987, 21, 1513.

[85] Namasivayam C., Prabha D., Kumutha M., *Bioresour Technol*, 1998, 64, 77.

[86] Ho Y.S., McKay G., *Resour Conserv Recy*, 1999, 25, 171.

[87] Namasivayam C., Radhika R., Suba S., *Waste Manage*, 2001, 21, 381.

[88] Namasivayam C, Kavitha D., *Dyes Pigments*, 2002, 54, 47.

[89] Atun G., Hisarli G., Sheldrick W.S., Muhler M., *Journal of Colloid and Interface Science*, 2003, 261, 32.

[90] McKayG., Otterburn M.S., Aga J.A., *Water, Air & Soil Pollution*, 1985, 24,

307.

[91] Poots V.J.P., McKay G., Healy J.J., *Water Research*, 1976, 10, 1067.

[92] Asfour H.M., Nassar M.M., Fadali O.A., Elgeundi M.S., *J Chem Technol Biotechnol*, 1985, 35, 28.

[93] Lim S.H., Hudson S.M., *J Macromol Sci Polym Rev*, 2003, 43, 223.

[94] Ravi Kumar M.N.V., *React Funct Polym*, 2000, 46, 1.

[95] Hennen William J., *Chitosan*, Woodland, 1996.

[96] Giunchedi P., Genta I., Conti B., Muzzarelli R.A.A., Conte U., *Biomaterials*, 1998, 19, 157.

[97] Illum L., *Pharmaceutical Research*, 1998, 15, 1326.

[98] Yoshida H., Okamoto A., Kataoka T., **Chemical Engineering Science**, 1993, 48, 2267.

[99] Yoshida H., Takemori T., *Water Science and Technology*, 1997, 35, 29.

[100]Yoshida H., Fukuda S., Okamoto A., Kataoka T., *Water Science and Technology*, 1991, 23, 1667.

[101]Chiou M.S., Li H.Y., *Chemosphere*, 2003, 50, 1095.

[102]Chang Y.C., Che D.H., *Macromolecular Bioscience*, 2005, 5, 254.

[103]Leon T.L., Carvalho E.L.S., Seijo B., *Journal of Colloid and Interface Science*, 2005, 283, 344.

[104]Stockman P.A., Bumgarner R.E., Suzuki S., Blake G.A., *Journal of Chemical Physics*, 1992, 96, 2496.

[105]Yeo G.A., Ford T.C., *Canada Journal of Chemistry*, 1991, 69, 632.

[106]Del Bene J.E., *Journal of American Chemical Society*, 1973, 95, 5460.

[107]Hu Y., Jiang X.Q., Ding Y., *Biomaterials*, 2002, 23, 3193.

[108]Wong Y.C., Szeto Y.S., Cheung W.H., McKay G., *Langmuir*, 2003, 19, 7888.

[109]Langmuir I., *Journal of American Chemical Society*, 1918, 40, 1361.

[110]Li X., Wang Z., *HUA XUE TONG BAO*, 2001, 5, 268.

[111]Xia H., Zhang C., Wang Q.Q., *Journal of Applied Polymer Science*, 2001, 80, 1130.

[112]Ryu J.G., Kim H.S., Lee J. W., *Annual Technical Conference - Society of Plastics Engineers*, 2002, 60th (Vol. 2), 2240.

[113]Danicher Louis, Frere Yves, Le Calve Anne, *Macromolecular Symposia*, 2000, 151, 387.

[114]Faerman V.T., Goryachko G.V., Slonimskii G.L., *Doklady Akademii Nauk SSSR*, 1964, 158, 446.

[115]Min Larng Tsaih, Rong Huei Chen, *Journal of Applied Polymer Science*, 2003, 90, 3526.

[116]Zhou S., Chen S., Tang W., *Strait Pharmaceutical Jourmal*, 2002, 14, 5.

[117]Liu S., Qiu Q., Cai C., Han S., *Journal of Guangdong University of Technology*, 2002, 19, 83.

[118]Ding M., Sun H., et al., *Heifei Lianhe Daxue Xuebao*, 1998, 2, 7.

[119]Ghohad G., et al., *Makromol. Chem*, 1998, 195, .

[120]Dong Y., Xu C., et al., *SCIENCE CHAINA (Series B)*, 2001, 31, 153.

[121]Dong Y., Wang M., et al., *Journal of Cellulose Science and Technology*, 2001,

9, 42.

[122]Alasdair Baxter, Michael Dillon, K. D. Anthony Taylor., *International Journal of Biological Macromolecules*, 1992, 14, 166.

[123]Tanveer Ahmad Khan, Kok Khiand Peh, Hung Seng Ch'ng. *J Pharm Pharmaceut Sci*, 2002, 5, 205.

[124]Duarte M. L., Ferreira M. C., et al., *International Journal of Biological Macromolecules*, 2002, 21, 1.

[125]Rabek, Jan F., *Experimental Methods in Polymer Chemistry: Physical Principles and Applocations*, Wiley-Interscience Publication, 1978.

[126]Stockman, P.A., Bumgarner R.E., Suzuki, S. Blake G.A., *Journal of Chemical Physics*, 1992, 96, 2496.

[127]Fraser G. T., Suenram R.D., *Journal of Chemical Physics*, 1992, 96, 7287.

[128]Herbine B., Nord L., *Journal of Chemical Physics*, 1985, 83, 3768.

[129] Sadle J., Moszynski, R., Dobrowolski, J.C., Mazurek, A.P., *Journal of Physical Chemistry A*, 1999, 103, 8528.

[130]Donaldson D. J., *Journal of Physical Chemistry A*, 1999, 103, 62.

[131]Robert Joel Samuels, *Journal of Polymer Science: Polymer Physics Edition*, 1981, 19, 1081.

[132]Masahisa Wada, Yukie Saito, *Journal of Polymer Science: Part B: Polymer Physics*, 2001, 39, 168.

[133] Tsaih M.L., Chen R.H., *Journal of Applied Polymer Science*, 2003, 90, 3526.

[134] Wang A., Yu X., *FINE CHEMICALS*, 1998, 15, 17.

[135]Djoric S.S., Burre R.E., *Journal of The Electrochemical Society*, 1998, 145, 1426.

[136]Feng Q.L., Wu J., et al., *Journal of Biomedical Materials Research*, 2000, 52, 662.

[137]Kraft C.N., Hansis M., et al., *Journal of Biomedical Materials Research*, 2000, 49, 192.

[138]Williams R.L., Doherty P.J., Vince D.G., Grashoff G.J., Williams D.F., *Crit Rev Biocompat*, 1989, 5, 221.

[139]Berger T.J., Spadaro J.A., Chanpin S.E., Becher R.O., *Antimicrobial Agents and Chemotherapy*, 1976, 9, 357.

[140]Verne E., Nunzio S.D., Bosetti M., et al., *Biomaterials*, 2005, 26, 5111.

[141]Gosheger Georg, Jendrik Hardes, et al., *Biomaterials*, 2004, 25, 5547.

[142]Gray J.E., Norton P.R., et al., *Biomaterials*, 2003, 24, 2759.

[143]Alt Volker , Bechert Thorsten, et al., *Biomaterials*, 2004, 25, 4383.

[144]Grunlan Jaime C, Choi John K, Albert Lin., *Biomacromolecules*, 2005, 6, 1149.

[145]Kumar Radhesh, Münstedt Helmut, *Biomaterials*, 2005, 26, 2081.

[146]Zhang S.T., Fu R.W., Wu D.C., et al., *Carbon*, 2004, 42, 3209.

[147] Hennen, William J., *Chitosan*, Woodland Pub, 1996.

[148]Giunchedi P, Genta I, et al., *Biomaterials*, 1998, 19, 157.

[149]Li Z., Zhuang X.P., et al., *Polymer*, 2002, 43, 1541.

[150]Hu S.G., Jou C.H., Yang M.C., *Biomaterials*, 2003, 24, 2685.

[151]Qi L.F., Xu Z.R., et al., *Carbohydrate Research*, 2004, 339, 2693.

[152]Huang H.Z., Yang X.R., *Carbohydrate Research*, 2004, 339, 2627.

[153]Muzzarelli R.A.A., *Natural Chelating Polymers*, Pergamon Press, Oxford, 1973.

[154]Morni N.M., Mohamed N.S., Arof A.K., *Mat Sci Eng B*, 1997, 45, 140.

[155]Yoshizuka K., Lou Z.R., Inoue K., *React Funct Polym*, 2000, 44, 47.

[156]Yi Y., Wang Y.T., Liu H., *Carbohydrate Polymer*, 2003, 53, 425.

[157]Huang H.Z., Yuan Q., Yang X.R., *Colloid Surface B*, 2004, 39, 31.

[158]Cheng D.M., Xia H.B., Chan S.O., *Langmuir*, 2004, 20, 9909.

[159]Hu Z.G., Szeto Y.S., patent filed.

[160]Hu Z.G., Chan W.L., Chan K.W., Szeto Y.S., *New chitosan/silver oxide nano-composite and its antibacterial activity in cotton fabrics*, Abstract of 230th ACS National Meeting, in Washington, DC, Aug 28-Sept 1, 2005.

[161]Kesting Robert E, *Journal of Applied Polymer Science*, 1965, 9, 663.

[162]Samuels R.J., *J Polym Sci Pol Phys*, 1981, 19, 1081.

[163] Masahisa W., Yukie S., *J Polym Sci Pol Phys*, 2001, 39, 168.

[164]Jeon H.J., Yi S.C., Oh S.G., *Biomaterials*, 2003, 24, 4921.

[165]Park S.J., Jiang Y.S., *Journal of Colloid Interface Science*, 2003, 261, 238.

[166]Li L., Judith Yang C., *Mater. High Temp.*, 2003, 20, 601.

[167]Wang H.S., Qiao X.L., Chen J.G., Ding S.Y., *Colloids and Surfaces A*, 2005, 256, 111.

[168]Stockman P.A., Bumgarner R.E., Suzuki S., Blake G.A., J*ournal of Chemical*

Physics, 1992, 96, 2496.

[169]Yeo G.A., Ford T.A., *Canada Journal of Chemistry*, 1991, 69, 632.

[170]Janet E., Bene Del, *Journal of American Chemical Society*, 1973, 95, 5460.

[171]Antonietti M., *Topic in Current Chemistry: Colloid Chemistry II*, Berlin ; Hong Kong : Springer, c2003.

[172]Annadurai G., Krishnan M.R.V., *Iranian Polymer Journal*, 1997, 6, 169.

[173]Vandevivere P.C., Bianchi R., Verstraete W., *J. Chem. Technol.Biotechnol.*, 1998, 72, 289.

[174]Canal J.M., Rodriquez C., Caballero G., Julia M.R., *Int. Dyer*, 1998, 183, 16.

[175]Weltrowiski M., Masri M.S., US Patent 5,501,711, 1996.

[176]Hsieh C.Y., Tsai S.P., Wang D.M., *Biomaterials*, 2005, 26, 5617.

[177]Saha T.K., Karmaker S., Ichikawa H., *Journal of Colloid Interface Science*, 2005, 286, 433.

[178]Wu Y., Seo T., Maeda S., *J. Polym. Sci. Pol. Phys.*, 2005, 43, 1354.

[179]Uragami T., Katayama T., Miyata T., *Biomacromolecules*, 2004, 5, 1567.

[180]Jiang L.Y., Liu C.Y., L Jiang.P., *Anal. Sci.*, 2004, 20, 1055.

[181]Lim S.H., Hudson S.M., *J. Macromol. Sci.-Polym. Rev*, 2003, 43, 2223.

[182]Ravi Kumar M.N.V., *React. Funct. Polym.*, 2000, 46, 1.

[183]Yoshida H., Okamoto A., Kataoka T., *Chemical Engineering Science*, 1993, 48, 2267.

[184]Yoshida H., Takemori T., *Water Science and Technology*, 1997, 35, 29.

[185]Yoshida H., Fukuda S., Okamoto A., Kataoka T., *Water Science and*

Technology, 1991, 23, 1667.

[186]Dragan J., Susana V., Tatjana T., *Carbohydrate Polymer*, 2004, 60, 51.

[187]Wu Y.G., Chan W.L., Szeto Y.S., *Journal of Applied Polymer Science*, 2003, 90, 2500.

[188]Takeshi K., Akiko N., *Nippon Sanshigaku Zassh*, 2002, 71, 147.

[189]Takeshi K., *Nippon Sanshigaku Zasshi*, 2001, 70, 117.

[190]Yuri R., Yurko D., *Langmuir*, 2005, 21, 7057.

[191]Salamanca J.M., Ciampi E., Faux D.A., *Langmuir*, 2001, 17, 3202.

[192]Wang Y., Kats A., Juhue D., Winnik M., *Langmuir*, 1992, 8, 1435.

[193] Wallin M., Glover P.M., Hellgren A.C., *Macromolecules*, 2000, 33, 8443.

[194]Routh A., Zimmerman W.B., *Chemical Engineering Science*, 2004, 59, 2961.

[195]Ko H.Y., Park J., Shin H.M., *Journal of Chemical Materials*. 2004, 16, 4212.

[196]Blaaderen A. van, Wiltzius P., *Science*, 1995, 270, 1177.

[197]Hu Z.G., Chan W.L., Szeto Y.S., *Dyeability improvement of silk with chitosan nanoparticles*, Abstract of the 230th ACS National Meeting, Washington DC, August 2005.

[198]Hu Z.G., Szeto Y.S., Patent in application.

[199]Stockman P.A., Bumgarner R.E., Suzuki S., Blake G.A., *Journal of Chemical Physics*, 1992, 96, 2496.

[200]Yeo G.A., Ford T., *Canada Journal of Chemistry*, 1991, 69, 632.

[201]Del Bene J.E., *Journal of American Chemical Society*., 1973, 95, 5460.

[202]Dragan J., Susana V., Tatjana T., *Carbohydrate Polymer*, 2004, 60, 51.

[203]Juang R.S., Tseng R.L., Wu F.C., J*ournal of Chemical Technology & Biotechnology*, 1997, 70, 391.

[204]Heinrich Zollinger, *Color Chemistry*, WILEY-VCH, 2003, p194.

[205]J.R. Aspland, Textile Dyeing and Coloration, AATCC, 1997, p231.